2008-11-20

piRNA Function and Biogenesis in the *Drosophila* Female Germline: A Dissertation

Carla Andrea Klattenhoff
University of Massachusetts Medical School

piRNA FUNCTION AND BIOGENESIS IN THE *DROSOPHILA* FEMALE GERMLINE

A Dissertation Presented

By

CARLA ANDREA KLATTENHOFF

Submitted to the Faculty of the

University of Massachusetts Graduate School of Biomedical Sciences, Worcester

in partial fulfillment of the requirements for the degree of

DOCTOR OF PHILOSOPHY

NOVEMBER 20, 2008

INTERDISCIPLINARY GRADUATE PROGRAM

piRNA FUNCTION AND BIOGENESIS IN THE *DROSOPHILA* FEMALE GERMLINE

A Dissertation Presented By

Carla Andrea Klattenhoff

The signatures of the Dissertation Defense Committee signifies completion and approval as to style and content of the Dissertation

William Theurkauf, Ph.D., Thesis Advisor

Kirsten Hagstrom, Ph.D., Member of Committee

Craig Mello, Ph.D,, Member of Committee

Danesh Moazed, Ph.D., Member of Committee

Craig Peterson, Ph.D., Member of Committee

The signature of the Chair of the Committee signifies that the written dissertation meets the requirements of the Dissertation Committee

Stephen Doxsey, Ph.D., Chair of Committee

The signature of the Dean of the Graduate School of Biomedical Sciences signifies that the student has met all graduation requirements of the School

Anthony Carruthers, Ph.D.
Dean of the Graduate School of Biomedical Sciences

Interdisciplinary Graduate Program
November 20, 2008

COPYRIGHT INFORMATION

ACKNOWLEDGMENTS

First of all, I need to thank my mentor, Bill Theurkauf, for all the guidance and support over the course of my thesis. His door was always open to answer my questions and to have scientific discussions, which I truly enjoyed.

I would like to thank all the esteemed colleagues involved in the studies presented in this thesis. Very specially, Nadine Schultz was responsible for most of the genetics presented throughout this work. She also contributed in countless ways to making my life easier every day, offering just the best technical support.

Diana Bratu and Heather Cook were involved in generating the data for Chapter II. Birgit Koppetsch contributed to experiments presented in both Chapters II and III. Jaspreet Khurana generated the ChIP data presented in Chapter III.

Phil Zamore and the rest of his group were always supportive, providing us with a different point of view, constructive comments and their outstanding expertise in small RNA biochemistry. In particular, I want to thank Herve Seitz and Chengjian Li, for their contributions to the microarray analysis and experimental aspects of the deep sequencing of small RNAs for Chapter III.

The UMASS bioinformatics group, directed by Zhiping Weng, were just amazing help with the analysis of both the microarray and deep sequencing data presented in Chapter III.

Past and present members of the Theurkauf lab provided a rich work environment and interesting scientific discussion. Beatrice Benoit, Hanne Varmark and Byeong Cha

helped me with their friendship and contagious enthusiasm for science and discovery. I will never forget the philosophical meetings.

Finally, I will never be able to thank enough to my family and friends. My parents and sisters, selflessly allowed me to leave their side to pursue my dreams and have always supported me. Dear friends have provided the joy and comfort to keep going in times when experiments fail and results don't make sense. My husband has given enormous support to make this thesis possible, always reminding me of my potential. Last but not least, my baby, Olivia, has patiently shared her mother's energy and attention.

ABSTRACT

The studies presented in this thesis addressed mainly two aspects of Piwi-interacting RNA (piRNA) biology in the *Drosophila* germline.

We investigated the role of the piRNA pathway in embryonic axis specification. piRNAs mediate silencing of retrotransposons and the *Stellate* locus. Mutations in the *Drosophila* piRNA pathway genes *armitage* and *aubergine* disrupt embryonic axis specification, triggering defects in microtubule polarization and asymmetric localization of mRNA and protein determinants in the developing oocyte. Mutations in the ATR/Chk2 DNA damage signal transduction pathway dramatically suppress these axis specification defects, but do not restore retrotransposon or *Stellate* silencing. Furthermore, piRNA pathway mutations lead to germline-specific accumulation of γ–H2Av foci characteristic of DNA damage. We conclude that piRNA based gene silencing is not required for axis specification, and that the critical developmental function for this pathway is to suppress DNA damage signaling in the germline.

We have also identified a new member of the piRNA pathway. We show that mutations in *rhino*, which encodes a rapidly evolving Heterochromatin Protein 1 (HP1) chromo box protein, lead to germline specific DNA break accumulation, trigger Chk2 kinase dependent defects in axis specification, and disrupt germline localization of Piwi proteins. Mutations in *rhino* and the piRNA pathway gene *armitage* disrupt silencing of all major transposon families, but do not alter expression of euchromatic or heterochromatic protein coding genes. Deep sequencing studies show that *rhino* mutations significantly reduce or eliminate anti-sense piRNAs derived from the majority

of transposable elements in the *Drosophila* genome, and lead to a dramatic reduction in piRNAs derived from major piRNA production clusters on chromosomes 2R and 4. Rhino protein localizes to distinct nuclear foci, and associates with the chromosome 2R and 4 clusters by chromatin immunoprecipitation. The Rhino HP1 homologue is therefore required for piRNA biogenesis, transposon silencing, and maintenance of germline genome integrity.

TABLE OF CONTENTS

Chapter III.

The *Drosophila* HP1 homologue Rhino is required for piRNA biogenesis, transposon silencing and genome maintenance in the female germline

Chapter IV.

Perspectives and open questions

Appendix I.

LIST OF FIGURES

Appendix I

LIST OF CONTRIBUTIONS

Chapter II

- **Table 1.** Carla Klattenhoff, Nadine Schultz and Diana Bratu.
- **Figure 1.** Nadine Schultz and Diana Bratu.
- **Figure 2.** Carla Klattenhoff, Nadine Schultz and Diana Bratu.
- **Figure 3.** Nadine Schultz and Diana Bratu.
- **Figure 4.** Carla Klattenhoff.
- **Figure 5.** Nadine Schultz and Diana Bratu.
- **Figure 6.** Carla Klattenhoff.
- **Figure 7.** Carla Klattenhoff.
- **Figure 8.** Carla Klattenhoff, Nadine Schultz and Birgit Koppetsch.
- **Figure 9.** Carla Klattenhoff and William Theurkauf.

Chapter III

- **Table 1.** Carla Klattenhoff and Nadine Schultz.
- **Figure 1.** A. Carla Klattenhoff. B. Carla Klattenhoff
- **Figure 2.** Carla Klattenhoff.
- **Figure 3.** Carla Klattenhoff, Birgit Koppetsch, Phyllis Spatrick and Hualin Xi.
- **Figure 4.** Birgit Koppestch.
- **Figure 5.** Carla Klattenhoff, Chengjian Li and Zhiping Weng.
- **Figure 6.** Carla Klattenhoff, Chengjian Li and Zhiping Weng.
- **Figure 7.** Carla Klattenhoff, Chengjian Li and Zhiping Weng.
- **Figure 8.** Carla Klattenhoff and Chengjian Li.
- **Figure 9.** Carla Klattenhoff
- **Figure 10.** Carla Klattenhoff
- **Figure 11.** Carla Klattenhoff and Jaspreet Khurana.
- **Figure 12.** Carla Klattenhoff.
- **Figure 13.** Carla Klattenhoff.

Appendix I

- **Figure 1.** Carla Klattenhoff.
- **Figure 2.** Carla Klattenhoff.

CHAPTER I

INTRODUCTION

Biogenesis and germline functions of piRNAs

Introduction

In 1993, Ambros and colleagues showed that the *C. elegans lin-4* gene encodes a small regulatory RNA with complementarity to the *lin-14* transcription unit, which it negatively regulates (Lee et al., 1993). These pioneering studies thus identified the first microRNA (miRNA). Small non-coding RNAs have subsequently emerged as powerful experimental tools and critical developmental regulators in animals and plants (Baulcombe, 2004; Hannon, 2002; Kloosterman and Plasterk, 2006; Mello and Conte, 2004). 21 nt small interfering RNAs (siRNAs), now ubiquitously used to experimentally manipulate gene expression, are processed from long double-stranded RNA (dsRNA) precursors by the Dicer endonucleases. The resulting 21 nucleotide (nt) double stranded RNAs are incorporated into an intermediate RNA-protein complex. Displacement of one of the RNA strands (referred to as the "passenger strand") then produces the mature RNA Induced Silencing Complex (RISC), which contains a single "guide strand" bound to a member of the Argonaute protein family. When the guide strand siRNA is perfectly complementary to a target RNA, the Argonaute protein catalyzes sequence-specific endonucleolytic cleavage (for review see (Hannon, 2002; Meister and Tuschl, 2004). *In vivo,* the siRNA pathway destabilizes RNA intermediates generated during the viral life cycle, and thus plays an important role in limiting virus infectivity (Wang et al., 2006). By contrast, microRNAs are derived from stem loop transcripts encoded by chromosomal genes. Primary stem-loop RNAs (priRNA) are processed in the nucleus by the ribonuclease Drosha, producing pre-miRNAs that are exported from the nucleus and cleaved in the cytoplasm by a Dicer endonuclease to yield ~22nt mature miRNAs. These miRNAs associate with Argonaute proteins and induce the homology-dependent down-

regulation of target gene activity. Imperfect miRNA base pairing to target transcripts appears to induce translational silencing, while perfect base pairing triggers RNA destruction. Mutations in the miRNA pathway disrupt development and often lead to embryonic lethality (reviewed in (Du and Zamore, 2005; Kloosterman and Plasterk, 2006).

Recent studies have revealed the existence of a new class of 24-30 nt RNAs that are generated by a Dicer-independent mechanism and that interact with a subset of Argonaute proteins related to Piwi (Aravin et al., 2006; Brennecke et al., 2007; Girard et al., 2006; Grivna et al., 2006a; Gunawardane et al., 2007; Houwing et al., 2007; Lau et al., 2006; Saito et al., 2006; Vagin et al., 2006; Watanabe et al., 2006), which is required for female and male fertility in *Drosophila* (Lin and Spradling, 1997). In some systems, these Piwi-interacting RNAs (piRNAs) are primarily derived from transposons and other repeated sequence elements (Brennecke et al., 2007; Gunawardane et al., 2007; Saito et al., 2006), leading to their other designation as repeat associated small interfering RNA (rasiRNA) (Aravin et al., 2003). It is now clear that piRNAs can be derived from either repeated or complex DNA sequence elements (Aravin et al., 2007; Brennecke et al., 2007; Houwing et al., 2007), and that rasiRNAs are a subset of piRNAs. We therefore use the more generic term piRNA in the following discussions. Genetic studies in mice, *Drosophila*, and zebrafish indicate that piRNAs are critical to germline development (Carmell et al., 2007; Chen et al., 2007; Cook et al., 2004; Cox et al., 1998; Cox et al., 2000; Deng and Lin, 2002; Gillespie and Berg, 1995; Houwing et al., 2007; Kuramochi-Miyagawa et al., 2004; Pane et al., 2007; Schupbach and Wieschaus, 1991). However, proteins involved in piRNA production have also been implicated in control of gene

expression in somatic cells (Grimaud et al., 2006; Pal-Bhadra et al., 2002; Pal-Bhadra et al., 2004) and learning and memory (Ashraf et al., 2006), suggesting that piRNAs may impact a broad range of biological processes.

piRNA production

The 24 to 30 nt length of piRNAs is an indication that they are not generated by a Dicer, which produces 21 to 22 nt products from double stranded precursors (Bernstein et al., 2001). Recent genetic studies are consistent with the conclusion that piRNA production is a Dicer-independent process (Houwing et al., 2007; Vagin et al., 2006). Insight into the mechanism of piRNA production has come from studies of their genomic origin and of Argonaute binding in *Drosophila* (Aravin et al., 2006; Brennecke et al., 2007; Girard et al., 2006; Grivna et al., 2006a; Gunawardane et al., 2007; Houwing et al., 2007; Lau et al., 2006; Saito et al., 2006; Vagin et al., 2006). In *Drosophila* ovaries, the vast majority of piRNAs appear to be derived from a limited number of pericentromeric and telomeric sites that are enriched for retrotransposon sequences (Brennecke et al., 2007). The most abundant piRNAs derive from the antisense strand of retrotransposon sequences, and these RNAs preferentially associate with the Argonautes Piwi and Aubergine (Aub). Sense strand piRNAs, by contrast, preferentially associate with Argonaute 3 (Ago3) (Brennecke et al., 2007; Gunawardane et al., 2007). Piwi, Aub and Ago3, in complex with piRNAs, can cleave target RNAs between positions 10 and 11 of the guide strand (Gunawardane et al., 2007; Saito et al., 2006). Significantly, *Drosophila* piRNAs from opposite strands tend to have a 10 nt overlap. Furthermore, antisense piRNAs bound to Piwi and Aub show a strong bias toward a U at the 5’end, while sense

strand piRNAs bound to Ago3 tend to have an A residue at position 10 (Brennecke et al., 2007; Gunawardane et al., 2007). Based on these observations, two groups concurrently proposed a "ping-pong" model of piRNA production, in which Ago3 bound to sense strand piRNAs catalyzes antisense strand cleavage at an A:U base pair that generates the 5' end of anti-sense piRNAs (Figure 1) (Brennecke et al., 2007; Gunawardane et al., 2007). The 5' ends of the resulting cleavage products are proposed to associate with Aub or Piwi, with nucleolytic processing of the 3' overhangs generating mature 23 to 30 nt anti-sense piRNAs (Figure 1B). The mature anti-sense piRNA-Argonaute complexes are then proposed to bind and cleave sense strand RNAs, silencing gene expression and generating the 5'end of sense strand piRNA precursors that associate with Ago3 (Figure 1D). Processing of the 3' overhang produces mature sense strand piRNAs, completing the cycle (Figure 1E). This model is based on studies in *Drosophila,* but recent findings suggest that a similar mechanism may function in mouse (Aravin et al., 2007).

The proteins that mediate a number of the proposed steps in the "ping-pong" model of piRNA production have not been identified, but the results of recent studies might help fill some of these gaps. For example, mutations in the *Drosophila zucchini* and *squash* genes disrupt piRNA production and lead to a loss of retrotransposon silencing, and both of these genes encode putative nucleases (Pane et al., 2007). Zucchini and Squash may therefore process the 3' end extensions to generate mature piRNAs (Figure 1). In addition, the 3' end of mature piRNAs are methylated (Kirino and Mourelatos, 2007; Ohara et al., 2007). In *Drosophila* this reaction is carried out by the Hen1 RNA methyltransferase (DmHen1/Pimet), and methylation appears to take place after piRNAs bind to Argonautes (Horwich et al., 2007; Saito et al., 2007). A mutation in *Dmhen1*

reduces the length and steady state level of piRNAs, suggesting that methylation limits the extent of 3' processing and increases the stability of piRNAs (Horwich et al., 2007). Methylation could also influence interactions between piRNAs and additional components of the piRNA pathway. However, *Dmhen1* mutants are viable and fertile, indicating that this modification is not essential to piRNA function (Saito et al., 2007).

Genetic screens in *Drosophila* have identified several additional factors that are required for piRNA production or function. For example, the *armitage* and *spindle-E* genes encode putative helicases are required for piRNA production and retrotransposon silencing (Aravin et al., 2004; Vagin et al., 2006). These proteins could unwind duplex intermediates formed during piRNA production, target recognition, or cleavage. By contrast, the *cutoff* gene is required for retrotransposon silencing, but is not needed for piRNA production (Chen et al., 2007). Yeast homologues of Cutoff have been implicated in RNA decay (Kim et al., 2004; Xue et al., 2000). Cutoff could therefore facilitate gene silencing by enhancing the activity of piRNA-Argonaute complexes.

Figure 1.

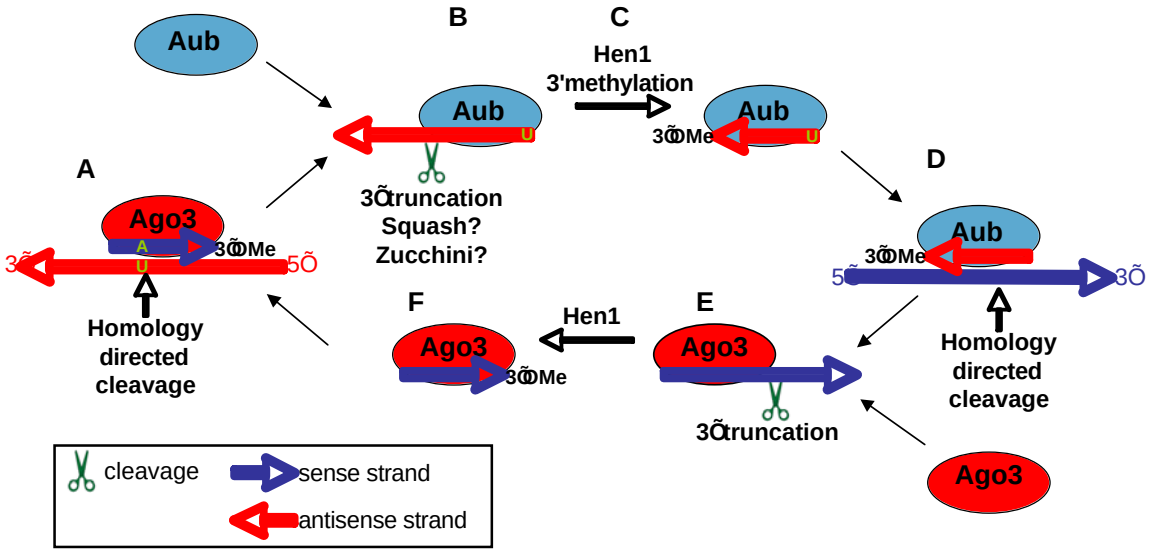
Aub
B
C
Hen1
3'methylation
Aub
Aub
3ÕOMe
U
A
D
Ago3
3ÕOMe
5Õ
3Õ
Aub
3ÕOMe
5Õ
3Õ
3Õtruncation
Squash?
Zucchini?
Homology
directed
cleavage
F
Hen1
E
Ago3
Ago3
3ÕOMe
Ago3
3Õtruncation
Homology
directed
cleavage
Ago3
cleavage
sense strand
antisense strand

Figure 1. Ping-pong model for piRNA production (modified from Brennecke et al., 2007).

(**A**) The Piwi-class Argonaute protein Argonaute 3 (Ago3) binds to sense-strand piRNAs (blue) and directs the cleavage of target antisense-strand transcripts (red), producing the 5' end of antisense-strand piRNAs. (**B**) Aubergine (Aub) and Piwi (not shown) bind to the resulting piRNA precursor, which is trimmed to its final length. This might be catalyzed by the putative nucleases Squash and Zucchini. (**C**) *Drosophila* Hen1 methylates the 3'ends of piRNAs (3'OMe). (**D**) Aub–antisense-strand piRNA complexes catalyze the cleavage of sense transcripts (blue), producing the 5' end of sense piRNAs. (**E**) Ago3 binds the resulting sense piRNA precursors, which are trimmed and (**F**) methylated, as described for antisense-strand piRNAs.

Compartmentalization of the piRNA pathway

Recently, the *Drosophila* Tudor domain protein Krimper has been implicated in both retrotransposon repression and piRNA production (Lim and Kai, 2007). This protein is a component of nuage, a germline-specific perinuclear structure that has been implicated in RNA processing, and *krimper* mutations block nuage assembly. Intriguingly, many piRNA pathway related proteins accumulate in nuage, which is prominent in nurse cells. The *Drosophila* oocyte develops in a cyst with 15 nurse cells, which synthesize RNAs and proteins that are transported through ring canals to the oocyte (Spradling, 1993). Nuage was first identified in electron micrographs as an amorphous electron dense cloud that surrounds the nurse cell nuclei (Allis et al., 1979; Mahowald, 1971). Nuage is enriched for the Piwi class Argonautes Aub and Ago3 (Figure 2A; (Brennecke et al., 2007; Harris and Macdonald, 2001), the helicases Armitage and Spindle-E (Cook et al., 2004; Lim and Kai, 2007), the nucleases Zucchini and Squash (Pane et al., 2007), Maelstrom and Cutoff (Chen et al., 2007; Findley et al., 2003). In contrast to most piRNA pathway proteins, *Drosophila* Piwi localizes almost exclusively to nurse cell nuclei (Figure 2A; (Brennecke et al., 2007; Cox et al., 2000; Saito et al., 2006). These observations suggest that piRNA production and function may be compartmentalized (Lim and Kai, 2007).

piRNA-argonaute complexes appear to be the catalytically active effectors of the pathway, and these localization studies thus suggest that Piwi mediates nuclear functions for the piRNA pathway, while Ago3 and Aub drive cytoplasmic functions (Figure 2B).

We speculate that piRNA biogenesis, which is proposed to require sense and antisense strand Argonaute complexes, take place in the nuage. In this model, the sense

strand piRNA precursor transcripts are exported to the nuage, where they are cleaved by Aub-antisense piRNA complexes, silencing target gene expression and generating precursors of sense strand piRNAs. These sense strand precursors associate with Ago3 and are trimmed to mature length. Ago3-sense strand complexes then catalyze the cleavage of the antisense transcripts, producing piRNA precursors that associate with Aub and Piwi.

Mature Aub complexes then remain in the nuage and function in piRNA production and sense strand transcript destruction, while mature Piwi complexes are imported into the nucleus and mediate heterochromatin assembly and transcriptional silencing, or co-transcriptional RNA destruction. This model is highly speculative, but makes a number of clear predictions and may therefore serve as a useful framework for further studies on piRNA biogenesis.

Genetic studies in *Drosophila*, mice and zebrafish have provided insight into the biological functions of piRNAs, and highlight the significance of these RNAs in germline development. The phenotypes of piRNA pathway mutations in each of these systems are outlined below.

Figure 2.

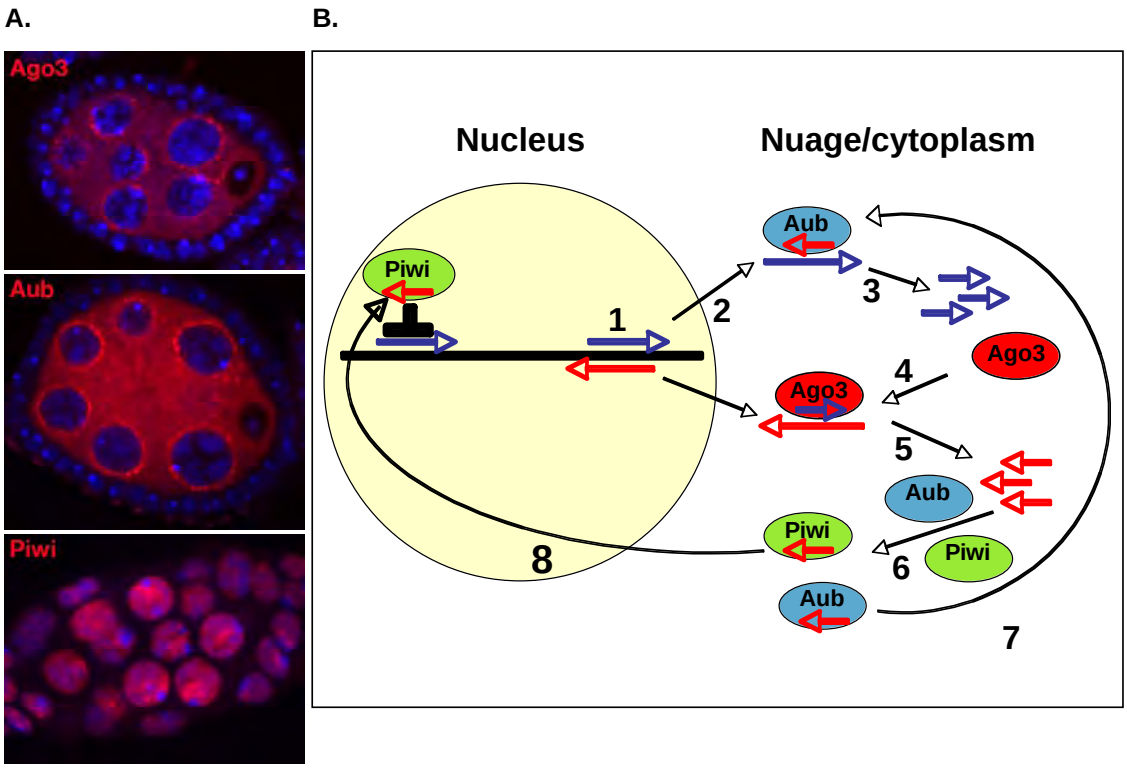
A.
B.
Ago3
Aub
Piwi
Nucleus
Nuage/cytoplasm
Piwi
1
2
Aub
3
Ago3
4
Ago3
5
Aub
Piwi
6
Piwi
Aub
7
8

Figure 2. Compartmentalization of piRNA production and function. (A). Localization of Piwi class Argonautes in the *Drosophila* ovary. Argonautes (red), DNA (Wakabayashi-Ito et al.). Argonaute 3 (Ago3) and Aubergine (Aub) localize to the cytoplasm and nuage, which is a perinuclear structure rich in RNA processing enzymes. Piwi localizes predominantly to germline nuclei. (B). Model for compartmentalized production and function of piRNAs. Sense and antisense strands of piRNA "master control" regions are transcribed (1) and exported from the nucleus (2). In the nuage, Aub-piRNA complexes cleave sense transcripts (3), leading to production of sense strand piRNAs that associate with Ago3 (4). Ago3-piRNA complexes cleave antisense transcripts (5), producing piRNAs that associate with Aub and Piwi (6). Aub complexes remain in the nuage and cleave sense strand complexes (7). Piwi-piRNA complexes are imported into the nucleus where they silence homologous genes in euchromatin and heterochromatin (8).

Stem cell division and axis specification in *Drosophila* females

Mutations in piRNA pathway genes were first identified in *Drosophila* through screens for mutations that disrupt oogenesis and embryonic axis specification (Gillespie and Berg, 1995; Schupbach and Wieschaus, 1991). *Drosophila* oogenesis begins with a germline stem cell division that produces a cystoblast, which divides four times with incomplete cytokinesis to produce 16 interconnected cells that form a single oocyte and 15 nurse cells (for review see (Spradling, 1993). The nurse cells provide most of the RNA and protein components of the oocyte, which remains transcriptionally silent through most of oogenesis. Embryonic axis specification in *Drosophila* depends on the asymmetric localization of a small number of morphogenetic RNAs in the oocyte. These RNAs are transferred from the nurse cells to the oocyte, where localization is driven by interactions with a polarized microtubule cytoskeleton. Microtubule polarization is controlled by a cascade of germline to soma and soma to germline signaling events (reviewed in (Grunert and St Johnston, 1996). Mutations in piRNA pathway genes disrupt both stem cell maintenance and oocyte production, and the localization of morphogenetic RNAs in the oocyte during axis specification (Chen et al., 2007; Cook et al., 2004; Cox et al., 1998; Cox et al., 2000; Gillespie and Berg, 1995; Lin and Spradling, 1997; Pane et al., 2007; Schupbach and Wieschaus, 1991).

The *piwi* gene encodes the founding member of the Piwi class of Argonautes (Cox et al., 1998). Mutations in *piwi* lead to severe defects in oogenesis, including loss of germline stem cells (Figure 3.A) (Cox et al., 1998; Cox et al., 2000; Lin and Spradling, 1997). Clonal studies indicate that stem cell maintenance and division require *piwi* expression in the somatic cells that form the stem cell niche. Loss of *piwi* in the germline,

by contrast, reduces stem cell division rate, but does not lead to loss of stem cells or block oogenesis (Cox et al., 2000). Mutations in other piRNA pathway genes, including *zucchini* and *squash,* also lead to germline stem cell loss (Chen et al., 2007; Pane et al., 2007). It is unclear if these genes are required in the germline, soma, or both. The molecular functions for Piwi and the piRNA pathway in germline stem cell division and maintenance have not been defined.

Mutations in most piRNA genes in *Drosophila*, including *aubergine, spindle-E, armitage, maelstrom, krimper, zucchini* and *squash,* disrupt the localization of dorsal and posterior RNAs (Cook et al., 2004; Gillespie and Berg, 1995; Pane et al., 2007; Schupbach and Wieschaus, 1991). These mutations do not disrupt anterior localization of *bicoid* mRNA or block oocyte development. Therefore, these genes were initially assumed to control the expression of a specific subset of genes that is required for anterior-posterior and dorsal-ventral patterning (Cook et al., 2004). Subsequent studies, however, have demonstrated that the dramatic axis specification defects that are associated with piRNA mutations are a secondary consequence of DNA damage signaling (Chen et al., 2007; Klattenhoff et al., 2007; Pane et al., 2007). These studies suggest that piRNAs have a primary function in maintaining germline DNA integrity.

The link between piRNAs and DNA damage signaling was suggested by studies of *Drosophila* meiotic DNA repair genes. Meiotic recombination requires DNA break formation by the Spo11 nuclease (Cao et al., 1990), and Schupbach and colleagues showed that mutations that disrupt meiotic DNA break repair also disrupt posterior and dorsal-ventral axis specification (Abdu et al., 2002; Ghabrial et al., 1998). Significantly, the *Drosophila* embryonic patterning defects that are linked to repair mutations are

dramatically suppressed by mutations in *mei-41* and *mnk*, which encode the ATR and Chk2 kinases, respectively, that function in DNA damage signaling, and by mutations in *mei-W68* (Abdu et al., 2002; Ghabrial et al., 1998), which encodes the fly Spo11 homologue (McKim and Hayashi-Hagihara, 1998). Unrepaired meiotic breaks thus appear to activate the ATR and Chk2 kinases, which in turn trigger the observed axis specification defects. Recent studies show that the axis specification defects in *armitage, aubergine, cutoff* and *squash* are also suppressed by *mei-41* and/or *mnk* (Chen et al., 2007; Klattenhoff et al., 2007; Pane et al., 2007). Furthermore, *armitage, aubergine* and *spindle-E* mutations lead to a dramatic accumulation of phosphorylated histone H2Av (γ–H2Av) foci in germline nuclei (Figure 3.B); and these foci are generally linked to DNA double strand breaks (Modesti and Kanaar, 2001). Significantly, *mei-W68* (Spo11) does not suppress the patterning defects associated with *armitage,* or the formation of γ–H2Av foci (Klattenhoff et al., 2007). piRNA mutations, like DNA repair mutations, thus disrupt axis specification through activation of the ATR/Chk2 pathway. However, unlike with DNA repair pathway mutations, meiotic breaks are not the source of damage.

All of the *Drosophila* piRNA pathway mutations lead to a significant over-expression of retrotransposons (Aravin et al., 2001; Chen et al., 2007; Kalmykova et al., 2005; Pane et al., 2007; Sarot et al., 2004; Vagin et al., 2006), and *piwi* mutants have been shown to mobilize at least one class of transposon in the male germline (Kalmykova et al., 2005). Retrotransposon mobilization can induce DNA damage (Belgnaoui et al., 2006; Gasior et al., 2006), and high rates of transposon insertion in piRNA mutants could overwhelm the DNA repair machinery, leading to the breaks that activate ATR and Chk2. However, there is no direct evidence for transposon mobilization in the female germline

when piRNA pathway components are disrupted, and this pathway could have a more direct role in DNA repair, or in establishing chromatin structures that resist damage. *Drosophila* telomeres are composed of retrotransposon repeats, and piRNA mutations increase the number of these repeats (Savitsky et al., 2006). These findings suggest that piRNA mutations could lead to a loss of telomere protection, leading to the recognition of chromosome ends as DNA breaks. However, it is currently unclear if the break sites in piRNA pathway mutations are random, linked to transposon insertions, or restricted to specific chromatin domains, and the precise functions of these RNAs in maintaining germline genome integrity remains to be determined.

The Oskar protein is essential to pole plasm assembly and embryonic patterning, and piRNA pathway mutations disrupt *osk* mRNA and protein localization (Cook et al., 2004). Translation of *osk* mRNA is tightly linked to posterior localization, which begins during oogenesis stage 9 (Kim-Ha et al., 1995; Markussen et al., 1995; Rongo et al., 1995). Mutations in a number of piRNA pathway mutations lead to Oskar protein expression during earlier stages of oogenesis, and the *mnk* (Chk2) mutation does not suppress premature *osk* mRNA translation (Cook et al., 2004; Pane et al., 2007). Therefore, premature Osk protein accumulation is not a consequence of DNA damage signaling. Piwi class Argonaute-piRNA complexes, like siRNA or miRNA-Argonaute complexes, can cleave perfectly matched RNA targets *in vitro* (Gunawardane et al., 2007; Lau et al., 2006; Saito et al., 2006). As noted above, miRNA-Argonaute complexes that imperfectly pair with target mRNAs induce translational silencing (Valencia-Sanchez et al., 2006). It is therefore possible that piRNA-Piwi class Argonaute complexes also trigger translational silencing of imperfectly matched targets, including mRNAs from

single copy genes like *oskar*. Consistent with this speculation, a subset of piRNAs associate with polysomes in the mouse (Grivna et al., 2006b).

Fertility and *Stellate* silencing in *Drosophila* males

Most of *Drosophila* piRNA pathway mutations reduce male fertility (Cox et al., 1998; Schmidt et al., 1999; Stapleton et al., 2001; Tomari et al., 2004), and this is linked to the overexpression of Stellate protein. The function of Stellate is not known, but it is encoded by repeated genes on the X chromosome that are suppressed by the Y-linked *Suppressor of Stellate* locus [*Su*(*Ste*)] (Aravin et al., 2001; Livak, 1990). *Su(Ste)* consists of bi-directionally transcribed repeats that are highly homologous to *stellate,* and deletion of the *Su*(*Ste*) locus leads to the massive over-expression of Stellate protein, which assembles into crystals in the testes (Bozzetti et al., 1995; Livak, 1984; Palumbo et al., 1994). 25-27nt piRNAs are produced from the *Su*(*Ste*) locus, and mutations in piRNA pathway genes lead to Stellate crystal formation (Aravin et al., 2001; Pane et al., 2007; Stapleton et al., 2001; Tomari et al., 2004). piRNAs from the *Su(Ste)* locus thus silence expression of *stellate* in trans. It is currently unclear if this reflects transcriptional or post-transcriptional silencing. Stellate over-expression alone could induce sterility, but defects in silencing of other genes could also impact male fertility. piRNA pathway mutations lead to mobilization of at least a subset of transposons in the male germline (Kalmykova et al., 2005), and insertional mutations associated with transposon mobilization could also reduce male fertility.

Male germline development in the mouse

The mouse genome encodes three Piwi homologues, Miwi, Miwi2 and Mili, and all three are expressed at high levels in testes and are required for male fertility (Aravin et al., 2006; Deng and Lin, 2002; Girard et al., 2006; Grivna et al., 2006a; Kuramochi-Miyagawa et al., 2001; Sasaki et al., 2003). Both Mili and Miwi bind piRNAs, and knock out mutations in the *Mili* and *Miwi* genes block piRNA production (Aravin et al., 2006; Girard et al., 2006; Grivna et al., 2006a). Single null mutations in each of the three genes lead to male sterility (Carmell et al., 2007; Deng and Lin, 2002; Kuramochi-Miyagawa et al., 2004). Spermatogenesis in the mouse is a coordinated process that can be divided into three phases; mitosis, meiosis and spermiogenesis (de Rooij and Grootegoed, 1998). In the first phase, stem cells localized in the basal layer of the epithelium divide mitotically to self-renew and generate a population of primary spermatocytes. In the second phase, the primary spermatocytes progress through meiosis to generate haploid round spermatids. During leptotene of meiotic prophase I, duplicated chromosomes condense and begin to pair. Pairing is completed and the synaptonemal complex forms during zygotene, and crossing over occurs in pachytene. The homologs begin to separate in diplotene and finally resolve in diakinesis. During the third phase, round spermatids mature and elongate and are then released into the lumen of the tubule. In *Mili, Miwi and Miwi2* mutants, the testes appear normal until about two weeks post partum, which roughly corresponds with the first round of meiosis. However, post-meiotic cells do not form (Figure 3.C). Mutations in *Mili* and *Miwi2* block progression through pachytene, while *Miwi* mutant spermatocytes develop to the round spermatid stage but do not complete spermiogenesis (Carmell et al., 2007; Deng and Lin, 2002; Kuramochi-Miyagawa et al.,

2004). The timing of developmental arrest correlates with the temporal expression of Mili and Miwi proteins. Mili is first detected in male primordial germ cells and is present throughout pachytene, whereas Miwi is expressed only from mid-pachytene to the round spermatid stage (Deng and Lin, 2002; Kuramochi-Miyagawa et al., 2004). The temporal expression pattern of Miwi2 during spermatogenesis has not been reported.

Mutations in each of the three genes lead to the degeneration of the male germline, while somatic cells appear to remain relatively unaffected (Carmell et al., 2007; Deng and Lin, 2002; Kuramochi-Miyagawa et al., 2004); Figure 3.C). Similar spermatogenesis arrest phenotypes have been observed in mutants that disrupt synapsis or DNA repair (Baarends et al., 2001; Barchi et al., 2005; Xu et al., 2003). Additionally, high levels of γ-H2AX staining, indicative of DNA break formation, have been observed *Miwi2* mutants (Carmell et al., 2007). All of the above suggests that mutations in *piwi* homologues in the mice, like piRNA pathway mutations in *Drosophila*, lead to DNA damage and activation of a DNA damage response, including apoptotic degeneration of germline cells.

In piRNA pathway mutants in flies, germline DNA damage is associated with the massive over-expression of retrotransposon, and most of the piRNAs are linked to retrotransposon and repeated sequences (Brennecke et al., 2007; Klattenhoff et al., 2007; Vagin et al., 2006). These observations suggest that germline DNA damage is caused by transposon mobilization, although this has not been demonstrated (Klattenhoff et al., 2007). By contrast, the piRNAs from adult mouse testes are depleted of repeated and retrotransposon sequences (Aravin et al., 2006; Girard et al., 2006; Grivna et al., 2006a). However, a recent study has identified a pre-pachytene cluster of Mili-interacting piRNAs that include a substantial number of repeat and retrotransposon sequences (Aravin et al.,

2007). Moreover, *Mili* and *Miwi2* mutations in mice lead to the de-repression of retrotransposon transcripts (Aravin et al., 2007; Carmell et al., 2007). The piRNA pathway may therefore have a conserved function in silencing retrotransposons and preventing DNA damage in germline. However, in contrast to flies, the female germline is not affected by single mutations in mouse Piwi class Argonaut genes (Carmell et al., 2007; Deng and Lin, 2002; Kuramochi-Miyagawa et al., 2004). This could indicate that a distinct pathway fulfills this role in the mammalian female germline. However, the Piwi class Argonautes could also act redundantly during oogenesis, and double or triple mutants may therefore reveal a role for piRNAs in the mouse female germline.

Sex determination and germline development in zebrafish

The zebrafish genome encodes two clear Piwi homologues, *ziwi* and *zili*. Ziwi appears to be an ortholog of the mouse Miwi protein, while Zili is more similar to mouse Mili. Only Ziwi, which is expressed specifically in the male and female germline cells, has been characterized (Houwing et al., 2007). Ziwi, like the *Drosophila* Ago-3 and Aub proteins, is primarily cytoplasmic and localizes to perinuclear nuage. Strikingly, null *ziwi* mutations also result in apoptotic loss of germ cells from the testes (Figure 3.D). Reduced levels of *ziwi* function permit the survival of male germ cells to the adult stage, but lead to elevated levels of apoptosis in adult germ cells and to varying levels of infertility. piRNAs isolated from zebrafish testes and ovaries show the same molecular properties as piRNAs from other organisms, and many are derived from repetitive sequences. Mutations in *ziwi* also affect sex determination, and all surviving mutant animals are male (Houwing et al., 2007). As a result, the role of *ziwi* in the female germline could not be

assessed. Other mutations that reduce germ cell number also lead to male development, suggesting that the sex determination phenotype is secondary to the loss of germ cells (Slanchev et al., 2005). However, a more direct role for piRNAs in sex determination cannot be excluded.

Figure 3

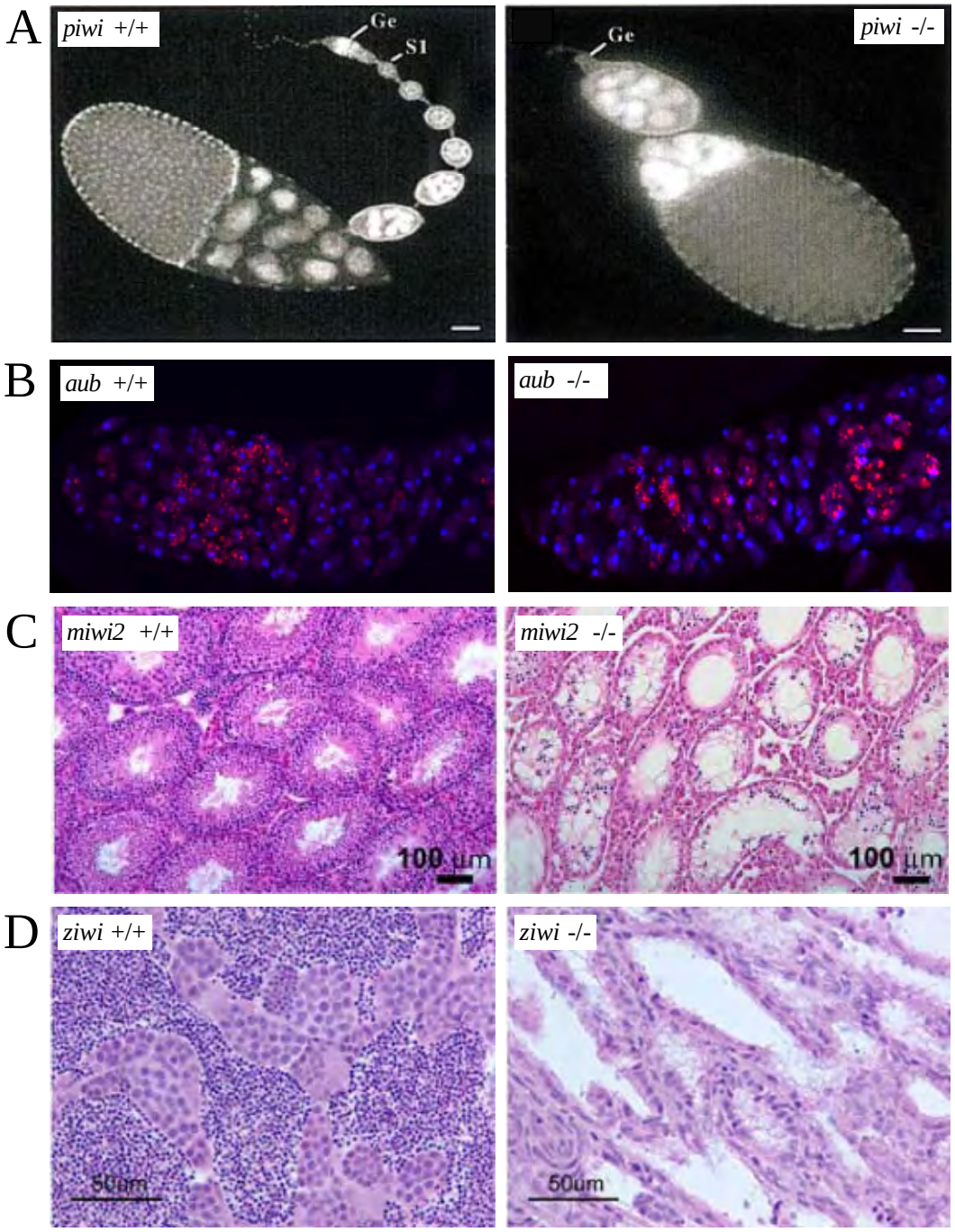
A
piwi +/+
Ge
S1
Ge
piwi -/-
B
aub +/+
aub -/-
C
miwi2 +/+
100 µm
miwi2 -/-
100 µm
D
ziwi +/+
50um
ziwi -/-
50um

Figure 3. The piRNA pathway is required for germline development. (A). *piwi* is required for the self-renewing division of germline stem cells during oogenesis. DAPI images of 0-to-1-day old adult ovarioles from wild-type and *piwi2* mutant flies. Wild-type ovarioles contain a long string of developing egg chambers produced through continuous stem cell divsion (Ge). In contrast, *piwi* mutant ovarioles typically contain only 2 egg chambers, derived though stem cell differntiation and loss (Cox et al., 1998). (B). Increased DNA damage in the germline cells of *aub* mutant ovaries. *Drosophila* ovaries immunostained to reveal phosphorylated form of histone H2Av (g-H2Av) (red) and DNA (Wakabayashi-Ito et al.). γ-H2Av accumulates near double-strand break sites. In wild-type, γ-H2Av foci are restricted to region 2 of the germarium, where meiotic DSBs form. In aub mutant ovaries g-H2Av foci accumulate in cells within the germarium and persist and increase in intensity only in the germline as cysts bud from the germarium to form egg chambers (Klattenhoff et al., 2007). (C). *Miwi2* mutants deplete germ cell lineages in mouse testes. Hematoxylin and eosin staining of wild type and *Miwi2* mutants adult testes shows germline degeneration in *Miwi2* mutant mouse testes (Carmell et al., 2007). (D). Ziwi is necessary for the maintenance of the germline. Hematoxylin and eosin staining of wild-type and *ziwi* testis shows *ziwi* mutants have germ cell-depleted testis (Houwing et al., 2007).

Conclusion and open questions

In flies, fish and mice, piRNA pathway mutations lead to germline-specific defects, and studies in *Drosophila* indicate that some of these defects result from DNA damage signaling. piRNAs may therefore have a conserved function in preserving germline genome integrity. In flies, piRNA mutations lead to the over-expression of retrotransposons, and retrotransposon mobilization could cause the DNA lesions that lead to germline DNA damage. However, piRNA pathway mutations have been linked to the mobilization of a single transposon in the *Drosophila* male germline (Kalmykova et al., 2005), and there is no direct evidence that the breaks that accumulate in piRNA pathway mutations in the female germline are associated with transposition events. piRNAs could therefore directly promote repair, induce the assembly of damage resistant chromosome structures, or suppress the expression of euchromatic genes that induce DNA breaks.

The mechanism of piRNA-based gene silencing also remains to be determined. Mutations in genes involved in the piRNA pathway in *Drosophila* have been reported to disrupt position effect variegation (PEV), a form of transcription silencing caused by heterochromatin spreading from peri-centromeric and telomeric regions (Pal-Bhadra et al., 2002; Pal-Bhadra et al., 2004). piRNAs could therefore silence gene expression by promoting heterochromatin assembly, which could directly suppress transcription. Alternatively, piRNA-Argonaute complexes could associate with heterochromatin and catalyze the co-transcriptional destruction of nascent transcripts. The latter possibility is suggested by studies in fission yeast that indicate that siRNA-containing Argonaute proteins are recruited to heterochromatic regions, where they degrade transcripts as they are produced (Verdel and Moazed, 2005). However, mouse and *Drosophila* Piwi class

Argonautes are also present in the cytoplasm, and piRNA-Piwi class Argonaut complexes could silence gene expression by targeting the destruction of mature mRNA following exit from the nucleus. It is also possible that piRNA-Argonaute function in both the nucleus and the cytoplasm during the development of complex multi-cellular organisms.

The studies presented in this thesis addressed mainly two aspects of Piwi-interacting RNA (piRNA) biology in the *Drosophila* germline.

In Chapter II, we investigated the role of the piRNA pathway in embryonic axis specification. piRNAs mediate silencing of retrotransposons and the *Stellate* locus. Mutations in the *Drosophila* piRNA pathway genes *armitage* and *aubergine* disrupt embryonic axis specification, triggering defects in microtubule polarization and asymmetric localization of mRNA and protein determinants in the developing oocyte. Mutations in the ATR/Chk2 DNA damage signal transduction pathway dramatically suppress these axis specification defects, but do not restore retrotransposon or *Stellate* silencing. Furthermore, piRNA pathway mutations lead to germline-specific accumulation of γ–H2Av foci characteristic of DNA damage. We conclude that piRNA based gene silencing is not required for axis specification, and that the critical developmental function for this pathway is to suppress DNA damage signaling in the germline.

In the studies presented in Chapter III we identified a new member of the piRNA pathway. We show that mutations in *rhino*, which encodes a rapidly evolving Heterochromatin Protein 1 (HP1) chromo box protein, lead to germline specific DNA break accumulation, trigger Chk2 kinase dependent defects in axis specification, and disrupt germline localization of Piwi proteins. Mutations in *rhino* and the piRNA pathway

gene *armitage* disrupt silencing of all major transposon families, but do not alter expression of euchromatic or heterochromatic protein coding genes. Deep sequencing studies show that *rhino* mutations significantly reduce or eliminate anti-sense piRNAs derived from the majority of transposable elements in the *Drosophila* genome, and lead to a dramatic reduction in piRNAs derived from major piRNA production clusters on chromosomes 2R and 4. Rhino protein localizes to distinct nuclear foci, and associates with the chromosome 2R and 4 clusters by chromatin immunoprecipitation. The Rhino HP1 homologue is therefore required for piRNA biogenesis, transposon silencing, and maintenance of germline genome integrity.

References.

Abdu, U., Brodsky, M., and Schupbach, T. (2002). Activation of a meiotic checkpoint during Drosophila oogenesis regulates the translation of Gurken through Chk2/Mnk. Curr Biol *12*, 1645-1651.

Allis, C. D., Underwood, E. M., Caulton, J. H., and Mahowald, A. P. (1979). Pole cells of Drosophila melanogaster in culture. Normal metabolism, ultrastructure, and functional capabilities. Dev Biol *69*, 451-465.

Aravin, A., Gaidatzis, D., Pfeffer, S., Lagos-Quintana, M., Landgraf, P., Iovino, N., Morris, P., Brownstein, M. J., Kuramochi-Miyagawa, S., Nakano, T., *et al.* (2006). A novel class of small RNAs bind to MILI protein in mouse testes. Nature *442*, 203-207.

Aravin, A. A., Klenov, M. S., Vagin, V. V., Bantignies, F., Cavalli, G., and Gvozdev, V. A. (2004). Dissection of a natural RNA silencing process in the Drosophila melanogaster germ line. Mol Cell Biol *24*, 6742-6750.

Aravin, A. A., Lagos-Quintana, M., Yalcin, A., Zavolan, M., Marks, D., Snyder, B., Gaasterland, T., Meyer, J., and Tuschl, T. (2003). The small RNA profile during Drosophila melanogaster development. Dev Cell *5*, 337-350.

Aravin, A. A., Naumova, N. M., Tulin, A. V., Vagin, V. V., Rozovsky, Y. M., and Gvozdev, V. A. (2001). Double-stranded RNA-mediated silencing of genomic tandem repeats and transposable elements in the D. melanogaster germline. Curr Biol *11*, 1017-1027.

Aravin, A. A., Sachidanandam, R., Girard, A., Fejes-Toth, K., and Hannon, G. J. (2007). Developmentally regulated piRNA clusters implicate MILI in transposon control. Science *316*, 744-747.

Ashraf, S. I., McLoon, A. L., Sclarsic, S. M., and Kunes, S. (2006). Synaptic protein synthesis associated with memory is regulated by the RISC pathway in Drosophila. Cell *124*, 191-205.

Baarends, W. M., van der Laan, R., and Grootegoed, J. A. (2001). DNA repair mechanisms and gametogenesis. Reproduction *121*, 31-39.

Barchi, M., Mahadevaiah, S., Di Giacomo, M., Baudat, F., de Rooij, D. G., Burgoyne, P. S., Jasin, M., and Keeney, S. (2005). Surveillance of different recombination defects in mouse spermatocytes yields distinct responses despite elimination at an identical developmental stage. Mol Cell Biol *25*, 7203-7215.

Baulcombe, D. (2004). RNA silencing in plants. Nature *431*, 356-363.

Belgnaoui, S. M., Gosden, R. G., Semmes, O. J., and Haoudi, A. (2006). Human LINE-1 retrotransposon induces DNA damage and apoptosis in cancer cells. Cancer Cell Int *6*, 13.

Bernstein, E., Caudy, A. A., Hammond, S. M., and Hannon, G. J. (2001). Role for a bidentate ribonuclease in the initiation step of RNA interference. Nature *409*, 363-366.

Bozzetti, M. P., Massari, S., Finelli, P., Meggio, F., Pinna, L. A., Boldyreff, B., Issinger, O. G., Palumbo, G., Ciriaco, C., Bonaccorsi, S., and et al. (1995). The Ste locus, a component of the parasitic cry-Ste system of Drosophila melanogaster, encodes a protein that forms crystals in primary spermatocytes and mimics properties of the beta subunit of casein kinase 2. Proc Natl Acad Sci U S A *92*, 6067-6071.

Brennecke, J., Aravin, A. A., Stark, A., Dus, M., Kellis, M., Sachidanandam, R., and Hannon, G. J. (2007). Discrete small RNA-generating loci as master regulators of transposon activity in Drosophila. Cell *128*, 1089-1103.

Cao, L., Alani, E., and Kleckner, N. (1990). A pathway for generation and processing of double-strand breaks during meiotic recombination in S. cerevisiae. Cell *61*, 1089-1101.
Carmell, M. A., Girard, A., van de Kant, H. J., Bourc'his, D., Bestor, T. H., de Rooij, D. G., and Hannon, G. J. (2007). MIWI2 is essential for spermatogenesis and repression of transposons in the mouse male germline. Dev Cell *12*, 503-514.
Chen, Y., Pane, A., and Schupbach, T. (2007). Cutoff and aubergine mutations result in retrotransposon upregulation and checkpoint activation in Drosophila. Curr Biol *17*, 637-642.
Cook, H. A., Koppetsch, B. S., Wu, J., and Theurkauf, W. E. (2004). The Drosophila SDE3 homolog armitage is required for oskar mRNA silencing and embryonic axis specification. Cell *116*, 817-829.
Cox, D. N., Chao, A., Baker, J., Chang, L., Qiao, D., and Lin, H. (1998). A novel class of evolutionarily conserved genes defined by piwi are essential for stem cell self-renewal. Genes Dev *12*, 3715-3727.
Cox, D. N., Chao, A., and Lin, H. (2000). piwi encodes a nucleoplasmic factor whose activity modulates the number and division rate of germline stem cells. Development *127*, 503-514.
de Rooij, D. G., and Grootegoed, J. A. (1998). Spermatogonial stem cells. Curr Opin Cell Biol *10*, 694-701.
Deng, W., and Lin, H. (2002). miwi, a murine homolog of piwi, encodes a cytoplasmic protein essential for spermatogenesis. Dev Cell *2*, 819-830.
Du, T., and Zamore, P. D. (2005). microPrimer: the biogenesis and function of microRNA. Development *132*, 4645-4652.
Findley, S. D., Tamanaha, M., Clegg, N. J., and Ruohola-Baker, H. (2003). Maelstrom, a Drosophila spindle-class gene, encodes a protein that colocalizes with Vasa and RDE1/AGO1 homolog, Aubergine, in nuage. Development *130*, 859-871.
Gasior, S. L., Wakeman, T. P., Xu, B., and Deininger, P. L. (2006). The human LINE-1 retrotransposon creates DNA double-strand breaks. J Mol Biol *357*, 1383-1393.
Ghabrial, A., Ray, R. P., and Schupbach, T. (1998). okra and spindle-B encode components of the RAD52 DNA repair pathway and affect meiosis and patterning in Drosophila oogenesis. Genes Dev *12*, 2711-2723.
Gillespie, D. E., and Berg, C. A. (1995). Homeless is required for RNA localization in Drosophila oogenesis and encodes a new member of the DE-H family of RNA-dependent ATPases. Genes Dev *9*, 2495-2508.
Girard, A., Sachidanandam, R., Hannon, G. J., and Carmell, M. A. (2006). A germline-specific class of small RNAs binds mammalian Piwi proteins. Nature *442*, 199-202.
Grimaud, C., Bantignies, F., Pal-Bhadra, M., Ghana, P., Bhadra, U., and Cavalli, G. (2006). RNAi components are required for nuclear clustering of Polycomb group response elements. Cell *124*, 957-971.
Grivna, S. T., Beyret, E., Wang, Z., and Lin, H. (2006a). A novel class of small RNAs in mouse spermatogenic cells. Genes Dev *20*, 1709-1714.
Grivna, S. T., Pyhtila, B., and Lin, H. (2006b). MIWI associates with translational machinery and PIWI-interacting RNAs (piRNAs) in regulating spermatogenesis. Proc Natl Acad Sci U S A *103*, 13415-13420.
Grunert, S., and St Johnston, D. (1996). RNA localization and the development of asymmetry during Drosophila oogenesis. Curr Opin Genet Dev *6*, 395-402.

Gunawardane, L. S., Saito, K., Nishida, K. M., Miyoshi, K., Kawamura, Y., Nagami, T., Siomi, H., and Siomi, M. C. (2007). A slicer-mediated mechanism for repeat-associated siRNA 5' end formation in Drosophila. Science *315*, 1587-1590.
Hannon, G. J. (2002). RNA interference. Nature *418*, 244-251.
Harris, A. N., and Macdonald, P. M. (2001). Aubergine encodes a Drosophila polar granule component required for pole cell formation and related to eIF2C. Development *128*, 2823-2832.
Horwich, M. D., Li, C., Matranga, C., Vagin, V., Farley, G., Wang, P., and Zamore, P. D. (2007). The Drosophila RNA Methyltransferase, DmHen1, Modifies Germline piRNAs and Single-Stranded siRNAs in RISC. Curr Biol *17*, 1265-1272.
Houwing, S., Kamminga, L. M., Berezikov, E., Cronembold, D., Girard, A., van den Elst, H., Filippov, D. V., Blaser, H., Raz, E., Moens, C. B., *et al.* (2007). A role for Piwi and piRNAs in germ cell maintenance and transposon silencing in Zebrafish. Cell *129*, 69-82.
Kalmykova, A. I., Klenov, M. S., and Gvozdev, V. A. (2005). Argonaute protein PIWI controls mobilization of retrotransposons in the Drosophila male germline. Nucleic Acids Res *33*, 2052-2059.
Kim, M., Krogan, N. J., Vasiljeva, L., Rando, O. J., Nedea, E., Greenblatt, J. F., and Buratowski, S. (2004). The yeast Rat1 exonuclease promotes transcription termination by RNA polymerase II. Nature *432*, 517-522.
Kim-Ha, J., Kerr, K., and Macdonald, P. M. (1995). Translational regulation of oskar mRNA by bruno, an ovarian RNA-binding protein, is essential. Cell *81*, 403-412.
Kirino, Y., and Mourelatos, Z. (2007). Mouse Piwi-interacting RNAs are 2'-O-methylated at their 3' termini. Nat Struct Mol Biol *14*, 347-348.
Klattenhoff, C., Bratu, D. P., McGinnis-Schultz, N., Koppetsch, B. S., Cook, H. A., and Theurkauf, W. E. (2007). Drosophila rasiRNA pathway mutations disrupt embryonic axis specification through activation of an ATR/Chk2 DNA damage response. Dev Cell *12*, 45-55.
Kloosterman, W. P., and Plasterk, R. H. (2006). The diverse functions of microRNAs in animal development and disease. Dev Cell *11*, 441-450.
Kuramochi-Miyagawa, S., Kimura, T., Ijiri, T. W., Isobe, T., Asada, N., Fujita, Y., Ikawa, M., Iwai, N., Okabe, M., Deng, W., *et al.* (2004). Mili, a mammalian member of piwi family gene, is essential for spermatogenesis. Development *131*, 839-849.
Kuramochi-Miyagawa, S., Kimura, T., Yomogida, K., Kuroiwa, A., Tadokoro, Y., Fujita, Y., Sato, M., Matsuda, Y., and Nakano, T. (2001). Two mouse piwi-related genes: miwi and mili. Mech Dev *108*, 121-133.
Lau, N. C., Seto, A. G., Kim, J., Kuramochi-Miyagawa, S., Nakano, T., Bartel, D. P., and Kingston, R. E. (2006). Characterization of the piRNA complex from rat testes. Science *313*, 363-367.
Lee, R. C., Feinbaum, R. L., and Ambros, V. (1993). The C. elegans heterochronic gene lin-4 encodes small RNAs with antisense complementarity to lin-14. Cell *75*, 843-854.
Lim, A. K., and Kai, T. (2007). Unique germ-line organelle, nuage, functions to repress selfish genetic elements in Drosophila melanogaster. Proc Natl Acad Sci U S A *104*, 6714-6719.
Lin, H., and Spradling, A. C. (1997). A novel group of pumilio mutations affects the asymmetric division of germline stem cells in the Drosophila ovary. Development *124*, 2463-2476.

Livak, K. J. (1984). Organization and mapping of a sequence on the Drosophila melanogaster X and Y chromosomes that is transcribed during spermatogenesis. Genetics *107*, 611-634.
Livak, K. J. (1990). Detailed structure of the Drosophila melanogaster stellate genes and their transcripts. Genetics *124*, 303-316.
Mahowald, A. P. (1971). Polar granules of Drosophila. 3. The continuity of polar granules during the life cycle of Drosophila. J Exp Zool *176*, 329-343.
Markussen, F. H., Michon, A. M., Breitwieser, W., and Ephrussi, A. (1995). Translational control of oskar generates short OSK, the isoform that induces pole plasma assembly. Development *121*, 3723-3732.
McKim, K. S., and Hayashi-Hagihara, A. (1998). mei-W68 in Drosophila melanogaster encodes a Spo11 homolog: evidence that the mechanism for initiating meiotic recombination is conserved. Genes Dev *12*, 2932-2942.
Meister, G., and Tuschl, T. (2004). Mechanisms of gene silencing by double-stranded RNA. Nature *431*, 343-349.
Mello, C. C., and Conte, D., Jr. (2004). Revealing the world of RNA interference. Nature *431*, 338-342.
Modesti, M., and Kanaar, R. (2001). DNA repair: spot(light)s on chromatin. Curr Biol *11*, R229-232.
Ohara, T., Sakaguchi, Y., Suzuki, T., Ueda, H., Miyauchi, K., and Suzuki, T. (2007). The 3' termini of mouse Piwi-interacting RNAs are 2'-O-methylated. Nat Struct Mol Biol *14*, 349-350.
Pal-Bhadra, M., Bhadra, U., and Birchler, J. A. (2002). RNAi related mechanisms affect both transcriptional and posttranscriptional transgene silencing in Drosophila. Mol Cell *9*, 315-327.
Pal-Bhadra, M., Leibovitch, B. A., Gandhi, S. G., Rao, M., Bhadra, U., Birchler, J. A., and Elgin, S. C. (2004). Heterochromatic silencing and HP1 localization in Drosophila are dependent on the RNAi machinery. Science *303*, 669-672.
Palumbo, G., Berloco, M., Fanti, L., Bozzetti, M. P., Massari, S., Caizzi, R., Caggese, C., Spinelli, L., and Pimpinelli, S. (1994). Interaction systems between heterochromatin and euchromatin in Drosophila melanogaster. Genetica *94*, 267-274.
Pane, A., Wehr, K., and Schupbach, T. (2007). zucchini and squash encode two putative nucleases required for rasiRNA production in the Drosophila germline. Dev Cell *12*, 851-862.
Rongo, C., Gavis, E. R., and Lehmann, R. (1995). Localization of oskar RNA regulates oskar translation and requires Oskar protein. Development *121*, 2737-2746.
Saito, K., Nishida, K. M., Mori, T., Kawamura, Y., Miyoshi, K., Nagami, T., Siomi, H., and Siomi, M. C. (2006). Specific association of Piwi with rasiRNAs derived from retrotransposon and heterochromatic regions in the Drosophila genome. Genes Dev *20*, 2214-2222.
Saito, K., Sakaguchi, Y., Suzuki, T., Suzuki, T., Siomi, H., and Siomi, M. C. (2007). Pimet, the Drosophila homolog of HEN1, mediates 2'-O-methylation of Piwi- interacting RNAs at their 3' ends. Genes Dev *21*, 1603-1608.
Sarot, E., Payen-Groschene, G., Bucheton, A., and Pelisson, A. (2004). Evidence for a piwi-dependent RNA silencing of the gypsy endogenous retrovirus by the Drosophila melanogaster flamenco gene. Genetics *166*, 1313-1321.

Sasaki, T., Shiohama, A., Minoshima, S., and Shimizu, N. (2003). Identification of eight members of the Argonaute family in the human genome small star, filled. Genomics *82*, 323-330.
Savitsky, M., Kwon, D., Georgiev, P., Kalmykova, A., and Gvozdev, V. (2006). Telomere elongation is under the control of the RNAi-based mechanism in the Drosophila germline. Genes Dev *20*, 345-354.
Schmidt, A., Palumbo, G., Bozzetti, M. P., Tritto, P., Pimpinelli, S., and Schafer, U. (1999). Genetic and molecular characterization of sting, a gene involved in crystal formation and meiotic drive in the male germ line of Drosophila melanogaster. Genetics *151*, 749-760.
Schupbach, T., and Wieschaus, E. (1991). Female sterile mutations on the second chromosome of Drosophila melanogaster. II. Mutations blocking oogenesis or altering egg morphology. Genetics *129*, 1119-1136.
Slanchev, K., Stebler, J., de la Cueva-Mendez, G., and Raz, E. (2005). Development without germ cells: the role of the germ line in zebrafish sex differentiation. Proc Natl Acad Sci U S A *102*, 4074-4079.
Spradling, A. C. (1993). Developmental Genetics of Oogenesis, In The Development of *Drosophila Melanogaster*, M. Bate, and A. M. Arias, eds., pp. 1-70.
Stapleton, W., Das, S., and McKee, B. D. (2001). A role of the Drosophila homeless gene in repression of Stellate in male meiosis. Chromosoma *110*, 228-240.
Tomari, Y., Du, T., Haley, B., Schwarz, D., Bennett, R., Cook, H., Koppetsch, B., Theurkauf, W., and Zamore, P. D. (2004). RISC Assembly Defects in the Drosophila RNAi Mutant armitage. Cell *116*, 831-841.
Vagin, V. V., Sigova, A., Li, C., Seitz, H., Gvozdev, V., and Zamore, P. D. (2006). A distinct small RNA pathway silences selfish genetic elements in the germline. Science *313*, 320-324.
Valencia-Sanchez, M. A., Liu, J., Hannon, G. J., and Parker, R. (2006). Control of translation and mRNA degradation by miRNAs and siRNAs. Genes Dev *20*, 515-524.
Verdel, A., and Moazed, D. (2005). RNAi-directed assembly of heterochromatin in fission yeast. FEBS Lett *579*, 5872-5878.
Wakabayashi-Ito, N., Belvin, M. P., Bluestein, D. A., and Anderson, K. V. (2001). fusilli, an essential gene with a maternal role in Drosophila embryonic dorsal-ventral patterning. Dev Biol *229*, 44-54.
Wang, X. H., Aliyari, R., Li, W. X., Li, H. W., Kim, K., Carthew, R., Atkinson, P., and Ding, S. W. (2006). RNA interference directs innate immunity against viruses in adult Drosophila. Science *312*, 452-454.
Xu, X., Aprelikova, O., Moens, P., Deng, C. X., and Furth, P. A. (2003). Impaired meiotic DNA-damage repair and lack of crossing-over during spermatogenesis in BRCA1 full-length isoform deficient mice. Development *130*, 2001-2012.
Xue, Y., Bai, X., Lee, I., Kallstrom, G., Ho, J., Brown, J., Stevens, A., and Johnson, A. W. (2000). Saccharomyces cerevisiae RAI1 (YGL246c) is homologous to human DOM3Z and encodes a protein that binds the nuclear exoribonuclease Rat1p. Mol Cell Biol *20*, 4006-4015.

CHAPTER II

Drosophila rasiRNA pathway mutations disrupt embryonic axis specification through activation of an ATR/Chk2 DNA damage response

Abstract:

Small repeat associated siRNAs (rasiRNAs) mediate silencing of retrotransposons and the *Stellate* locus. Mutations in the *Drosophila* rasiRNA pathway genes *armitage* and *aubergine* disrupt embryonic axis specification, triggering defects in microtubule polarization and asymmetric localization of mRNA and protein determinants in the developing oocyte. Mutations in the ATR/Chk2 DNA damage signal transduction pathway dramatically suppress these axis specification defects, but do not restore retrotransposon or *Stellate* silencing. Furthermore, rasiRNA pathway mutations lead to germline-specific accumulation of γ–H2Av foci characteristic of DNA damage. We conclude that rasiRNA based gene silencing is not required for axis specification, and that the critical developmental function for this pathway is to suppress DNA damage signaling in the germline.

Introduction

RNA interference (Simeone et al.) and related processes utilize short RNAs to direct protein complexes to chromatin and RNA, triggering heterochromatin formation, transcriptional silencing, translational repression, or RNA destruction (Hannon, 2002; Hutvagner and Zamore, 2002; Wassenegger, 2005). Mutations that disrupt small RNA functions affect a remarkable range of processes, including early embryogenesis in mice (Bernstein et al., 2003), embryonic morphogenesis in zebrafish (Giraldez et al., 2005), chromosome segregation in cultured chicken cells (Fukagawa et al., 2004) and yeast (Provost et al., 2002; Volpe et al., 2003), and developmental timing in worms (Grishok et al., 2001). In *Drosophila,* RNAi related functions are required for stem cell division, stem cell maintenance and viral immunity (Forstemann et al., 2005; Hatfield et al., 2005) (Galiana-Arnoux et al., 2006; Wang et al., 2006). However, the full scope of biological functions controlled by small RNAs is only beginning to emerge, and the targets for most small RNAs have not been identified.

Mutations in the *Drosophila armitage* (Jaronczyk et al.), *spindle-E* (*spn-E*), and *aubergine* (*aub*) genes disrupt siRNA-guided RNA cleavage and assembly of the RNA induced silencing complex (RISC) in ovary extracts and production of 24 to 30 nt repeat associated siRNAs (rasiRNAs), which are linked to retrotransposon and *Stellate* locus silencing (Aravin et al., 2004; Tomari et al., 2004a; Vagin et al., 2006). Strong loss of function mutations in these genes disrupt embryonic axis specification, triggering defects in microtubule organization and microtubule-dependent localization of mRNA and protein determinants in the developing oocyte (Cook et al., 2004). By contrast, mutations in *argonaute-2* (*ago-2*) and *dicer-2* (*dcr-2*) that disrupt the siRNA pathway, but do not block

rasiRNA production, are viable and fertile (Deshpande et al., 2005; Lee et al., 2004; Okamura et al., 2004; Tomari et al., 2004b; Vagin et al., 2006). The rasiRNA pathway thus appears to have an essential function in embryonic axis specification; however, the critical developmental targets for this pathway have not been defined.

Mutations in the *armi*, *aub*, and *spn-E* genes lead to premature expression of Oskar (Drees et al.) protein during early oogenesis (Cook et al., 2004), suggesting that over-expression of axis specification genes could lead to the patterning defects associated with rasiRNA pathway defects. However, here we show that the axis specification defects associated with *armi* and *aub* are dramatically suppressed by null mutations in *mei-41* and *mnk*, which encode ATR and Chk2 kinases that function in DNA double strand break signaling. We also show that rasiRNA pathway mutations lead to germline specific accumulation of γ–H2Av foci characteristic of DNA double strand breaks (DSBs). Significantly, the ATR/Chk2 mutations do not suppress the defects in retrotransposon and *Stellate* silencing. We therefore conclude that rasiRNA based gene silencing is not required for axis specification, and that the critical developmental function for the *Drosophila* rasiRNA pathway is to suppress DNA damage signaling in the germline.

Results

ATR and Chk2 mutations suppress *armi* and *aub* axis specification defects

The *armi, spn-E* and *aub* genes are required for production of rasiRNAs, and mutations in these genes lead to Stellate over-expression during spermatogenesis and premature Osk protein expression during oogenesis (Aravin et al., 2001; Cook et al., 2004; Vagin et al., 2006). These mutations also lead to female sterility and disrupt embryonic axis specification, suggesting that rasiRNAs control expression of genes involved in patterning the oocyte (Cook et al., 2004). However, mutations in the meiotic DSB repair pathway also lead to axis specification defects, and these defects result from activation of a damage signaling pathway that includes the ATR and Chk2 kinases (Bartek et al., 2001) (Abdu et al., 2002; Ghabrial and Schupbach, 1999). These findings raised the alternative possibility that rasiRNA pathway mutations disrupt axis specification by activating ATR and Chk2.

To genetically test the role of DNA damage signaling in the rasiRNA pathway mutant phenotype, we analyzed double mutant combinations with *mei-41* or *mnk*, which encode the *Drosophila* ATR and Chk2 homologues. We were unable to recover *mnk; spn-E* double mutants, and it is unclear if this reflects a significant negative genetic interaction between these genes or the presence of background mutations on the *mnk* or *spn-E* chromosome. Our analyses thus focused on *armi* and *aub,* which we were able to combine with both *mei-41* and *mnk.* If *armi* and *aub* mutations block axis specification through ATR/Chk2 activation, the patterning defects associated with these mutations will be suppressed in the double mutants. Initial suppression analysis focused on the dorsal appendages, which are easily scored eggshell structures that are induced through Gurken

(Grk) signaling from the oocyte to the somatic follicle cells during mid-oogenesis (Schupbach, 1987). Appendages do not form in the absence of Grk, a single appendage forms with low Grk levels, and two appendages form when signaling is normal (Gonzalez-Reyes et al., 1995; Roth et al., 1995). As shown in Table 1, *mei41* and *mnk* dramatically suppress the appendage defects associated with *armi* and *aub.* Two appendages are present on 100% of the embryos derived from wild type and *mei-41* females, and on 94% of the embryos derived from *mnk* single mutants (Table 1). By contrast, only 3.5% of the embryos derived from $armi^{72.1}/armi^{1}$ mutant females have 2 dorsal appendages. Strikingly, 92% of the embryos derived from *mnk;* $armi^{72.1}/armi^{1}$ double mutants show wild type appendage morphology. Similarly, 2 appendages are present on 48% of embryos derived from *aub* single mutants, and 98% of the embryos from *mnk, aub* double mutants have 2 appendages.

Mutations in *mei-41* also suppressed the eggshell patterning defects associated with *armi* and *aub*, although suppression by *mei-41* was consistently less dramatic than suppression by *mnk.* 56 % of the embryos from *mei-41;* $armi^{72.1}/armi^{1}$ double mutants show normal appendages. The *mei-41* mutation was also less effective than *mnk* in suppressing appendage defects associated with homozygous $armi^{1}$ (data not shown) and *aub* (Table 1). Therefore, partial suppression of the patterning defects by *mei-41* is not allele or gene specific. Chk2 can be activated by both ATR and ATM kinases (Bartek et al., 2001; Bartek and Lukas, 2003; Hirao et al., 2002), and the lower level of suppression by *mei-41*/ATR relative to *mnk*/Chk2 may therefore reflect redundant Chk2 activation by the *Drosophila* ATM homologue. However, null alleles of the *Drosophila atm* gene are lethal (Oikemus et al., 2004), making direct tests of this hypothesis difficult. Nonetheless,

these initial observations indicated that the axis specification defects associated with rasiRNA pathway mutations result from activation of an ATR/Chk2 kinase DNA damage signal.

The axis specification defects associated with repair mutations are suppressed by mutations in *mei-W68,* which encodes the *Drosophila* homologue of the Spo11 nuclease that catalyzes meiotic double strand break formation (McKim and Hayashi-Hagihara, 1998). By contrast, *mei-W68* has no effect on the dorsal appendage defects associated with *armi* (Table 1). Meiotic breaks thus do not appear to be the source of damage in *armi* mutations.

Table 1

Maternal Genotype	Dorsal Appendage Phenotype (%)			Hatch Rate (%)	N
	2 (wild type)	1 (fused)	0 (absent)		
mnk^{P6} / mnk^{P6}	94.1	2.3	3.6	73.9	827
mei41^{D3} / mei41^{D3}	100	0	0	0	920
meiW68^{1} / meiW68^{K05603}	94.3	4	1.7	67.2	1281
armi$^{72.1}$ / armi^{1}	3.5	67.6	28.9	0	765
mnk^{P6} / mnk^{P6} ; armi$^{72.1}$ / armi^{1}	91.9	2.5	5.6	0	1062
mei41^{D3} / mei41^{D3} ; armi$^{72.1}$ / armi^{1}	56	38.4	5.6	0	575
meiW68^{1} / meiW68^{K05603} ; armi$^{72.1}$ / armi^{1}	3.6	37.9	58.5	0	280
aub^{HN2} / aub^{QC42}	47.7	40.3	12	0	1212
mnk^{P6}, aub^{HN2} / mnk^{P6}, aub^{QC42}	97.6	2	0.4	0	296
mei41^{D3} / mei41^{D3} ; aub^{HN2}/ aub^{QC42}	85.2	8.6	6.2	0	859
spn-E^{1} / spn-E^{1}	16.6	55.4	27.9	0	123

mei41^{D3} / mei41^{D3} ; spn-E^{1} / spn-E^{1}	23.9	56.2	19.9	0	233
spn-D^{2} / spn-D^{2}	34.8	54	11.2	17.3	1245
mnk^{P6} / mnk^{P6} ; spn-D^{2} / spn-D^{2}	98.8	0.5	0.7	45.9	812

Table 1. *mnk* and *mei-41* mutations suppress D-V patterning defects in rasiRNA mutants.

Localization of axis specification determinants

During early oogenesis, the TGFα homologue Grk localizes to the posterior of the oocyte and signals to the overlying follicle cells, inducing posterior differentiation. During mid-oogenesis, Grk signals from the oocyte to the dorsal follicle cells to generate the dorsal-ventral axis (Gonzalez-Reyes et al., 1995; Roth et al., 1995). Mutations in *armi* and *aub* disrupt Grk protein localization at both stages, leading to posterior and dorsal-ventral axis specification defects (Cook et al., 2004). To determine if the DNA damage signaling mutations suppress the Grk localization defects in *armi* and *aub* mutants, we analyzed the distribution of this protein by indirect immunofluorescence and laser scanning confocal microscopy (Figure 1). For these studies, Grk protein levels within cross sections of stage 6 oocytes were measured and an average fluorescence intensity profile for each genotype was generated (Figure 1B, inset). In wild type stage 6 oocytes, Grk protein accumulates near the posterior cortex (Figure 1A, a). In *armi* and *aub* single mutants, by contrast, low levels of Grk protein are uniformly distributed in the oocyte and nurse cells (Figure 1A, c and e). However, Grk shows almost wild type accumulation near the posterior cortex of *mnk*; *armi* and *mnk*, *aub* double mutants oocytes (Figure 1A, d and f). The defects in dorsal-anterior localization of Grk during mid-oogenesis (Figure 1A, c' and e') are also restored in the *mnk* double mutants (Figure 1A, d' and f'). Weaker suppression is observed with *mei-41*, consistent with our analysis of the dorsal appendages (Figure 2).

To determine if *mnk* and *mei-41* suppress the *armi* and *aub* induced defects in posterior morphogen localization (Cook et al., 2004), we analyzed the distribution of the pole plasm proteins Vasa (Vas) and Osk during mid oogenesis. Osk localizes to the

posterior in only 10% of stage 9 and 10 oocytes from *armi* females (2 of 23), with no detectable localization in the remaining egg chambers (Figure 3c). By contrast, Osk shows wild type posterior accumulation in over 80% of stage 9 and 10 *mnk*;*armi* double mutants (27 of 33; Figure 3d). Vas localization to the posterior pole is similarly restored in the double mutants (not shown). *mei-41* leads to a less dramatic suppression of the posterior patterning defects (not shown). Osk and Vas localization are also disrupted in *aub* mutants (Figure 3e and data not shown), and localization is restored in double mutants with *mnk* and *mei-41* (Figure 3f). The defects in posterior and dorsal-ventral morphogen localization associated with both *armi* and *aub* thus require ATR and Chk2, which function in DNA damage signal transduction.

Figure 1.

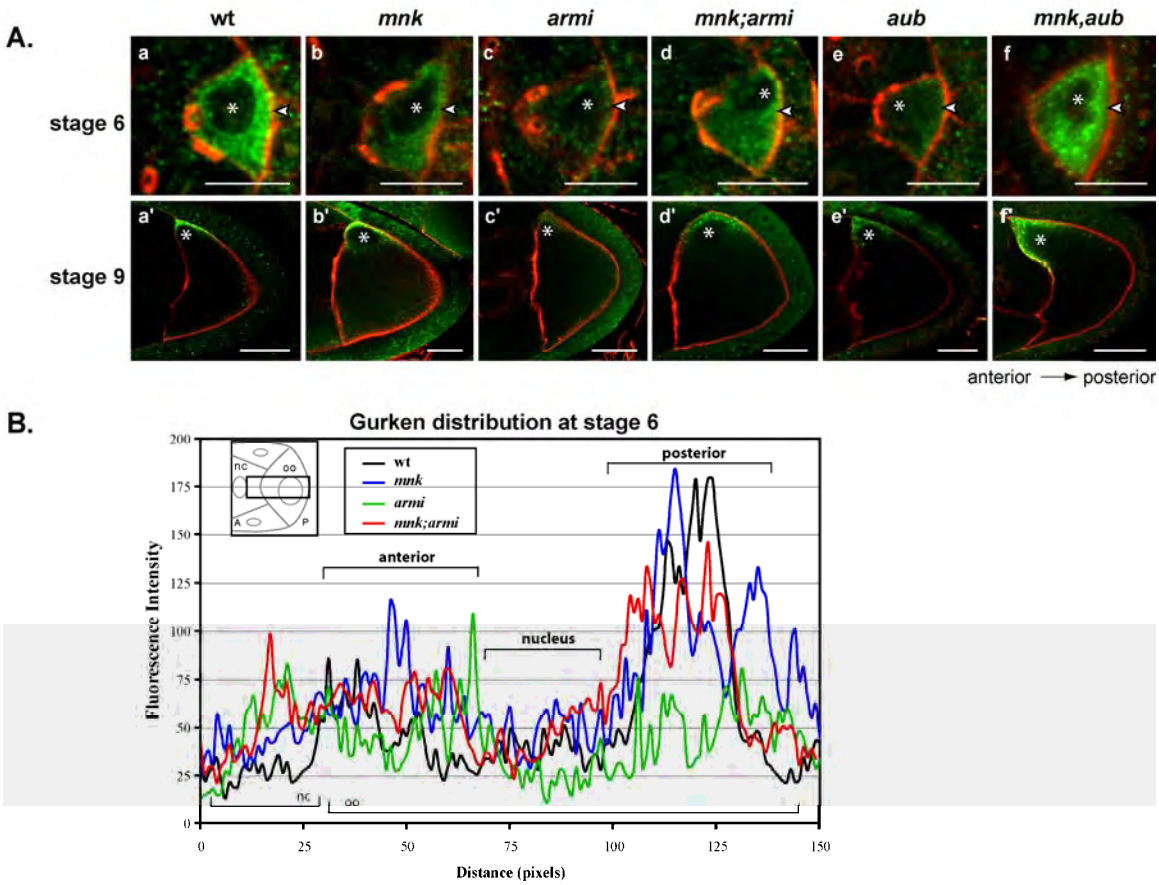
A.
wt
mnk
armi
mnk;armi
aub
mnk,aub
stage 6
stage 9
anterior → posterior
B.
Gurken distribution at stage 6
wt
mnk
armi
mnk;armi
posterior
anterior
nucleus
nc
oo
Fluorescence Intensity
Distance (pixels)

Figure 1. *mnk* suppresses Gurken protein localization defects in rasiRNA mutants.

A. (a) In wild type stage 6 egg chambers, Gurken (Grk) protein (green) accumulates at the posterior cortex (arrowhead). (a') By stage 9, Grk is localized at the dorsal anterior cortex. Actin filaments (red) mark the cell boundaries. (b-b') In mnk^{p6} oocytes, Grk localization is the same as in wild type. (c-c') In $armi^{72.1}/armi^{1}$ egg chambers, only low levels of Grk are present, and the protein is dispersed throughout the oocyte-nurse cell complex. (d-d') Posterior and dorsal accumulation of Grk is restored in mnk^{p6}/ mnk^{p6} ;$armi^{72.1}/armi^{1}$ double mutants. (e) In aub^{QC42}/aub^{HN2} stage 6 egg chambers, Grk localization is similar to that of $armi^{72.1}/armi^{1}$ oocytes. (e') At stage 9, Grk is localized correctly in aub^{QC42}/aub^{HN2}, but not at wild type levels. (f-f') In mnk^{p6}, aub^{QC42}/ mnk^{p6}, aub^{HN2} egg chambers Grk localization level is restored. Images were acquired under identical conditions for either stage. Projections of 3 serial 0.6 μm optical sections are shown The oocyte nucleus is indicated (asterisk). Scale bars are 10 μm and 25 μm for stage 6 and 9 egg chambers, respectively.

B. Quantification of Gurken localization in stage 6 oocytes. The average fluorescence intensity along a line beginning in the nurse cell cytoplasm and extending through a cross section of the oocyte is shown (inset, see Experimental Procedures).

Figure 2.

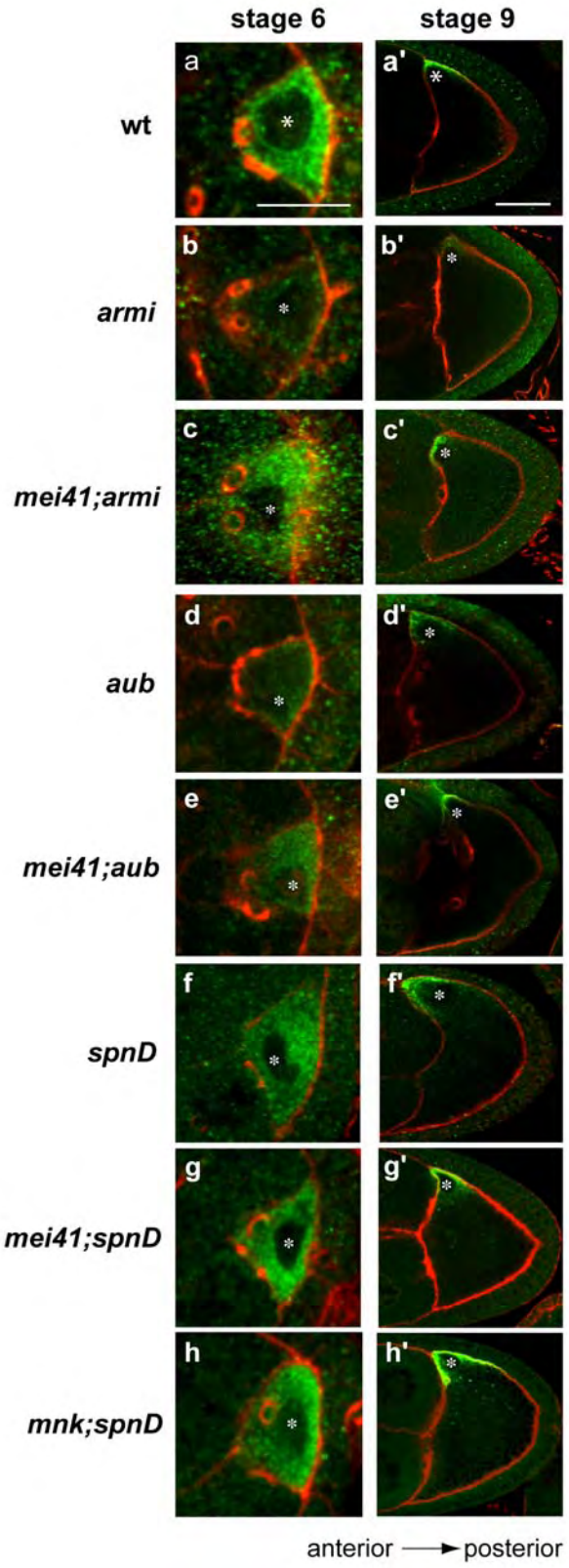
stage 6
stage 9
wt
armi
mei41;armi
aub
mei41;aub
spnD
mei41;spnD
mnk;spnD
a
a'
b
b'
c
c'
d
d'
e
e'
f
f'
g
g'
h
h'
anterior → posterior

Figure 2. Suppression of Gurken protein localization defects by *mei-41* and *mnk* mutants. (a) In wild type stage 6 egg chambers, Gurken (Grk) protein (green) is tightly localized at the posterior cortex near the oocyte nucleus. (a') By stage 9, Grk is localized at the dorsal anterior cortex near the oocyte nucleus. Actin filaments (red) mark the cell boundaries. (b-b') In $armi^{72.1}/armi^{1}$ egg chambers, this localization pattern is lost both at stage 6 and 9, with Grk dispersed throughout the oocyte. (c-c') $mei\text{-}41^{D3}$ partially suppresses the $armi^{72.1}/armi^{1}$ phenotype, and increases Grk localization during early and late oogenesis. (d) In $aub^{QC42}/\ aub^{HN2}$ stage 6 egg chambers, Grk localization is similar to that of $armi^{72.1}/armi^{1}$ oocytes. (d') At stage 9, Grk is localized correctly in $aub^{QC42}/\ aub^{HN2}$, but not at wild type levels. (e-e') In *mei-41D3;* $aub^{QC42}/\ aub^{HN2}$ egg chambers Grk localization level is partially restored. (f-f') In the weak allele $spn\text{-}D^{2}$ Grk is localized properly, but not at wild type levels. (g-g') In $mei\text{-}41^{D3}$; $spn\text{-}D^{2}$ double mutants Grk localization is similar to wild type. (h-h') mnk^{p6} mutation restores Grk localization to wild type levels in $spn\text{-}D^{2}$ mutants. Images were acquired under identical conditions. Projections of 3 serial 0,6 μm optical sections are shown. The oocyte nucleus is marked by an asterisk in all panels. Posterior is oriented to the right. Scale bars are 10 μm and 25 μm for stage 6 and stage 9 egg chambers, respectively.

Figure 3.

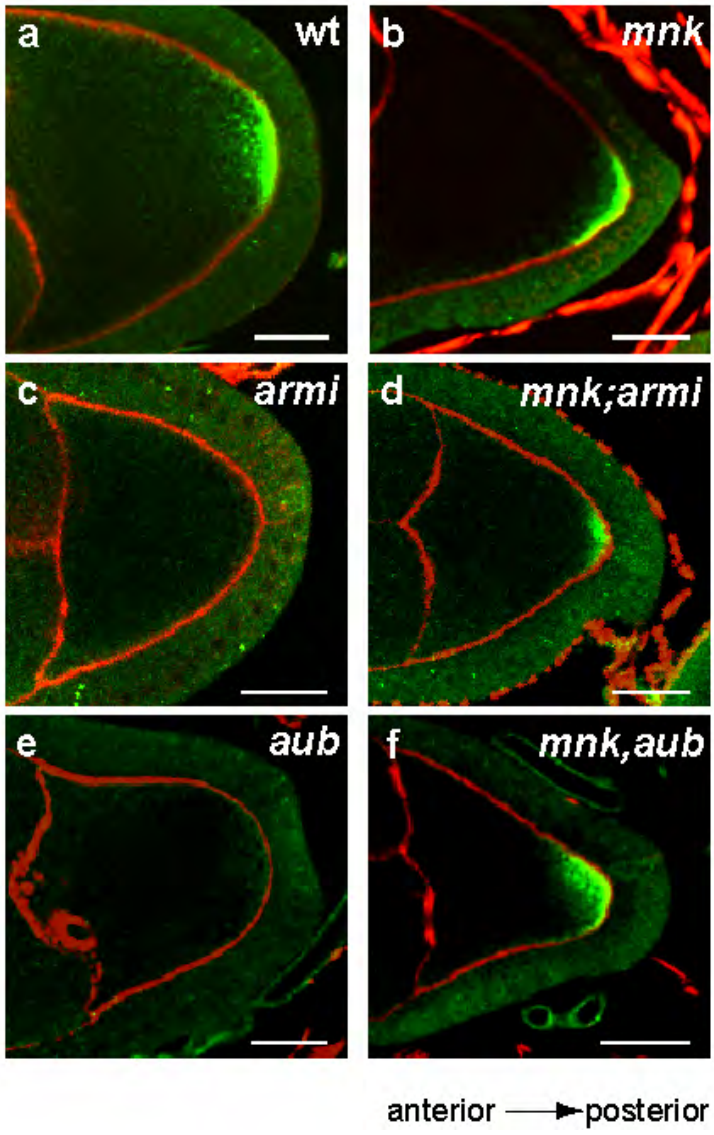

Figure 3. Oskar protein localization defects associated with rasiRNA mutations are suppressed by *mnk*. Egg chambers were fixed and labeled against Oskar (Drees et al.) protein (green) and Actin (red). In stage 9-10 wild type (a) and mnk^{p6} mutant (b) oocytes, Osk localizes tightly to the posterior cortex. In similarly staged $armi^{72.1}/armi^{1}$ (c) and aub^{QC42}/aub^{HN2} (e) oocytes, Osk fails to localize to the posterior pole. Osk localization is restored in double mutants for mnk^{p6} and $armi^{72.1}/armi^{1}$ (d) or aub^{QC42}/aub^{HN2}(f). Egg chambers are oriented with posterior to the right. Images were acquired under identical conditions. Single optical section are shown. Scale bar is 20 μm.

Microtubule organization and Vas phosphorylation

Specification of the posterior pole is initiated during early oogenesis, when the microtubule cytoskeleton reorganizes to form a polarized scaffold in the oocyte-nurse cell complex. While these complexes are in the germarium, a prominent microtubule organizing center (MTOC) forms at the anterior pole of the oocyte, and this MTOC appears to be required for oocyte differentiation (Figure 4A, a) (Theurkauf et al., 1993). After cysts bud from the germarium, a posterior MTOC is established (Figure 4A, a'). This asymmetric microtubule array directs Grk to the posterior pole of the oocyte, which signals to the overlying somatic follicle cells to induce posterior differentiation (Gonzalez-Reyes et al., 1995; Roth et al., 1995). In *armi* mutants, both the early anterior and later posterior MTOCs are much less prominent than in wild type (Cook et al., 2004) (Figure 4A, b and b', and Figure 5). By contrast, egg chambers double mutant for *armi* and *mnk* show near wild type anterior and posterior MTOCs (Figure 4A, c and c'). Restoration of normal microtubule organization correlates with suppression of the Grk localization defects (Figure 1A, d). Egg chambers double mutant for *armi* and *mei-41* show a phenotype intermediate between the *armi* mutants and wild type controls, consistent with partial suppression of posterior patterning defects later in oogenesis (Figure 5). The microtubule organization defects in *aub* are also strongly suppressed by *mnk*, and more weakly suppressed by *mei-41* (Figure 5). Mutations in *armi* and *aub* thus trigger Chk2 dependent defects in microtubule organization. These cytoskeletal defects are likely to contribute to the loss of axial patterning later in oogenesis.

The axis specification defects associated with mutations that disrupt meiotic DSB repair are also suppressed by *mnk.* To determine if Chk2-dependent disruption of the

oocyte cytoskeleton contributes to these defects, we analyzed microtubule organization in ovaries mutant for *spn-D*, which encodes a rad51C homologue required for DSB repair (Abdu et al., 2003). Mutations in *spn-D*, like mutations in *armi* and *aub*, disrupt both the prominent MTOC at the anterior of stage 1 egg chambers and the posterior MTOC during stages 2 through 6 (Figure 4A, d and d'). These defects are suppressed in *mnk; spn-D* double mutants (Figure 4A, e and e'), suggesting that DSB repair mutations and rasiRNA mutations trigger a common Chk2-dependent pathway that disrupts microtubule organization.

DSB repair mutations induce Chk2 dependent phosphorylation of Vas, a conserved RNA helicase required for posterior and dorsal-ventral patterning (Ghabrial and Schupbach, 1999; Styhler et al., 1998). To determine if rasiRNA mutations also trigger Chk2-dependent Vas phosphorylation, we probed western blots of *armi* and *mnk; armi* double mutants for Vas protein. Vas protein levels are also somewhat lower in the *armi* mutant egg chambers, but this may reflect differences in egg chamber stage distribution in the isolated ovaries (Figure 4B). More significantly, a lower electrophoretic mobility species is observed in ovaries homozygous for a strong loss of function allele, $armi^{72.1}$, and both species are observed with a weaker allelic combination $armi^{72.1}/armi^{1}$. Only the faster migrating species is present in *mnk;* $armi^{72.1}/armi^{1}$ double mutant extracts. Following phosphatase treatment, the lower mobility species present in *armi* mutant extracts disappears and the faster migrating species increases in intensity (not shown), indicating that the lower mobility band is a phosphorylated form of Vas. Mutations in *armi,* like meiotic DSB repair mutations, thus trigger Chk2-dependent phosphorylation of Vas. While the physiological significance of Vas phosphorylation has not been

established, these finding support the hypothesis that *armi* mutations lead to Chk2 kinase activation.

Figure 4.

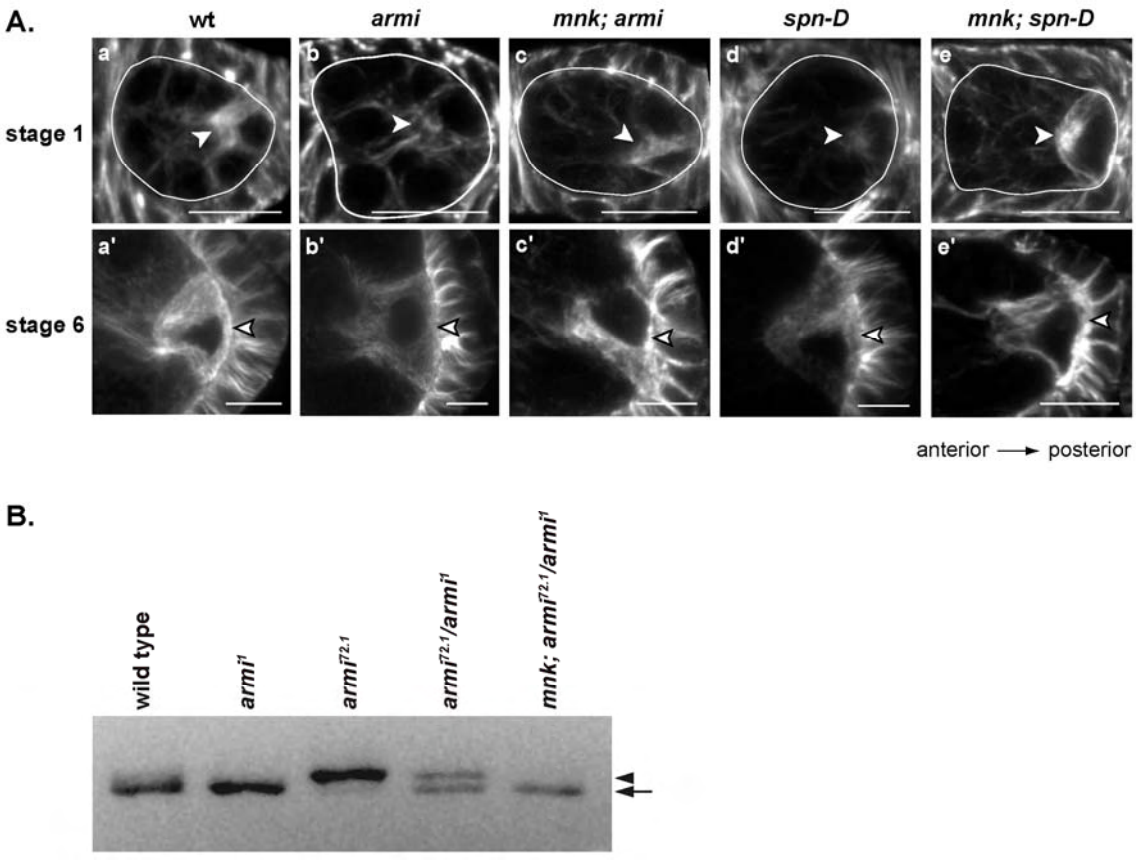
A.
wt
armi
mnk; armi
spn-D
mnk; spn-D
stage 1
stage 6
a
b
c
d
e
a'
b'
c'
d'
e'
anterior → posterior
B.
wild type
armi1
armi72.1
armi72.1/armi1
mnk; armi72.1/armi1

Figure 4. *mnk* suppresses microtubule organization defects and Vasa phosphorylation in rasiRNA pathway mutants. A. Microtubules were labeled with an anti-α-tubulin antibody. (a) A bright microtubule organizing center (MTOC) is localized to the anterior pole of the oocyte in wild type stage 1 egg chambers (arrowhead). (a') By stage 6, the MTOC is localized along the posterior cortex (arrowhead). In $armi^{72.1}/armi^{1}$ and $spn\text{-}D^{2}$ egg chambers, the anterior MTOC (b and d) and later posterior MTOC (b' and d') are much less prominent (arrowheads). (c and e) In mnk^{p6}; $armi^{72.1}/armi^{1}$and mnk^{p6}; $spn\text{-}D^{2}$ egg chambers, anterior MTOC during stage 1 (c and e, arrowheads) and the posterior MTOC during stage 6 (c' and e', arrowheads) are restored. Stage 1 oocytes are outlined. Images were acquired under identical conditions. Projections of 4 serial 0.6 μm optical sections are shown. Posterior is oriented to the right. Scale bar is 10 μm.

B. Western blot analysis of Vasa (Vas) protein in wild type, $armi^{1}$, $armi^{72.1}$, $armi^{72.1}/armi^{1}$and mnk^{p6}; $armi^{72.1}/armi^{1}$ovary extracts. Vas from homozygous $armi^{72.1}$ovaries has a reduced electrophoretic mobility relative Vas from wild type ovaries. Low mobility and wild type mobility forms of Vas are present in $armi^{72.1}/armi^{1}$ ovary extracts. Only the faster migrating form is present in mnk^{p6}; $armi^{72.1}/armi^{1}$ extracts (arrow).

Figure 5.

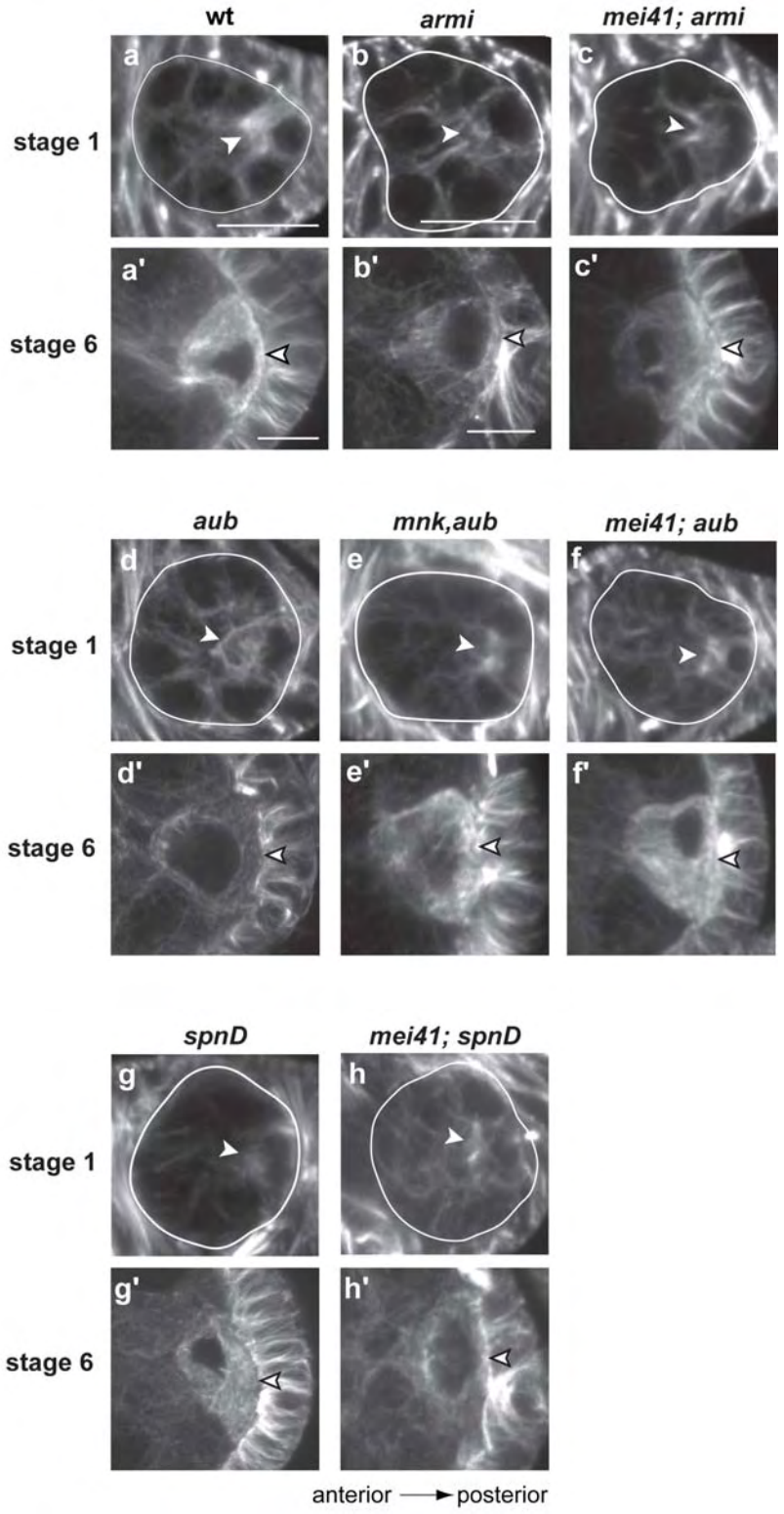
wt
armi
mei41; armi
stage 1
stage 6
a
b
c
a'
b'
c'
aub
mnk,aub
mei41; aub
d
e
f
d'
e'
f'
spnD
mei41; spnD
g
h
g'
h'
anterior → posterior

Figure 5. Suppression of the microtubule organization defects by *mei-41* and *mnk*. Egg chambers were fixed and labeled with FITC-conjugated anti-α-tubulin antibody. (a) A bright microtubule organizing center (MTOC) is localized to the anterior pole of the oocyte in wild type stage 1 egg chambers (arrowhead). (a') By stage 6, the MTOC is localized along the posterior cortex (arrowhead). (b', d' and g') In $armi^{72.1}/armi^{1}$, aub^{QC42}/aub^{HN2} and $spn\text{-}D^{2}$ mutant egg chambers the posterior MTOC localization at stage 6 is disrupted (arrowheads), moreover, (b, d and g) the stage 1 anterior localization of the MTOC is also defective (arrowheads). (c, c', f, f', h and h') *mei-41D3* mutation partially suppresses the microtubule organization defects in $armi^{72.1}/armi^{1}$, aub^{QC42}/aub^{HN2} and $spn\text{-}D^{2}$ egg chambers during stages 1 and 6 (arrowheads). (e and e') Microtubule polarization is restored to near wild type levels in mnk^{p6}, aub^{QC42} mnk^{p6}, aub^{HN2} double mutants (arrowheads). Stage 1 oocytes are outlined. Images were acquired under identical conditions. Projections of 4 serial 0,6 μm optical sections are shown. Posterior is oriented to the right. Scale bar is 10 μm.

rasiRNA pathway mutations lead to germline γ–H2Av accumulation

The above observations indicate that the axis specification defects associated with *armi* and *aub* are mediated by ATR and Chk2 kinases, which are normally activated by DNA DSBs. To determine if *armi* and *aub* lead to DSB accumulation, we labeled mutant ovaries for the phosphorylated form of the *Drosophila* histone H2AX variant (γ–H2Av), which accumulates on chromosomes near break sites (Modesti and Kanaar, 2001; Redon et al., 2002). Following chromosome breakage, *Drosophila* H2Av, like H2AX, is phosphorylated at a conserved SQ motif within an extended C-terminal tail (Madigan et al., 2002; Rogakou et al., 1998). We therefore used an anti-phosphoprotein antibody specific for γ-H2Av (Gong et al., 2005). In wild type ovaries, γ–H2Av foci are restricted to region 2 of the germarium, where meiotic DSBs are formed (Figure 6a) (Jang et al., 2003). Consistent with earlier observations, this labeling is significantly reduced in *mei-W68* mutants, which do not initiate meiotic breaks (Figure 6g). In *armi* and *aub* mutants, prominent γ–H2Av foci are present in germline cells of the germarium. Unlike wild type, these foci persist and increase in intensity as cysts mature and bud to form stage 2 egg chambers (Figure 6c and e). γ–H2Av foci persist in double mutants with *mnk*, indicating that suppression of the patterning defects by *mnk* is not the result of enhanced DNA repair. γ–H2Av foci also persist in egg chambers mutant for a third rasiRNA gene, *spn-E* (Figure 7). The pattern of germline specific γ–H2Av accumulation in *armi*, *aub*, and *spn-E* is similar to the pattern γ–H2Av accumulation in mutants for the DNA repair gene *spn-D*, although the foci appear to arise at somewhat earlier stages in the rasiRNA mutants (Figure 6c, e and i). Accumulation of γ–H2Av foci in *spn-D* mutants is suppressed by *mei-W68*, consistent with a function for this gene in meiotic DSB repair (Abdu et al.,

2002). By contrast, γ–H2Av foci persist in *mei-W68; armi* double mutants (Figure 6h). We have not yet assayed *mei-W68* double mutants with *aub* or *spn-E*, but the above observation suggests that the γ–H2Av foci in rasiRNA pathway mutations are independent of meiotic DSB formation.

Figure 6.

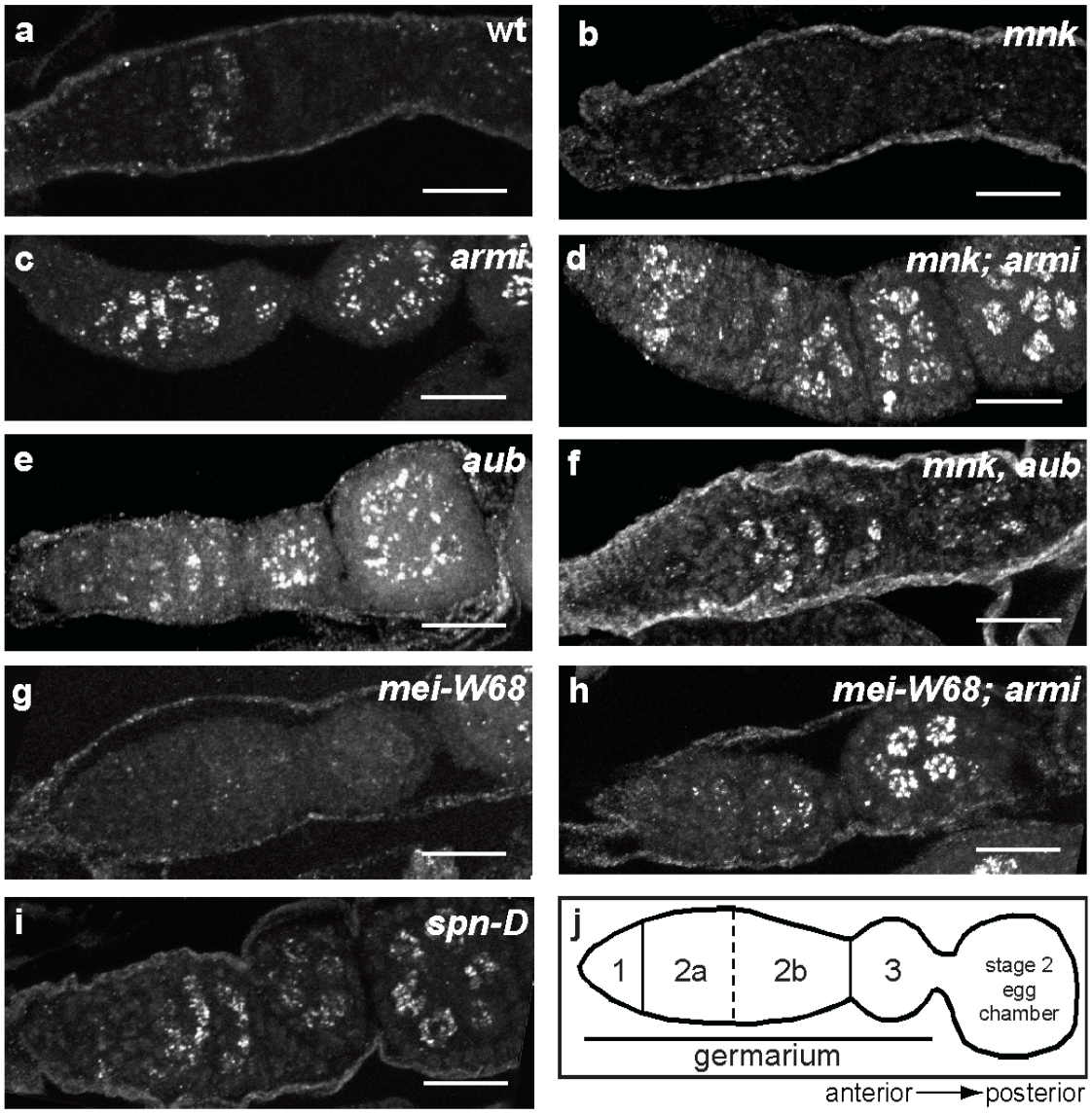
a
wt
b
mnk
c
armi
d
mnk; armi
e
aub
f
mnk, aub
g
mei-W68
h
mei-W68; armi
i
spn-D
j
1
2a
2b
3
stage 2
egg
chamber
germarium
anterior
posterior

Figure 6. γ–H2Av foci accumulate in *armi* and *aub* mutant ovaries. The phosphorylated form of Histone H2Av (γ–H2Av) accumulates near double strand break sites. (a and b) In wild type and mnk^{p6} mutants, γ–H2Av foci are restricted to region 2 of the germarium, where meiotic DSBs form. In (c) $armi^{72.1}/armi^{1}$, (d) mnk^{p6}; $armi^{72.1}/armi^{1}$, (e) aub^{QC42}/aub^{HN2}, and (f) mnk^{p6}, aub^{QC42}/ mnk^{p6}, aub^{HN2} ovaries, γ–H2Av foci accumulate in germline cells within the germarium, and persist and increase in intensity as cysts bud from the germarium to form egg chambers. (i) A similar pattern is observed in ovaries mutant for $spn\text{-}D^{2}$, which is required for DSB repair. (g) Mutations in *mei-W68* ($mei\text{-}W68^{1}/mei\text{-}W68^{k05603}$), which encodes the Spo11 nuclease that initiates meiotic DSBs, suppress formation of γ–H2Av foci in region 2 of the germarium. (h) However, *mei-W68* does not suppress γ–H2Av focus formation in *armi* mutants ($mei\text{-}W68^{1}/mei\text{-}W68^{k05603}$; $armi^{72.1}/armi^{1}$). (j) A schematic representation of the regions of the germarium and a developing egg chamber. Projections of 6 serial 1μm optical sections are shown. Posterior is to the right. Scale bar is 20 μm.

Figure 7.

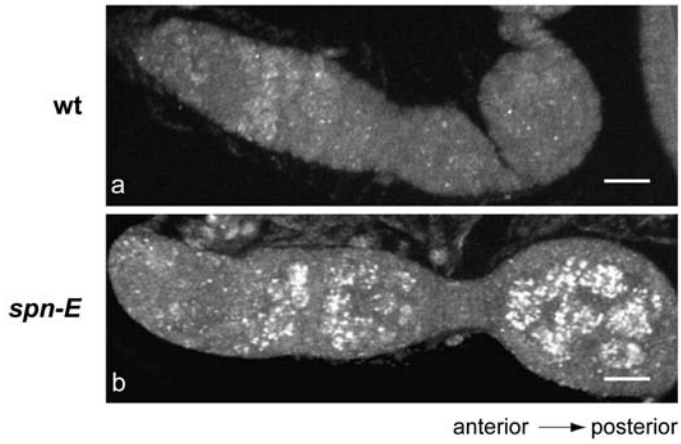

Figure 7. *spn-E* mutants have increased DNA damage in the germline. Ovaries from (a) wild type and (b) *spn-E1* flies were fixed and immunostained with an antibody against phosphorylated H2Av (γ–H2Av). (a) Foci of γ–H2Av are observed in wild type in region 2 of the germarium and correspond to the DSBs induced during meiotic recombination. (b) In *spn-E1* mutants, much larger foci also appear in region 2 of the germarium but persist in region 3 and the developing egg chambers. Images were acquired under identical conditions. Projections of 6 serial 1 μm optical sections are shown. Posterior is oriented to the right. Scale bar is 10 μm.

rasiRNA function

The observations presented above strongly suggested that the axial patterning defects associated with *armi* and *aub* are a consequence of DNA damage signaling, and that rasiRNA based gene silencing is not directly involved in embryonic patterning. However, the *mnk* and *mei-41* mutations could suppress the defects in rasiRNA function associated with *armi* and *aub*. We therefore analyzed rasiRNA dependent silencing of both the *Stellate (Ste)* gene during spermatogenesis and the *HeT-A* retrotransposon during oogenesis in single and double mutants. The *Ste* gene is repressed during spermatogenesis, apparently through mRNA turnover guided by rasiRNAs derived from the *Suppressor of Stellate* locus (Aravin et al., 2001; Gvozdev et al., 2003). Mutations in *armi* and *aub* lead to accumulation of full length *Ste* mRNA and Stellate (Ste) protein over-expression, which leads to assembly of Ste crystals in mutant testes (Aravin et al., 2004; Forstemann et al., 2005; Stapleton et al., 2001; Tomari et al., 2004a) (Figure 8A, b and c). Ste crystals are present in both *mnk; armi* and *mnk, aub* double mutant testes (Figure 8A, e and f). Ste over-expression is also linked to male sterility, and *mnk; armi* males are also sterile (data not shown).

HeT-A is a retrotransposon that contributes to telomere formation in *Drosophila* (Pardue et al., 2005), and *HeT-A* expression is dramatically de-repressed in *armi, aub* and *spn-E* mutant ovaries (Aravin et al., 2001; Vagin et al., 2004; Vagin et al., 2006). *HeT-A* is not expressed at detectable levels on Northern blots of wild type or *mnk* RNAs. However, *HeT-A* transcripts are abundant in *armi* and *aub* mutants (Figure 8C). Significantly, *HeT-A* is also over-expressed in *mnk; armi* and *mnk, aub* double mutants (Figure 8B and C). In fact, *HeT-A* expression is higher in the double mutants, relative to

the single mutants. FISH analyses indicate that this reflects increased expression in the germline and somatic cells of the ovary, during both early and mid-oogenesis (Figure 8B). Therefore, the *mnk* mutation does not suppress defects in rasiRNA based gene silencing during spermatogenesis or oogenesis, leading us to conclude that rasiRNA based silencing is not required for axis specification.

Figure 8.

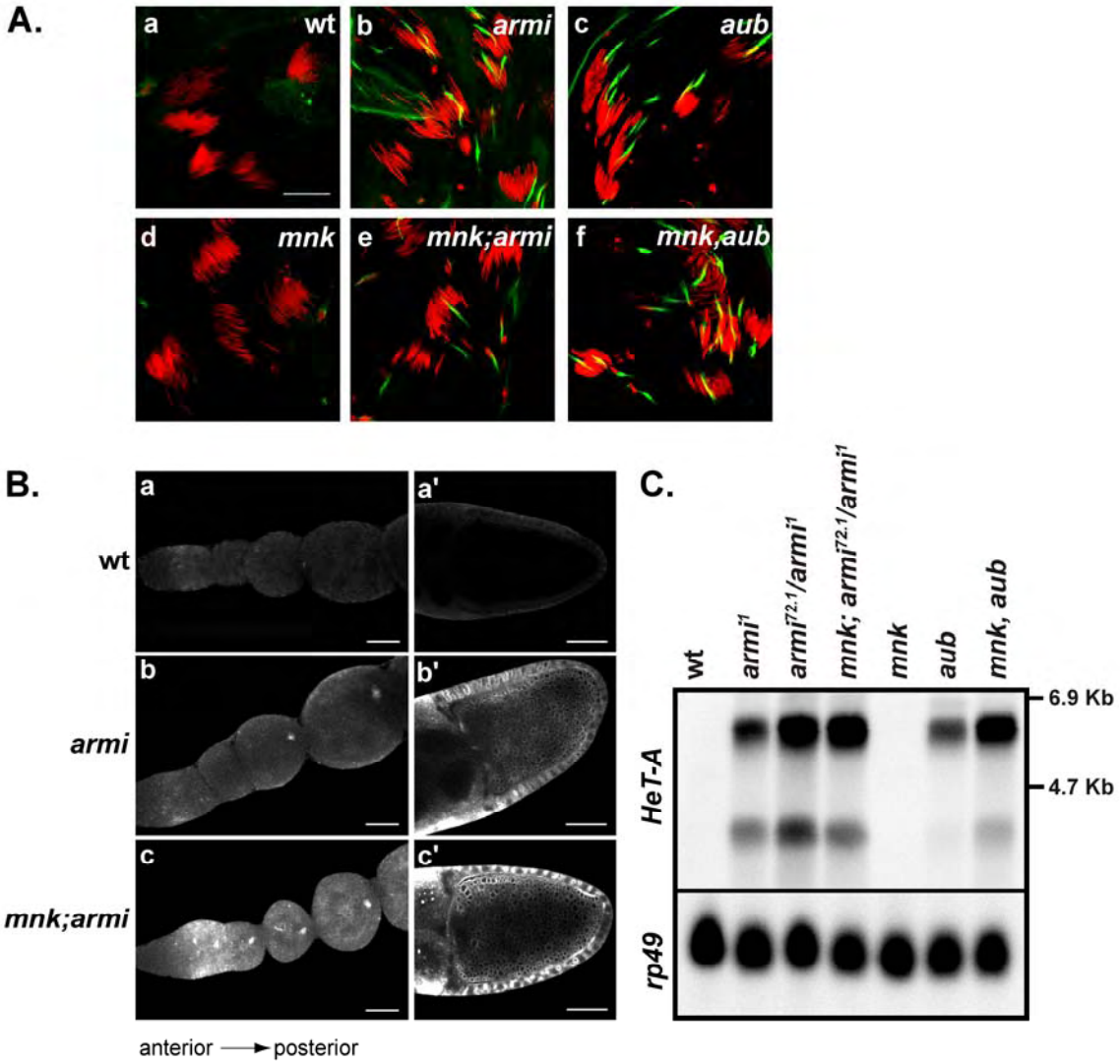
A.
a wt
b armi
c aub
d mnk
e mnk;armi
f mnk,aub
B.
wt
armi
mnk;armi
a
a'
b
b'
c
c'
anterior → posterior
C.
wt
armi1
armi72.1/armi1
mnk; armi72.1/armi1
mnk
aub
mnk, aub
HeT-A
rp49
6.9 Kb
4.7 Kb

Figure 8. The *mnk* mutation does not suppress defects in rasiRNA function.

A. Silencing of *Stellate* locus during spermatogenesis. *Stellate* is not expressed in (a) wild type or (d) mnk^{p6} mutant testes. However, *Stellate* is over-expressed and the protein assembles into crystals in testes from (b) $armi^{72.1}/armi^{1}$, (c) aub^{QC42}/aub^{HN2}, (e) mnk^{p6}; $armi^{72.1}/armi^{1}$, and (f) mnk^{p6}, aub^{QC42}/ mnk^{p6}, aub^{HN2} *males*. DNA (red) was labeled with TOTO3 and Stellate protein (green) was detected with anti-Stellate antibody. Projections of 5 serial 1μm optical sections are shown. Scale bar is 20 μm.

B. FISH analysis of *HeT-A* retrotransposon silencing. (a-a') In wild type ovaries, only background levels of *HeT-A* expression are detected. (b, b' and c, c') By contrast, *HeT-A* is expressed at high levels in the germline and somatic follicle cells of early and mid-oogenesis stage $armi^{72.1}/armi^{1}$ and mnk^{p6}; $armi^{72.1}/armi^{1}$ egg chambers. Panels (a), (b) and (c) are projections of 12-15 serial 1.5 μm optical sections. Panels (a'), (b') and (c') are single optical sections. Posterior is oriented to the right. Scale bar is 20 μm for the left panels and 50 μm for the right panels.

C. Northern blot for *HeT-A*. Total ovary RNA samples were resolved on a 1% agarose-formaldehyde gel, transferred to membrane, and probed for *HeT-A* transcript. *HeT-A* transcripts are undetectable in wild type and mnk^{p6} samples, but are abundant in RNA derived from $armi^{1}$, $armi^{72.1}/armi^{1}$, mnk^{p6}; $armi^{72.1}/armi^{1}$, aub^{QC42}/aub^{HN2} and mnk^{p6}, aub^{QC42}/aub^{HN2} mutant ovaries. Ribosomal protein 49 (rp49) was used as a loading control.

Discussion

Mutations in the *Drosophila armi*, *aub* and *spn-E* genes disrupt oocyte microtubule organization and asymmetric localization of mRNAs and proteins that specify the posterior pole and dorsal-ventral axis of the oocyte and embryo (Cook et al., 2004). Mutations in these genes block homology dependent RNA cleavage and RNA induced silencing complex (RISC) assembly in ovary lysates (Tomari et al., 2004a), RNAi based gene silencing during early embryogenesis (Kennerdell et al., 2002), rasiRNA production, and retrotransposon and *Stellate* silencing (Aravin et al., 2001; Vagin et al., 2006). Mutations in *dcr-2* and *ago-2* genes, by contrast, block siRNA function (Okamura et al., 2004; Tomari et al., 2004b) but do not disrupt the rasiRNA pathway or embryonic axis specification (Vagin et al., 2006). The rasiRNA pathway thus appears to be required for embryonic axis specification. However, the function of rasiRNAs in the axis specification pathway has not been previously established.

Here we show that the cytoskeletal polarization, morphogen localization, and eggshell patterning defects associated with *armi* and *aub* are efficiently suppressed by *mnk* and *mei-41*, which encode Chk2 and ATR kinase components of the DNA damage-signaling pathway (Table 1 and Figures 1-3). In addition, we show that *armi* and *aub* mutants accumulate γ–H2Av foci characteristic of DNA DSBs (Figure 4) and trigger Chk2-dependent phosphorylation of Vas (Figure 3B) , an RNA helicase required for posterior and dorsal-ventral specification (Styhler et al., 1998). Mutations in *spn-E* also disrupt the rasiRNA pathway (Aravin and Tuschl, 2005; Vagin et al., 2006), trigger axis specification defects (Cook et al., 2004) and lead to germline-specific accumulation of γ–H2Av foci (see Figure7). Significantly, the *mnk* and *mei-41* mutations do not suppress

Ste or *HeT-A* over-expression, indicating that axis specification does not directly require rasiRNA dependent gene silencing. Based on these findings, we conclude that the rasiRNA pathway suppresses DNA damage signaling in the female germline, and that mutations in this pathway disrupt axis specification by activating an ATR/Chk2 kinase pathway that blocks microtubule polarization and morphogen localization in the oocyte (Figure 9)..

The cause of DNA damage signaling in *armi, aub,* and *spn-E* mutants remains to be established. In wild type ovaries, γ–H2Av foci begin to accumulate in region 2 of the germarium (Jang et al., 2003), when the Spo11 nuclease (encoded by the *mei-W68* gene) initiates meiotic breaks (McKim and Hayashi-Hagihara, 1998). The axis specification defects associated with DNA DSB repair mutations are efficiently suppressed by *mei-W68* mutations, indicating that meiotic breaks are the source of DNA damage in these mutants (Abdu et al., 2002; Ghabrial and Schupbach, 1999; Staeva-Vieira et al., 2003). The axis specification defects and γ–H2Av foci formation associated with *armi,* by contrast, are not suppressed by *mei-W68* (Table 1, Figure 4). We have not yet analyzed *mei-W68* double mutants with *aub* or *spn-E,* but this observation strongly suggests that meiotic DSBs are not the source of DNA damage in rasiRNA pathway mutations. Retrotransposon silencing is disrupted in *armi, aub,* and *spn-E* mutants (Aravin et al., 2001; Vagin et al., 2006), and transcription of LINE retrotransposons in mammalian cells leads to DNA damage and DNA damage signaling (Belgnaoui et al., 2006; Gasior et al., 2006). Loss of retrotransposon silencing could therefore directly induce the DSBs in rasiRNA pathway mutants. However, DNA damage can also lead to loss of retrotransposon silencing (Bradshaw and McEntee, 1989; Farkash et al., 2006; Rudin and Thompson, 2001).

Mutations in the rasiRNA pathway could therefore disrupt DNA repair, and thus induce DNA damage that in turn induces loss of retrotransposon silencing. Finally, the *HeT-A* retrotransposon is associated with telomeres, and over-expression of this element could reflect a loss of telomere protection and damage signaling by chromosome ends in the rasiRNA pathway mutants. The available data do not distinguish between these alternatives.

In mouse, the *piwi* related Argonauts Miwi and Mili bind piRNAs, 30nt RNAs derived primarily from a single strand that appear to be related to rasiRNAs (Aravin et al., 2006; Girard et al., 2006; Grivna et al., 2006). Mutations in these genes disrupt spermatogenesis and lead to germline apoptosis (Deng and Lin, 2002; Kuramochi-Miyagawa et al., 2001), which can be induced by DNA damage signaling. Mammalian piRNAs and *Drosophila* rasiRNAs may therefore serve similar functions in suppressing a germline specific DNA damage response.

Figure 9.

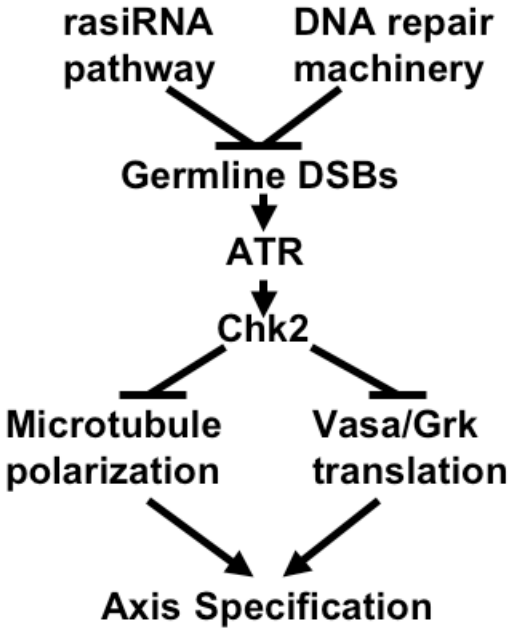
rasiRNA pathway
DNA repair machinery
Germline DSBs
ATR
Chk2
Microtubule polarization
Vasa/Grk translation
Axis Specification

Figure 9. Model for rasiRNA control of axis specification. The rasiRNA pathway and meiotic DSB repair machinery function independently to suppress DNA damage signaling in the female germline. Mutations that disrupt either pathway activate a common DNA damage response, mediated by the ATR and Chk2 kinases. Chk2 activation blocks axis specification by disrupting microtubule organization and phosphorylating Vas, an RNA helicase required for axis specification that has been implicated in *grk* mRNA translation.

Experimental Procedures

Drosophila stocks

All animals were raised at 25^{O}C on standard food. *Oregon R* was used for wild type control. The following alleles were used: *mnk*^{P6} (Brodsky et al., 2004; Takada et al., 2003); *armi*$^{72.1}$ and *armi*^{1} (Cook et al., 2004); *mei41*^{D3}, (Hari et al., 1995; Hawley and Tartof, 1983); *aub*^{QC42}, *aub*^{HN2} (Schupbach and Wieschaus, 1991); *spn-E*^{1} (Gillespie and Berg, 1995);(Gonzalez-Reyes et al., 1997); *spn-D*^{2} (Abdu et al., 2003) P[*lacW]mei-W68*^{K05603}, *mei-W68*^{1} (McKim and Hayashi-Hagihara, 1998). The *mnk*^{P6} allele was kindly provided by M. Brodsky (Brodsky et al., 2004). All other stocks were obtained from the Bloomington *Drosophila* Stock Center (Consortium, 2003; http://flybase.org/). Standard genetic procedures were used to generate double mutant combinations.

Antibody Production

Primers annealing to each of the translation start and stop sites of a *Stellate* cDNA (Bozzetti et al., 1995)were designed (Integrated DNA Technologies, Inc.) with attached Gateway (Invitrogen) sequences. The resulting PCR product was used to make a DONR clone which in turn was used to subclone into the 6X-His-tagged Gateway vector pDest17, yielding a 29kD 6X-His tagged Stellate fusion protein. The fusion protein was purified on a Probond Ni matrix (Invitrogen) under denaturing conditions, isolated by SDS-PAGE and used to immunize 2 rabbits (Pocono Rabbit Farm and Laboratory, Inc.) using standard protocols for antibody production. Antiserum was used at 1:1000 for immunohistochemistry.

Immunohistochemistry

Egg chamber fixation and whole-mount antibody labeling were performed as previously described (Theurkauf, 1994). Microtubules were labeled with FITC-conjugated mouse monoclonal anti-α-tubulin (Sigma Chemical Co.) used at 1:200. Osk protein was labeled with rabbit polyclonal anti-Osk antibody (Vanzo and Ephrussi, 2002) at 1:1000. Vas protein was labeled with rabbit polyclonal anti-Vas antibody (Liang et al., 1994) at 1:1000. Gurken protein was labeled with mouse monoclonal anti-Gurken antibody (obtained from the Developmental Studies Hybridoma Bank, University of Iowa) at 1:10. Antibody against γ-H2Av was kindly provided by Kim McKim (Gong et al., 2005) and egg chambers were labeled as described previously (Belmont et al., 1989). Rhodamine-conjugated phalloidin (Molecular Probes) was used at 1:100 to stain F-actin, and TOTO3 (Molecular Probes) was used at 1:500 (0.2 μM final concentration) to visualize DNA.

Fluorescence *in situ* Hybridization (FISH)

An anti-sense *HeT-A* digoxygenin (DIG)-labeled RNA probe was synthesized *in vitro* from a 500bp PCR-amplified cDNA fragment carrying a T7 promoter (generously provided by P. Zamore) using a DIG RNA Labeling Kit following manufacturer's instructions (Roche). Whole mount *in situ* hybridization was performed as described previously (Cha et al., 2001). Tyramide signal amplification (TSA^{TM}) was performed following manufacturer's instructions (Perkin Elmer).

Northern Blots

Fly ovaries were dissected in 1× Robb's medium (55mM Potassium Acetate, 40mM Sodium Acetate, 100mM Sucrose, 10mM Glucose, 1.2mM $MgCl_2$, 1mM $CaCl_2$, and 100mM HEPES, pH7.4). Total RNA was isolated from approximately 30 mg of ovaries using RNeasy® Mini Kit following manufacturer's instructions (Qiagen). Approximately 20µg of total RNA /sample was resolved electrophoretically on a 1%Agarose/Formaldehyde gel. RNA was transferred to a positively charge nylon membrane (Roche) by standard capillary transfer. Following transfer, RNA was fixed to the membrane via UV crosslinking (Stratalinker UV Crosslinker 2400). Following pre-hybridization, blots were probed with DIG labeled RNA following manufacturer's recommendations (Roche). *rp49* was used as a loading control. Blots were developed using CDP-Star (Tropix) according to manufacturer's directions. Images were acquired using the Kodak 4000MM Image Station.

Western Blot Analysis

The Western blot was performed as described (Ghabrial et al., 1998; Ghabrial and Schupbach, 1999) using the rabbit polyclonal anti-Vas antibody at 1:5000.

Microscopy

All tissues were mounted in 90% glycerol / PBS, with 1 mg/ml p-Phenylenediamine (Sigma). Samples were analyzed using a Leica TCS-SP inverted laser scanning microscope with 63X NA 1.32 PlanApo oil and 40X NA 1.25 Planapo oil objectives. Identical imaging conditions were used for each set of wild type and mutant samples. Images were processed using Image J software.

References:

Abdu, U., Brodsky, M., and Schupbach, T. (2002). Activation of a meiotic checkpoint during Drosophila oogenesis regulates the translation of Gurken through Chk2/Mnk. Curr Biol *12*, 1645-1651.
Abdu, U., Gonzalez-Reyes, A., Ghabrial, A., and Schupbach, T. (2003). The Drosophila spn-D gene encodes a RAD51C-like protein that is required exclusively during meiosis. Genetics *165*, 197-204.
Aravin, A., Gaidatzis, D., Pfeffer, S., Lagos-Quintana, M., Landgraf, P., Iovino, N., Morris, P., Brownstein, M. J., Kuramochi-Miyagawa, S., Nakano, T., *et al.* (2006). A novel class of small RNAs bind to MILI protein in mouse testes. Nature.
Aravin, A., and Tuschl, T. (2005). Identification and characterization of small RNAs involved in RNA silencing. FEBS Lett *579*, 5830-5840.
Aravin, A. A., Klenov, M. S., Vagin, V. V., Bantignies, F., Cavalli, G., and Gvozdev, V. A. (2004). Dissection of a natural RNA silencing process in the Drosophila melanogaster germ line. Mol Cell Biol *24*, 6742-6750.
Aravin, A. A., Naumova, N. M., Tulin, A. V., Vagin, V. V., Rozovsky, Y. M., and Gvozdev, V. A. (2001). Double-stranded RNA-mediated silencing of genomic tandem repeats and transposable elements in the D. melanogaster germline. Curr Biol *11*, 1017-1027.
Bartek, J., Falck, J., and Lukas, J. (2001). CHK2 kinase--a busy messenger. Nat Rev Mol Cell Biol *2*, 877-886.
Bartek, J., and Lukas, J. (2003). Chk1 and Chk2 kinases in checkpoint control and cancer. Cancer Cell *3*, 421-429.
Belgnaoui, S. M., Gosden, R. G., Semmes, O. J., and Haoudi, A. (2006). Human LINE-1 retrotransposon induces DNA damage and apoptosis in cancer cells. Cancer Cell Int *6*, 13.
Belmont, A. S., Braunfeld, M. B., Sedat, J. W., and Agard, D. A. (1989). Large-scale chromatin structural domains within mitotic and interphase chromosomes in vivo and in vitro. Chromosoma *98*, 129-143.
Bernstein, E., Kim, S. Y., Carmell, M. A., Murchison, E. P., Alcorn, H., Li, M. Z., Mills, A. A., Elledge, S. J., Anderson, K. V., and Hannon, G. J. (2003). Dicer is essential for mouse development. Nat Genet *35*, 215-217.
Bozzetti, M. P., Massari, S., Finelli, P., Meggio, F., Pinna, L. A., Boldyreff, B., Issinger, O. G., Palumbo, G., Ciriaco, C., Bonaccorsi, S., and et al. (1995). The Ste locus, a component of the parasitic cry-Ste system of Drosophila melanogaster, encodes a protein that forms crystals in primary spermatocytes and mimics properties of the beta subunit of casein kinase 2. Proc Natl Acad Sci U S A *92*, 6067-6071.
Bradshaw, V. A., and McEntee, K. (1989). DNA damage activates transcription and transposition of yeast Ty retrotransposons. Mol Gen Genet *218*, 465-474.
Brodsky, M. H., Weinert, B. T., Tsang, G., Rong, Y. S., McGinnis, N. M., Golic, K. G., Rio, D. C., and Rubin, G. M. (2004). Drosophila melanogaster MNK/Chk2 and p53 regulate multiple DNA repair and apoptotic pathways following DNA damage. Mol Cell Biol *24*, 1219-1231.
Cha, B. J., Koppetsch, B. S., and Theurkauf, W. E. (2001). In vivo analysis of Drosophila bicoid mRNA localization reveals a novel microtubule-dependent axis specification pathway. Cell *106*, 35-46.

Cook, H., Koppetsch, B., Wu, J., and Theurkauf, W. (2004). The *Drosophila* SDE3 homolog *armitage* is required for oskar mRNA silencing and embryonic axis specification. Cell *116*, 817-829.
Deng, W., and Lin, H. (2002). miwi, a murine homolog of piwi, encodes a cytoplasmic protein essential for spermatogenesis. Dev Cell *2*, 819-830.
Deshpande, G., Calhoun, G., and Schedl, P. (2005). Drosophila argonaute-2 is required early in embryogenesis for the assembly of centric/centromeric heterochromatin, nuclear division, nuclear migration, and germ-cell formation. Genes Dev *19*, 1680-1685.
Drees, B. L., Sundin, B., Brazeau, E., Caviston, J. P., Chen, G. C., Guo, W., Kozminski, K. G., Lau, M. W., Moskow, J. J., Tong, A., *et al.* (2001). A protein interaction map for cell polarity development. J Cell Biol *154*, 549-571.
Farkash, E. A., Kao, G. D., Horman, S. R., and Prak, E. T. (2006). Gamma radiation increases endonuclease-dependent L1 retrotransposition in a cultured cell assay. Nucleic Acids Res *34*, 1196-1204.
Forstemann, K., Tomari, Y., Du, T., Vagin, V. V., Denli, A. M., Bratu, D. P., Klattenhoff, C., Theurkauf, W. E., and Zamore, P. D. (2005). Normal microRNA maturation and germ-line stem cell maintenance requires Loquacious, a double-stranded RNA-binding domain protein. PLoS Biol *3*, e236.
Fukagawa, T., Nogami, M., Yoshikawa, M., Ikeno, M., Okazaki, T., Takami, Y., Nakayama, T., and Oshimura, M. (2004). Dicer is essential for formation of the heterochromatin structure in vertebrate cells. Nat Cell Biol *6*, 784-791.
Galiana-Arnoux, D., Dostert, C., Schneemann, A., Hoffmann, J. A., and Imler, J. L. (2006). Essential function in vivo for Dicer-2 in host defense against RNA viruses in drosophila. Nat Immunol *7*, 590-597.
Gasior, S. L., Wakeman, T. P., Xu, B., and Deininger, P. L. (2006). The human LINE-1 retrotransposon creates DNA double-strand breaks. J Mol Biol *357*, 1383-1393.
Ghabrial, A., Ray, R. P., and Schupbach, T. (1998). okra and spindle-B encode components of the RAD52 DNA repair pathway and affect meiosis and patterning in Drosophila oogenesis. Genes Dev *12*, 2711-2723.
Ghabrial, A., and Schupbach, T. (1999). Activation of a meiotic checkpoint regulates translation of Gurken during Drosophila oogenesis. Nat Cell Biol *1*, 354-357.
java/Propub/cellbio/ncb1099_1354.fulltext java/Propub/cellbio/ncb1099_1354.abstract.
Gillespie, D. E., and Berg, C. A. (1995). Homeless is required for RNA localization in Drosophila oogenesis and encodes a new member of the DE-H family of RNA-dependent ATPases. Genes Dev *9*, 2495-2508.
Giraldez, A. J., Cinalli, R. M., Glasner, M. E., Enright, A. J., Thomson, J. M., Baskerville, S., Hammond, S. M., Bartel, D. P., and Schier, A. F. (2005). MicroRNAs regulate brain morphogenesis in zebrafish. Science *308*, 833-838.
Girard, A., Sachidanandam, R., Hannon, G. J., and Carmell, M. A. (2006). A germline-specific class of small RNAs binds mammalian Piwi proteins. Nature.
Gong, W. J., McKim, K. S., and Hawley, R. S. (2005). All paired up with no place to go: pairing, synapsis, and DSB formation in a balancer heterozygote. PLoS Genet *1*, e67.
Gonzalez-Reyes, A., Elliott, H., and St Johnston, D. (1995). Polarization of both major body axes in Drosophila by gurken-torpedo signalling. Nature *375*, 654-658.

Gonzalez-Reyes, A., Elliott, H., and St Johnston, D. (1997). Oocyte determination and the origin of polarity in Drosophila: the role of the spindle genes. Development *124*, 4927-4937.
Grishok, A., Pasquinelli, A. E., Conte, D., Li, N., Parrish, S., Ha, I., Baillie, D. L., Fire, A., Ruvkun, G., and Mello, C. C. (2001). Genes and mechanisms related to RNA interference regulate expression of the small temporal RNAs that control C. elegans developmental timing. Cell *106*, 23-34.
Grivna, S. T., Beyret, E., Wang, Z., and Lin, H. (2006). A novel class of small RNAs in mouse spermatogenic cells. Genes Dev *20*, 1709-1714.
Gvozdev, V. A., Aravin, A. A., Abramov, Y. A., Klenov, M. S., Kogan, G. L., Lavrov, S. A., Naumova, N. M., Olenkina, O. M., Tulin, A. V., and Vagin, V. V. (2003). Stellate repeats: targets of silencing and modules causing cis-inactivation and trans-activation. Genetica *117*, 239-245.
Hannon, G. J. (2002). RNA interference. Nature *418*, 244-251.
Hari, K. L., Santerre, A., Sekelsky, J. J., McKim, K. S., Boyd, J. B., and Hawley, R. S. (1995). The mei-41 gene of D. melanogaster is a structural and functional homolog of the human ataxia telangiectasia gene. Cell *82*, 815-821.
Hatfield, S. D., Shcherbata, H. R., Fischer, K. A., Nakahara, K., Carthew, R. W., and Ruohola-Baker, H. (2005). Stem cell division is regulated by the microRNA pathway. Nature *435*, 974-978.
Hawley, R. S., and Tartof, K. D. (1983). The effect of mei-41 on rDNA redundancy in Drosophila melanogaster. Genetics *104*, 63-80.
Hirao, A., Cheung, A., Duncan, G., Girard, P. M., Elia, A. J., Wakeham, A., Okada, H., Sarkissian, T., Wong, J. A., Sakai, T., *et al.* (2002). Chk2 is a tumor suppressor that regulates apoptosis in both an ataxia telangiectasia mutated (ATM)-dependent and an ATM-independent manner. Mol Cell Biol *22*, 6521-6532.
Hutvagner, G., and Zamore, P. D. (2002). A MicroRNA in a Multiple-Turnover RNAi Enzyme Complex. Science *1*, 1.
Jang, J. K., Sherizen, D. E., Bhagat, R., Manheim, E. A., and McKim, K. S. (2003). Relationship of DNA double-strand breaks to synapsis in Drosophila. J Cell Sci *116*, 3069-3077.
Jaronczyk, K., Carmichael, J. B., and Hobman, T. C. (2005). Exploring the functions of RNA interference pathway proteins: some functions are more RISCy than others? Biochem J *387*, 561-571.
Kennerdell, J. R., Yamaguchi, S., and Carthew, R. W. (2002). RNAi is activated during Drosophila oocyte maturation in a manner dependent on aubergine and spindle-E. Genes Dev *16*, 1884-1889.
Kuramochi-Miyagawa, S., Kimura, T., Yomogida, K., Kuroiwa, A., Tadokoro, Y., Fujita, Y., Sato, M., Matsuda, Y., and Nakano, T. (2001). Two mouse piwi-related genes: miwi and mili. Mech Dev *108*, 121-133.
Lee, Y. S., Nakahara, K., Pham, J. W., Kim, K., He, Z., Sontheimer, E. J., and Carthew, R. W. (2004). Distinct roles for Drosophila Dicer-1 and Dicer-2 in the siRNA/miRNA silencing pathways. Cell *117*, 69-81.
Liang, L., Diehl-Jones, W., and Lasko, P. (1994). Localization of vasa protein to the Drosophila pole plasm is independent of its RNA-binding and helicase activities. Development *120*, 1201-1211.

Madigan, J. P., Chotkowski, H. L., and Glaser, R. L. (2002). DNA double-strand break-induced phosphorylation of Drosophila histone variant H2Av helps prevent radiation-induced apoptosis. Nucleic Acids Res *30*, 3698-3705.
McKim, K. S., and Hayashi-Hagihara, A. (1998). mei-W68 in Drosophila melanogaster encodes a Spo11 homolog: evidence that the mechanism for initiating meiotic recombination is conserved. Genes Dev *12*, 2932-2942.
Modesti, M., and Kanaar, R. (2001). DNA repair: spot(light)s on chromatin. Curr Biol *11*, R229-232.
Oikemus, S. R., McGinnis, N., Queiroz-Machado, J., Tukachinsky, H., Takada, S., Sunkel, C. E., and Brodsky, M. H. (2004). Drosophila atm/telomere fusion is required for telomeric localization of HP1 and telomere position effect. Genes Dev *18*, 1850-1861.
Okamura, K., Ishizuka, A., Siomi, H., and Siomi, M. C. (2004). Distinct roles for Argonaute proteins in small RNA-directed RNA cleavage pathways. Genes Dev *18*, 1655-1666.
Pardue, M. L., Rashkova, S., Casacuberta, E., DeBaryshe, P. G., George, J. A., and Traverse, K. L. (2005). Two retrotransposons maintain telomeres in Drosophila. Chromosome Res *13*, 443-453.
Provost, P., Silverstein, R. A., Dishart, D., Walfridsson, J., Djupedal, I., Kniola, B., Wright, A., Samuelsson, B., Radmark, O., and Ekwall, K. (2002). Dicer is required for chromosome segregation and gene silencing in fission yeast cells. Proc Natl Acad Sci U S A *99*, 16648-16653.
Redon, C., Pilch, D., Rogakou, E., Sedelnikova, O., Newrock, K., and Bonner, W. (2002). Histone H2A variants H2AX and H2AZ. Curr Opin Genet Dev *12*, 162-169.
Rogakou, E. P., Pilch, D. R., Orr, A. H., Ivanova, V. S., and Bonner, W. M. (1998). DNA double-stranded breaks induce histone H2AX phosphorylation on serine 139. J Biol Chem *273*, 5858-5868.
Roth, S., Neuman-Silberberg, F. S., Barcelo, G., and Schupbach, T. (1995). cornichon and the EGF receptor signaling process are necessary for both anterior-posterior and dorsal-ventral pattern formation in Drosophila. Cell *81*, 967-978.
Rudin, C. M., and Thompson, C. B. (2001). Transcriptional activation of short interspersed elements by DNA-damaging agents. Genes Chromosomes Cancer *30*, 64-71.
Schupbach, T. (1987). Germ line and soma cooperate during oogenesis to establish the dorsoventral pattern of egg shell and embryo in Drosophila melanogaster. Cell *49*, 699-707.
Schupbach, T., and Wieschaus, E. (1991). Female sterile mutations on the second chromosome of Drosophila melanogaster. II. Mutations blocking oogenesis or altering egg morphology. Genetics *129*, 1119-1136.
Simeone, A., Acampora, D., Mallamaci, A., Stornaiuolo, A., D'Apice, M. R., Nigro, V., and Boncinelli, E. (1993). A vertebrate gene related to orthodenticle contains a homeodomain of the bicoid class and demarcates anterior neuroectoderm in the gastrulating mouse embryo. Embo J *12*, 2735-2747.
Staeva-Vieira, E., Yoo, S., and Lehmann, R. (2003). An essential role of DmRad51/SpnA in DNA repair and meiotic checkpoint control. Embo J *22*, 5863-5874.
Stapleton, W., Das, S., and McKee, B. D. (2001). A role of the Drosophila homeless gene in repression of Stellate in male meiosis. Chromosoma *110*, 228-240.

Styhler, S., Nakamura, A., Swan, A., Suter, B., and Lasko, P. (1998). vasa is required for GURKEN accumulation in the oocyte, and is involved in oocyte differentiation and germline cyst development. Development *125*, 1569-1578.
Takada, S., Kelkar, A., and Theurkauf, W. E. (2003). Drosophila checkpoint kinase 2 couples centrosome function and spindle assembly to genomic integrity. Cell *113*, 87-99.
Theurkauf, W. E. (1994). Immunofluorescence analysis of the cytoskeleton during oogenesis and early embryogenesis. Methods Cell Biol *44*, 489-505.
Theurkauf, W. E., Alberts, B. M., Jan, Y. N., and Jongens, T. A. (1993). A central role for microtubules in the differentiation of Drosophila oocytes. Development *118*, 1169-1180.
Tomari, Y., Du, T., Haley, B., Schwarz, D., Bennett, R., Cook, H., Koppetsch, B., Theurkauf, W., and Zamore, P. D. (2004a). RISC Assembly Defects in the Drosophila RNAi Mutant armitage. Cell *116*, 831-841.
Tomari, Y., Matranga, C., Haley, B., Martinez, N., and Zamore, P. D. (2004b). A protein sensor for siRNA asymmetry. Science *306*, 1377-1380.
Vagin, V. V., Klenov, M. S., Kalmykova, A., Stolyarenko, A. D., Kotelnikov, R. N., and Gvozdev, V. (2004). The RNA interference Proteins and Vasa Locus are Involved in the Silencing of retrotransposons in the Female Germline of Drososophla melanogaster. RNA Biology *1*, 54-58.
Vagin, V. V., Sigova, A., Li, C., Seitz, H., Gvozdev, V., and Zamore, P. D. (2006). A small RNA mechanism distinct from the RNAi and microRNA pathways silences selfish genetic elements in Drosophila. Science, in press.
Vanzo, N. F., and Ephrussi, A. (2002). Oskar anchoring restricts pole plasm formation to the posterior of the Drosophila oocyte. Development *129*, 3705-3714.
Volpe, T., Schramke, V., Hamilton, G. L., White, S. A., Teng, G., Martienssen, R. A., and Allshire, R. C. (2003). RNA interference is required for normal centromere function in fission yeast. Chromosome Res *11*, 137-146.
Wang, X. H., Aliyari, R., Li, W. X., Li, H. W., Kim, K., Carthew, R., Atkinson, P., and Ding, S. W. (2006). RNA interference directs innate immunity against viruses in adult Drosophila. Science *312*, 452-454.
Wassenegger, M. (2005). The role of the RNAi machinery in heterochromatin formation. Cell *122*, 13-16.

CHAPTER III

The *Drosophila* HP1 homologue Rhino is required for piRNA biogenesis, transposon silencing and genome maintenance in the female germline

Abstract:

The *Drosophila* piRNA pathway silences transposon expression and maintains genome integrity during female germline development, but piRNA biogenesis and transposon silencing are not well understood. We show that mutations in *rhino*, which encodes a rapidly evolving Heterochromatin Protein 1 (HP1) chromo box protein, lead to germline specific DNA break accumulation, trigger Chk2 kinase dependent defects in axis specification, and disrupt germline localization of Piwi proteins. Mutations in *rhino* and the piRNA pathway gene *armitage* disrupt silencing transposons, but do not alter expression of euchromatic or heterochromatic protein coding genes. Deep sequencing studies show that *rhino* mutations significantly reduce or eliminate anti-sense piRNAs derived from the majority of transposable elements in the *Drosophila* genome, and lead to a dramatic reduction in piRNAs derived from major piRNA production clusters on chromosomes 2R and 4. Rhino protein localizes to distinct nuclear foci, and associates with the chromosome 2R and 4 clusters by chromatin immunoprecipitation. The Rhino HP1 homologue is therefore required for piRNA biogenesis, transposon silencing, and maintenance of germline genome integrity.

Introduction

Piwi class Argonautes bind to endogenous 24-30 nt non-coding RNAs (piRNAs) and are required for germline development in mouse, flies and fish (Aravin et al., 2007). In each of these systems, at least a subset of piRNAs are derived from transposons and other repeated sequence elements (Brennecke et al., 2007; Gunawardane et al., 2007; Saito et al., 2006), and mutations in the *Drosophila* piRNA pathway genes lead to DNA break accumulation and a dramatic loss of silencing for at least a subset of transposable elements (Klattenhoff et al., 2007). These findings suggest that piRNA mutations lead to transposon mobilization in the germline, which may overwhelm the DNA repair machinery, compromising chromosome integrity and germline development. However, there is no direct evidence that breaks in germline DNA are linked to new transposon insertions, and other mechanisms of damage accumulation are possible.

Insight into the mechanism of piRNA dependent transposon silencing has come from both deep sequencing and genetic studies. Deep sequencing in *Drosophila* indicates that most piRNAs are derived from a limited number of loci, termed piRNA clusters, that are largely localized to pericentromeric and telomeric heterochromatin (Brennecke et al., 2007). By contrast, full-length transposons are present throughout the genome. Significantly, the *flamenco* locus defines a piRNA cluster located on the X chromosome, and a P-element insertion in this locus disrupts silencing of *gypsy* elements located elsewhere in the genome (Brennecke et al., 2007; Prud'homme et al., 1995) . These findings suggest that piRNAs generated at a heterochromatic cluster can silence euchromatic transposons in trans. piRNA-Argonaute complexes can mediate homology dependent target cleavage *in vitro* (Gunawardane et al., 2007; Saito et al., 2006),

suggesting that trans-silencing reflects co-transcriptional or post-transcriptional destruction of target transcripts. However, mutations in the *Drosophila* piRNA pathway have been reported to modify position effect variegation (PEV) in somatic tissues (Brower-Toland et al., 2007; Pal-Bhadra et al., 2002; Pal-Bhadra et al., 2004), which is a stochastic form of silencing linked to spreading of transcriptionally silent heterochromatin from pericentric and telomeric regions. Piwi has also been found to physically and genetically interact with heterochromatin protein-1 (HP1) (Brower-Toland et al., 2007). Trans-silencing could therefore reflect piRNA-Piwi protein directed heterochromatin assembly and transcriptional repression. In *S. pombe,* siRNAs and Argonautes appear to recognize nascent transcripts at the centromere, triggering both transcript destruction and assembly of centromeric heterochomatin (Verdel and Moazed, 2005) . It is therefore possible that similar hybrid mechanisms drive piRNA based silencing in the germline.

Biogenesis of piRNAs is independent of Dicer (Houwing et al., 2007; Vagin et al., 2006), which catalyzes production of miRNAs and siRNAs from double strand precursors (reviewed in (Du and Zamore, 2005; Hannon, 2002). Deep sequencing of small RNAs from *Drosophila* ovaries reveals a subset of sense and anti-sense piRNAs with a 10 base overlap. Within this pool, there is bias toward an A at position 10 of the sense strand piRNA and a U at the 5' end of the anti-sense strand piRNA (Brennecke et al., 2007; Gunawardane et al., 2007). Argonautes cleave targets between positions 10 and 11 of the guide strand (Gunawardane, 2007; Saito, 2006). These results thus suggest that piRNAs are produced by a ping-pong mechanism in which sense strand piRNAs bound to Argonaute proteins generate the 5' end of antisense piRNAs, and anti-sense piRNA-Argonaute complexes generate the 5' end of sense strand piRNAs (Brennecke et al., 2007;

Gunawardane et al., 2007). However, the mechanism of 3" end generation is not understood, and most piRNAs cannot be assigned to "ping-pong" pairs. In addition, the precursor RNAs for piRNA production have not been identified.

The mechanisms that drive piRNA biogenesis and piRNA dependent silencing thus remain to be determined. To gain insight into these critical processes, we have exploited forward genetic approaches in *Drosophila* to identify new components of the piRNA pathway. Mutations in the piRNA pathway produce characteristic defects in posterior and dorsal-ventral axis specification, which lead to easily scored changes in eggshell shape (Chen et al., 2007; Cook et al., 2004; Pane et al., 2007). Volpe et al. previously reported that mutations in the *rhino (rhi) locus*, which encodes a member of the Heterochromatin Protein 1 (HP1) subfamily of chromo box proteins, produce similar defects (Volpe et al., 2001). The axis specification defects in piRNA mutants are linked to DNA break formation in the germline, and are suppressed by mutations that disrupt DNA damage signaling (Klattenhoff et al., 2007). Here, we show that *rhino* mutations also lead to DNA break accumulation in the germline, and that the axis specification defects associated with these mutations result from DNA damage signaling. Whole genome tiling array studies show that *rhi* mutations, and mutations in the piRNA pathway gene *armitage (armi),* lead to dramatic increases in expression of a significant fraction of the transposable elements in the *Drosophila* genome. By contrast, *rhi* and *armi* do not significantly alter expression of euchromatic or heterochromatic protein coding genes. Deep sequencing of small RNAs demonstrate the *rhino* mutations lead to a significant reduction in piRNA production from a number of piRNA clusters, including major piRNA clusters on chromosome 2R and 4, and chromatin immunoprecipitation (ChIP) studies

indicate that Rhino protein is physically associated with these loci. Furthermore, mutations in *rhino* lead to a dramatic reduction in minus strand piRNAs from the majority of transposable elements, and a loss of overlapping sense and anti-sense strand piRNAs characteristic of ping-pong biogenesis. Interestingly, *rhino* is one of the fastest evolving genes in the *Drosophila* genome, suggesting a role in host-pathogen competition. Our findings demonstrate that Rhi is required for piRNA biogenesis and transposon silencing, and strongly suggest that competition with selfish genetic elements drives *rhi* evolution.

Results

rhino (*rhi*) mutations trigger Chk2-dependent axis specification defects

Mutations that disrupt the piRNA pathway lead to female sterility and defects in posterior and dorsal-ventral axis specification, which result from activation of DNA damage signaling through ATR and Chk2. Mutations in the *rhi* locus, which encodes an HP1 homologue, also lead to female sterility and defects in dorsal-ventral and posterior patterning (Volpe et al., 2001). We analyzed double-mutant combinations with *mei-41* and *mnk*, which encode ATR and Chk2, to determine the role of DNA-damage signaling in the *rhi* mutant phenotype. For these studies, we initially scored defect in dorsal appendages. These eggshell structures are induced through Gurken (Grk) signaling from the oocyte to the dorsal somatic follicle cells during midoogenesis (Schupbach, 1987). Appendages do not form in the absence of Grk, a single appendage forms with low Grk levels, and two appendages form when signaling is normal (Gonzalez-Reyes et al., 1995; Roth et al., 1995). As shown in Table 1, *mnk* dramatically suppresses the appendage defects associated with *rhi*. Two appendages are present on 100% of the embryos derived from wild type and on 93.6% of the embryos derived from *mnk* single mutants (Table 1). By contrast, only 17.2% of the embryos derived from rhi^{KG}/rhi^{2} mutant females have 2 dorsal appendages. However, 80.5% of the embryos derived from *mnk rhi* double mutants show wild type appendage morphology. Consistent with these observations, rhi^{KG}/rhi^{2} disrupt dorsal localization of Grk and posterior localization of Vasa (Vas) during mid-oogenesis, and localization of both morphogens is restored in *mnk rhi* double mutants (Figure 1).

Mutations in *mei-41,* which encodes ATR, partially suppress the eggshell defects associated with rhi^{KG}/rhi^{2}, with 32.9 % of the embryos from *mei-41;*rhi^{KG}/rhi^{2} double mutants showing normal appendages. *mei-41* mutations are also less effective than *mnk* in suppressing appendage defects associated with the piRNA pathway mutants *armi* and *aub* (Klattenhoff et al., 2007). Chk2 can be activated by both ATM and ATR (Wang et al., 2006). We therefore speculated that partial suppression of *rhi* and *armi* by *mei-41* reflects redundant Chk2 activation by both of these kinases. Caffeine inhibits ATM and to a lesser extent ATR (Sarkaria JN et al., 1999). We therefore tested caffeine for the ability to suppress the patterning defect in *rhi* and *armi* mutants by feeding adults a 2% solution of drug mixed with yeast paste (Table 1). 17% of the embryos from rhi^{KG}/rhi^{2} females have wild type appendages, while 88.4 % of the embryos from rhi^{KG}/rhi^{2} females fed caffeine show normal appendages (5 fold increase). Similarly, 1.8% of embryos from $armi^{72.1}/armi^{1}$ females have 2 appendages, while 10.6% of the embryos from $armi^{72.1}/armi^{1}$ females that were fed caffeine show wild type appendages (6 fold increase). Strikingly, 83% of embryos from *mei-41; armi* double mutants fed caffeine had 2 appendages. These results suggest that *rhi* and *armi* mutations lead to both ATR and ATM dependent activation of Chk2.

Mutations in the meiotic DSB repair pathway also lead to axis specification defects that result from activation of a damage signaling pathway that includes the ATR and Chk2 kinases (Bartek et al., 2001) (Abdu et al., 2002; Ghabrial and Schupbach, 1999). The axis specification defects associated with these mutations are also suppressed by *mei-W68,* which encodes the *Drosophila* homologue of the Spo11 nuclease that catalyzes meiotic double strand break formation (McKim and Hayashi-Hagihara, 1998). By contrast, *mei-*

W68 does not suppress the dorsal appendage defects associated with *rhi* (Table 1). Similarly, the axis specification defects associated with *armi* are not suppressed by *mei-W68* (Klattenhoff et al., 2007). Activation of DNA damage signaling in *rhi* and piRNA pathway mutants thus appears to be independent of meiotic break formation.

To determine if *rhi* nonetheless leads to DSBs in the germline, we labeled mutant ovaries for the phosphorylated form of the *Drosophila* histone H2AX (γ–H2Av), which accumulates on chromosomes near break sites (Modesti and Kanaar, 2001; Redon et al., 2002). Labeling with an anti-phosphoprotein antibody specific for γ-H2Av (Gong et al., 2005) reveals foci in region 2 of the germarium, where meiotic DSBs are formed (Figure 1B) (Jang et al., 2003). In *rhi* mutants, by contrast, prominent γ–H2Av foci are present in germline cells of the germarium, and these foci persist and increase in intensity as cysts mature and bud to form stage 2 egg chambers (Figure 1B). These findings indicate that the axis specification defects in *rhi* mutants are due to DNA breakage and activation of and ATM/ATR/Chk2 damage signaling pathway.

Table 1.

Maternal Genotype	Dorsal Appendage Phenotype (%)			Hatch Rate (%)	N
	2 (wild type)	1 (fused)	0 (absent)		
mnk^{P6} / mnk^{P6}	93.6	2.5	3.9	72.6	827
mei41^{D3} / mei41^{D3}	100	0	0	0	920
meiW68^{1} / meiW68^{K05603}	94.3	4	1.7	67.2	1281
rhi^{02086} / rhi^{KG00910}	17.2	66.5	16.3	0	700
mnk^{P6} rhi^{02086} / mnk^{P6} rhiK^{G00910}	80.5	14.5	5	0	689
mei41^{D3} / mei41^{D3} ; rhi^{02086} / rhi^{KG00910}	32.9	53.3	13.8	0	732
meiW68^{K05603} rhi^{02086} / meiW68^{1} rhi^{KG00910}	18.7	58.5	22.8	0	244
rhi^{02086} / rhi^{KG00910} 2% caffeine	88.4	6.6	5	0	473
armi$^{72.1}$ / armi^{1}	1.8	24.7	73.6	0	227
armi$^{72.1}$ / armi^{1} 2% caffeine	10.6	29.6	59.8	0	477
mei41^{D3} / mei41^{D3} ; armi$^{72.1}$ / armi^{1}	56	38.4	5.6	0	575
mei41^{D3} / mei41^{D3} ; armi$^{72.1}$ / armi^{1} 2% Caffeine	83.2	11.9	4.9	0	226
rhi^{02086} / rhi^{KG00910}; GFP-Rhino/Gal4 nos	96.1	3.6	0.3	74	483

Table 1. *mnk* and *mei-41* mutations suppress D-V patterning defects in *rhi* mutants. Treatment with 2% caffeine also strongly suppresses D-V patterning defects in *rhi* mutants and to a lesser extent in *armi* mutants. Two dorsal appendages are normally present at the dorsal side of a wild type *Drosophila* egg. The mutant phenotypes are classified as weakly ventralized, which results in fusion of the dorsal appendages, and strongly ventralized, resulting in absence of dorsal appendages.

Figure 1.

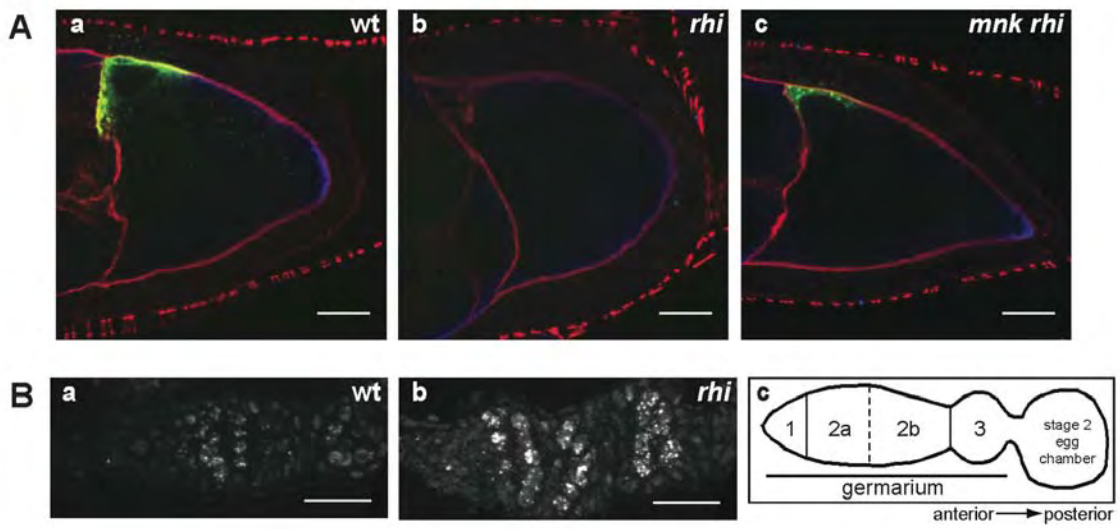
A
a
wt
b
rhi
c
mnk rhi
B
a
wt
b
rhi
c
1
2a
2b
3
stage 2
egg
chamber
germarium
anterior
posterior

Figure 1. A. *mnk* mutation restores Gurken and Vasa protein localization in *rhi* mutants. (a) In a stage 9 wild type oocyte, Grk (green) is localized at the dorsal anterior cortex near the oocyte nucleus and Vas (blue) is localized at the posterior cortex. Actin filaments (red) mark the cell boundaries (b) In rhi^{KG}/rhi^{2} egg chambers, this localization pattern is lost, with Grk and Vas dispersed throughout the oocyte. (c) mnk^{p6} suppresses the rhi^{KG}/rhi^{2} phenotype, and rescues Grk and Vas localization during late oogenesis. Images were acquired under identical conditions for either stage. Projections of 2 serial 0,6 μm optical sections are shown. Scale bars for are 20 μm.

B. *rhi* mutants have increased DNA damage in the germline. Ovaries from (a) wild type and (b) rhi^{KG}/rhi^{2} flies were fixed and immunostained with an antibody against phosphorylated H2Av (γ–H2Av). (a) Foci of γ–H2Av are observed in wild type in region 2a and 2b of the germarium and correspond to the DSBs induced during meiotic recombination. (b) In rhi^{KG}/rhi^{2} mutants, much larger foci also appear in region 2a of the germarium but persist in region 3 and the developing egg chambers. Samples were labeled and images were acquired under identical conditions. Projections of 5 serial 1μm optical sections are shown. Posterior is oriented to the right. Scale bar is 20 μm. (c) A schematic representation of the regions of the germarium and a developing egg chamber.

Rhino is required for transposon silencing in the female germline

The above observations suggested that *rhino* could function in the piRNA pathway, which is required for silencing of the *stellate* locus during spermatogenesis and transposable elements during female germline development. Over-expression of *Stellate (Ste)* leads to accumulation of Stellate protein crystals in the testes (Bozzetti et al., 1995). However, we did not find *Stellate* crystals in *rhi* mutant testes (Figure 2). This finding is consistent with the observation that Rhi is expressed at very low levels during spermatogenesis (Volpe et al., 2001), and we find that *rhino* mutant males are fertile (not shown). By contrast, *rhino* mutant females are sterile and show patterning defects characteristic of defects in the piRNA pathway. We therefore focused our analysis of transposon expression during oogenesis.

The piRNA pathway has been implicated in heterochromatic silencing of protein coding genes in somatic cells, as well as transposon silencing in the germline. We therefore initiated a genome wide analysis of both transposon and protein coding gene expression using tiling arrays that include heterochromatic and repeated sequences. For these studies, we assayed transcript expression in ovaries from 2 to 4 day old females. The dissected ovaries were visually inspected to confirm similar egg chamber stage distribution, and analysis of protein coding gene expression indicates that similar stages were present in each sample (see below). Mutations in *rhino* and the piRNA pathway gene *armi* lead to over-expression of a significant fraction of transposons in the *Drosophila* genome, with a subset showing up to 80 fold increases in transcript accumulation (Figure 3A-B). The telomeric transposon *Het-A* shows the greatest fold induction in *rhino* and *armi* and we have confirmed this dramatic increase in expression by northern blot (Figure

4). *Het-A* is a LINE element, but genome wide we find that retrotransposons are enriched in the pool of highly over-expressed elements (Figure 3F).

The *rhino* gene encodes an HP1 homologue, and HP1 is known to function in heterochromatic silencing in somatic cells. In addition, several genes in the piRNA pathway has been implicated in position effect variegation (PEV), which reflects changes in gene expression that are linked to spreading of heterochromatin from centromeric and telomeric regions. We therefore speculated that *rhino* and mutations in known piRNA pathway genes would lead to over-expression of germline protein coding genes located in heterochromatin. However, the expression of protein coding genes, including genes in heterochromatin, is not significantly altered by *rhino* or *armi* mutations (Figure 3C-D). This is visually displayed in plots of expression level of annotated genes in mutant vs. control samples, where all points scatter around a line with a slope of 1 (Figure 3C-D). Note that linear scales are used in the plots, and none of genes show a change of more that 25% up or down. These observations indicate that the changes in transposon expression in piRNA pathway and *rhino* mutants are unlikely to reflect changes in general heterochromatin structure. Most of the RNA in the ovary samples used in these studies is derived from germline cells, and these results may differ from observations in somatic cells due to properties of heterochromatin that are specific to the germline.

These findings demonstrate that the mutations in *rhi* and the piRNA pathway gene *armi* lead to nearly identical defects in oocyte patterning and transposon expression, suggesting a direct role for the Rhino protein in piRNA production or function. To distinguish between these alternatives, we used deep sequencing to assay piRNA

production in *rhino* mutant ovaries and ovaries derived from control females (see methods).

Figure 2.

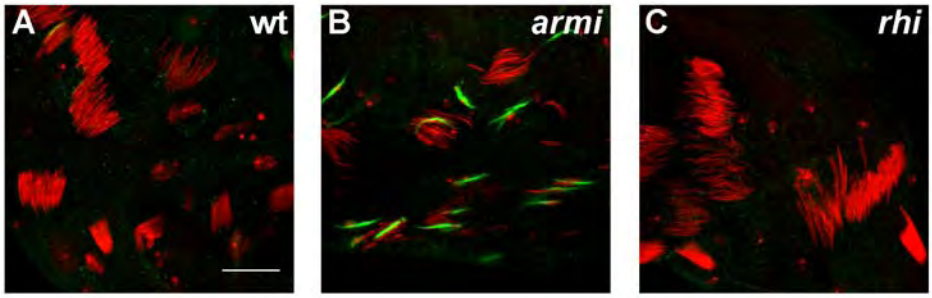

Figure 2. *Stellate* locus is properly silenced in *rhi* mutant testes. The testes from (A) wild type, (B) *armi72.1/armi1,* (C) *rhiKG/rhi2* flies were stained for DNA (red) and Stellate protein (green). (A and C) No Stellate protein is expressed in wild type and *rhiKG/rhi2* testes. (B) In *armi72.1/armi1* mutant testes Stellate protein accumulates and forms crystals. Projections of 5 serial 1μm optical sections are shown. Images were acquired under identical conditions. Scale bar is 20 μm.

Figure 3.

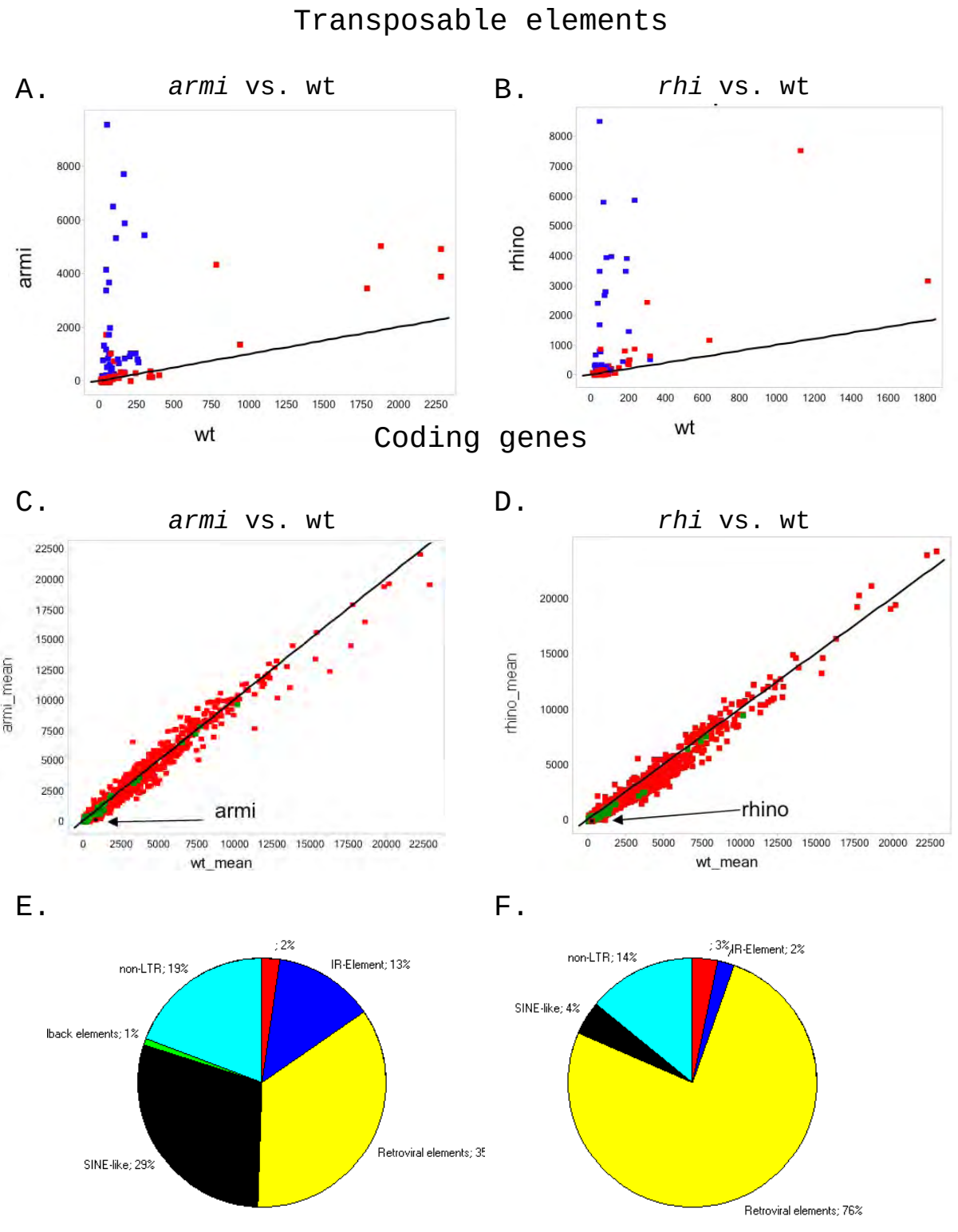
Transposable elements
A.
armi vs. wt
armi
wt
B.
rhino vs. wt
rhino
wt
Coding genes
C.
armi vs. wt
armi_mean
wt_mean
armi
D.
rhino vs. wt
rhino_mean
wt_mean
rhino
E.
non-LTR; 19%
IR-Element; 13%
Iback elements; 1%
SINE-like; 29%
Retroviral elements; 3
F.
non-LTR; 14%
IR-Element; 2%
SINE-like; 4%
Retroviral elements; 76%

Figure 3. *rhi* is required to silence transposable elements in the female germline.

(A-D) Scatter plots representing transcript expression levels in mutant vs control ovaries. (A-B) transposable element transcripts in the *Drosophila* genome, significantly over-expressed subfamilies shown in blue. Each point represents a subfamily. (A) *armi* vs control. (B) *rhi* vs control. (C-D) coding gene transcripts in the *Drosophila* genome, euchromatic genes shown in red, heterochromatic genes shown in green, *armi* and *rhi* transcripts shown in black (C) *armi* vs control. (D) *rhi* vs control.

(E-F) Distribution of copy numbers of each transposable element family encoded in the *Drosophila* genome (E) and over-expressed in rhi mutant ovaries (F).

Figure 4.

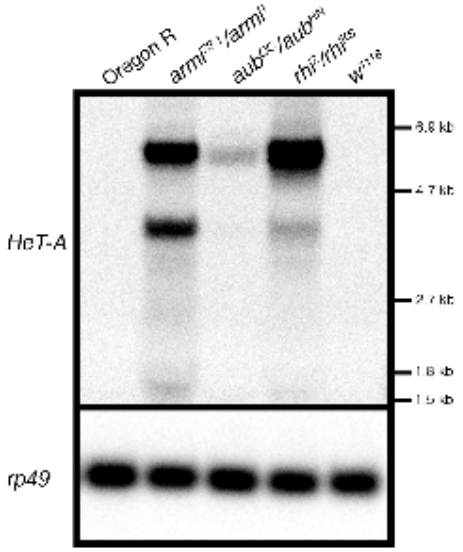
Oregon R
armi72.1/armi1
aub5C/aub5N
rhi2/rhi2
w1118
HeT-A
rp49
8.8 kb
4.7 kb
2.4 kb
1.8 kb
1.5 kb

Figure 4. *HeT-A* retrotransposon is over-expressed in *rhi* mutant ovaries.

HeT-A transcript can be detected by Northern blot in RNA from $armi^{72.1}/armi^{1}$, rhi^{KG}/rhi^{2} and aub^{QC42}/aub^{HN2} mutant ovaries, but not from wild type or w^{1118} ovaries.

Rhino is required for piRNA production

HP1 and the piRNA pathway have been implicated in PEV and heterochromatin formation In somatic tissues (Brower-Toland et al., 2007; Pal-Bhadra et al., 2002; Pal-Bhadra et al., 2004), and we speculated that the Rhino HP1 homolgue could have a similar function in the germline. Additionally, Rhino could be required for piRNA production. We therefore performed small RNA deep sequencing to assay piRNA production in *rhi* mutants. *rhi* mutations lead to a substantial reduction in piRNA production from a number of piRNA clusters (as defined by Brennecke et al., 2007), including major piRNA clusters on chromosome 2R and 4 (Figure 5A and C). However, clusters located in chromosomes 3 and X chromosomes are not noticeably affected in *rhi* mutants (Figure 5B and D).

We also find that production of piRNAs from 126 of the 138 transposable element families in the *Drosophila* genome are significantly reduced in *rhino* mutants, with the most pronounced decrease in the anti-sense piRNAs, which are putative effectors in the silencing process (examples shown in Figure 6A'-B'). Figure 6A'D-F shows sense and anti-sense piRNAs for *HeT-A*, a telomeric transposon that is highly over-expressed in *rhi* and other piRNA pathway mutants. We have confirmed that piRNAs for *HeT-A* decrease in *rhi* mutants by northern blot (Figure 8). To determine the effect of *rhino* on piRNA production genome wide, we plotted the abundance of sense and antisense piRNAs in control vs *rhi* mutants, for all of the transposon families in *Drosophila.* As shown in Figure 7, *rhi* mutations lead to a significant loss of sense and anti-sense strand piRNAs from the vast majority of elements.

Intriguingly, a subset of 12 elements show little change in antisense piRNAs and an increase in sense strand piRNAs. As an example we show *mdg1* (Figure 6C'). Some of

these elements may be expressed primarily in the soma, and Rhino appears to be restricted to the germline (see below). A subset of sense and anti-sense piRNAs show a 10 bp overlap and have sense strand A bias at position 10 and an antisense strand bias for a U a position 1. These pairs suggest that piRNA may be produced by a ping-pong mechanism. In *rhi* mutants, most elements show a reduction in these ping-pong pairs (Figure 6A' and B', B,G and H), including elements that do not show a decrease total piRNA production (i.e. *mdg1*; Figure 6C', B,G an H). These observations suggest that ping-pong pairs, rather than total piRNAs, have a critical role in transposon silencing.

Figure 5

A.

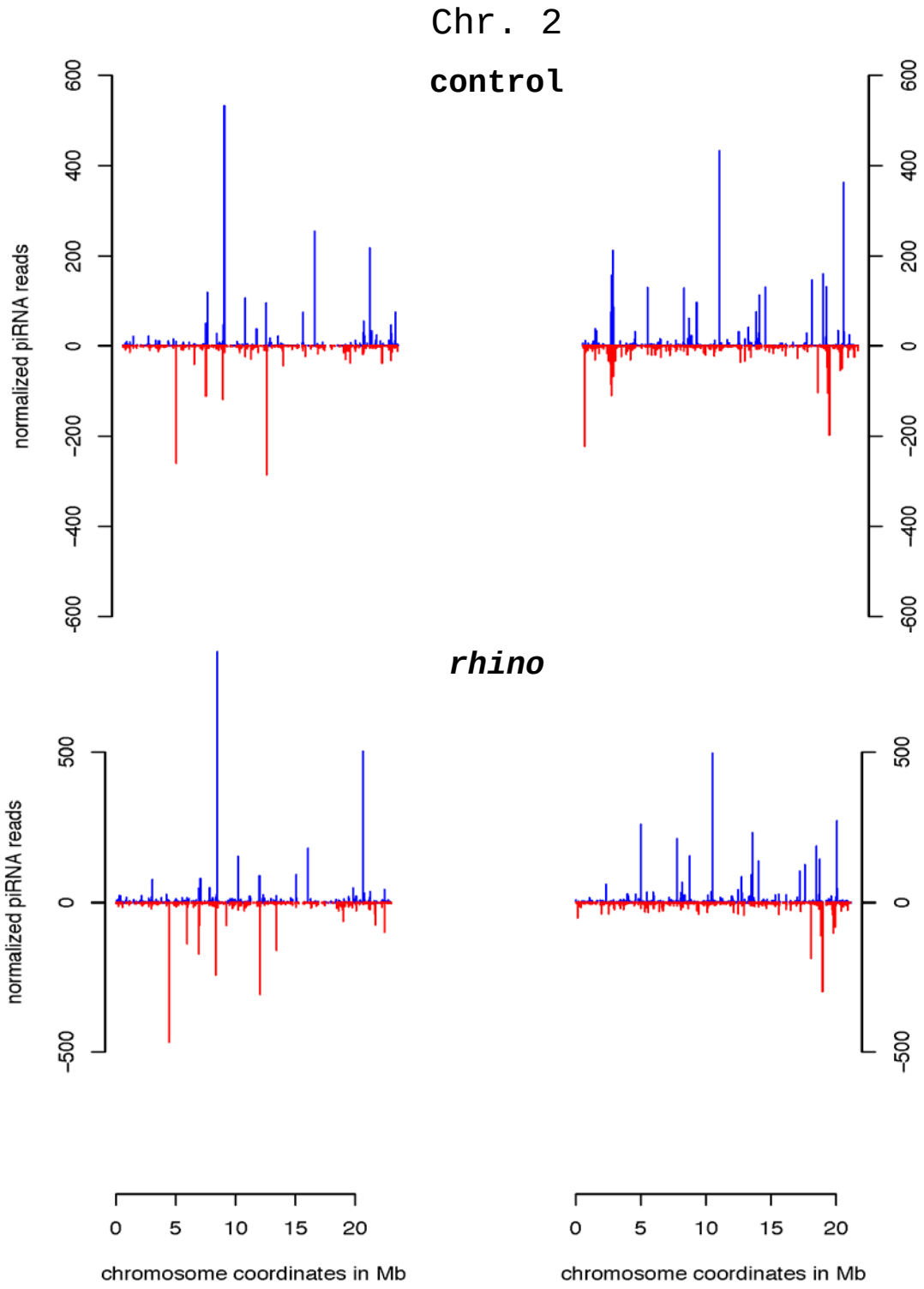
Chr. 2
control
rhino
normalized piRNA reads
normalized piRNA reads
600
400
200
0
-200
-400
-600
500
0
-500
0
5
10
15
20
chromosome coordinates in Mb
chromosome coordinates in Mb

B.

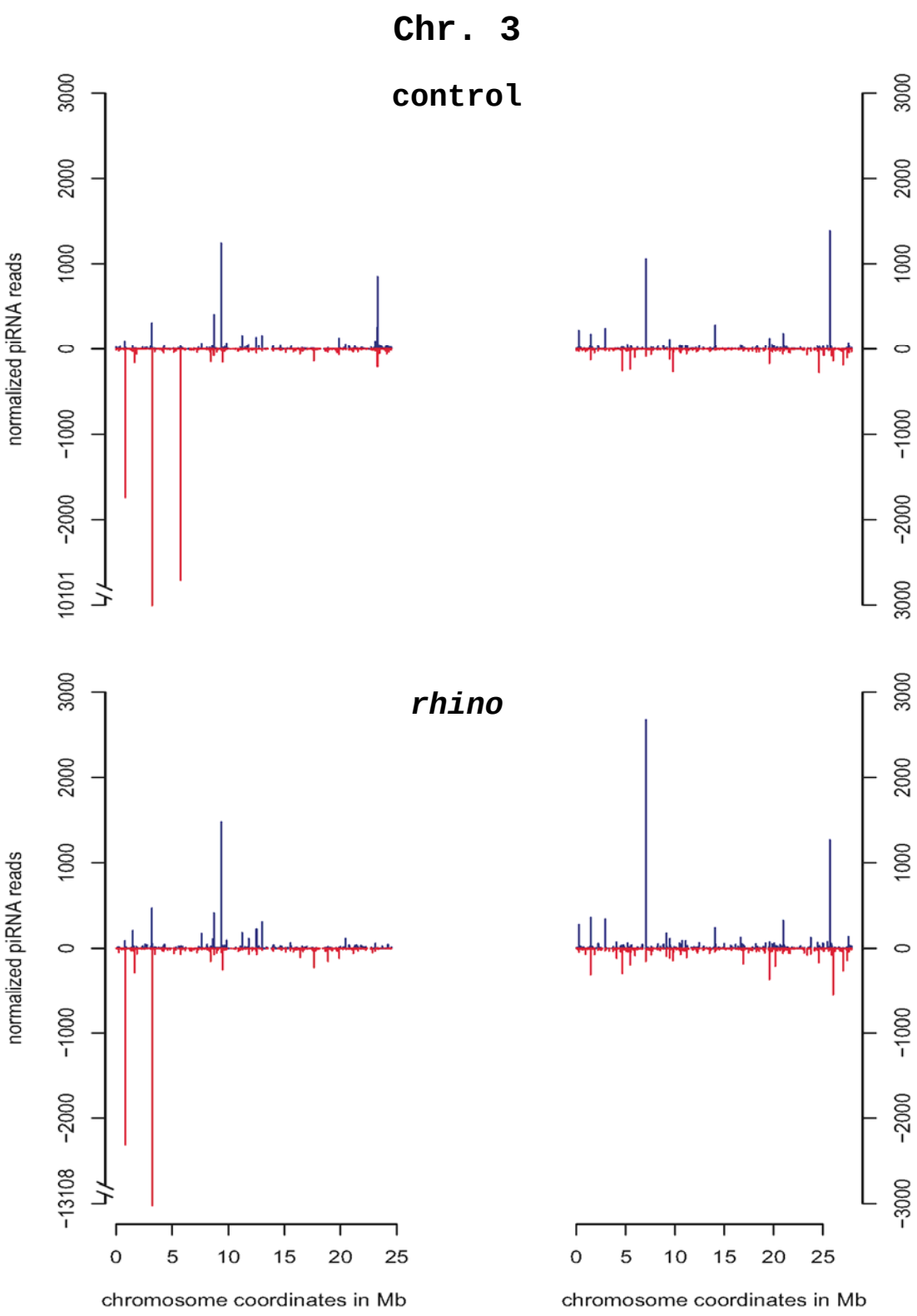
Chr. 3
control
rhino
normalized piRNA reads
normalized piRNA reads
3000
2000
1000
0
−1000
−2000
10101
−13108
−3000
0
5
10
15
20
25
chromosome coordinates in Mb
chromosome coordinates in Mb

C.

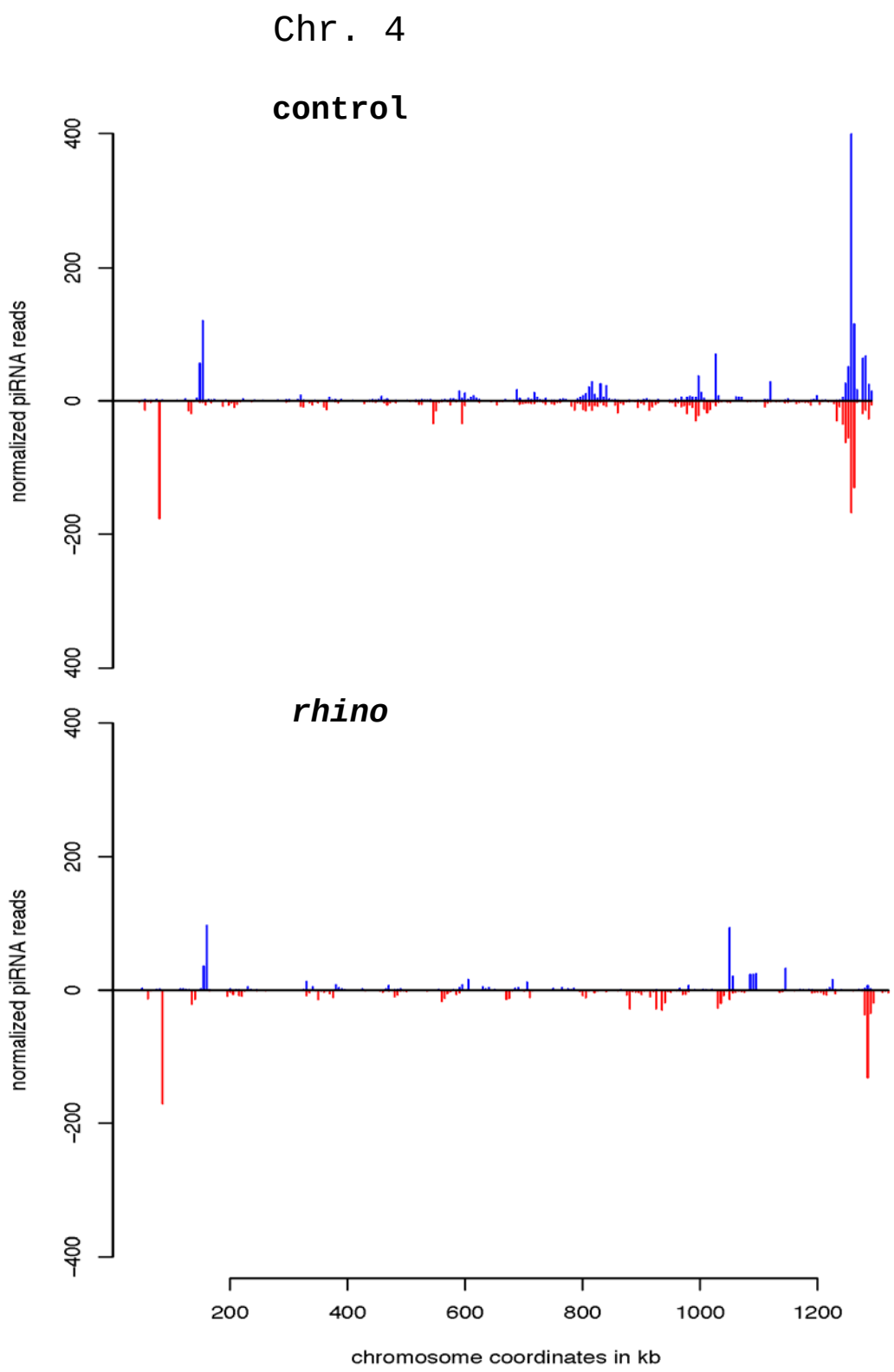
Chr. 4
control
rhino
normalized piRNA reads
normalized piRNA reads
400
200
0
-200
400
400
200
0
-200
-400
200
400
600
800
1000
1200
chromosome coordinates in kb

D.

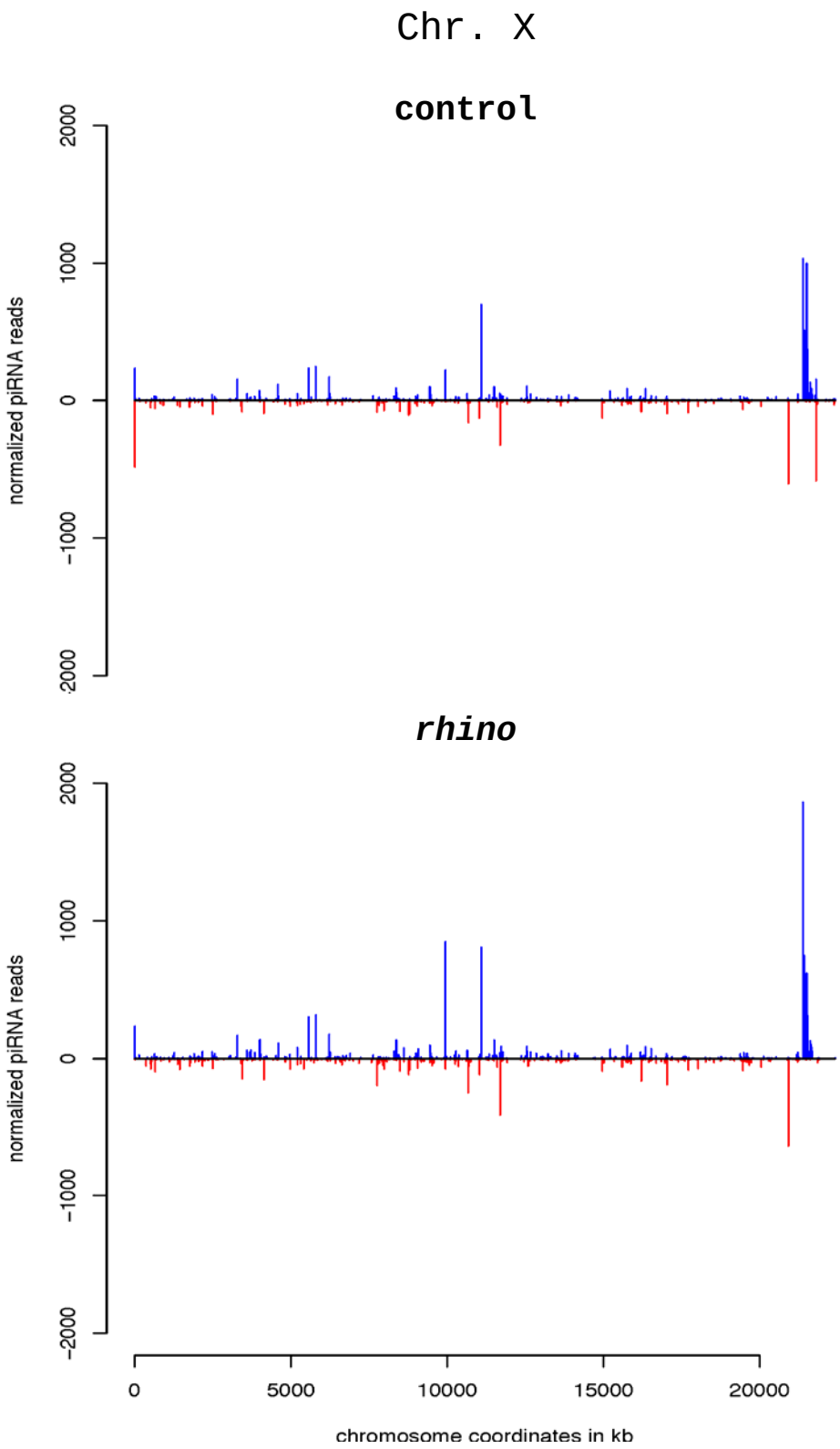
Chr. X
control
rhino
normalized piRNA reads
2000
1000
0
−1000
−2000
0
5000
10000
15000
20000
chromosome coordinates in kb

Figure 5. *rhi* is required to produce piRNAs from distinct loci.

Normalized piRNA read distribution mapping across chromosome arms in $cn^{1}; ry^{506}$ used as control (top panel) and *rhi* mutant ovaries (bottom panel). Blue bars represent + strand and red bars represent - strand. (A) Chromosome 2. (B) Chromosome 3. (C) Chromosome 4. (D) Chromosome X.

Figure 6.

A’.

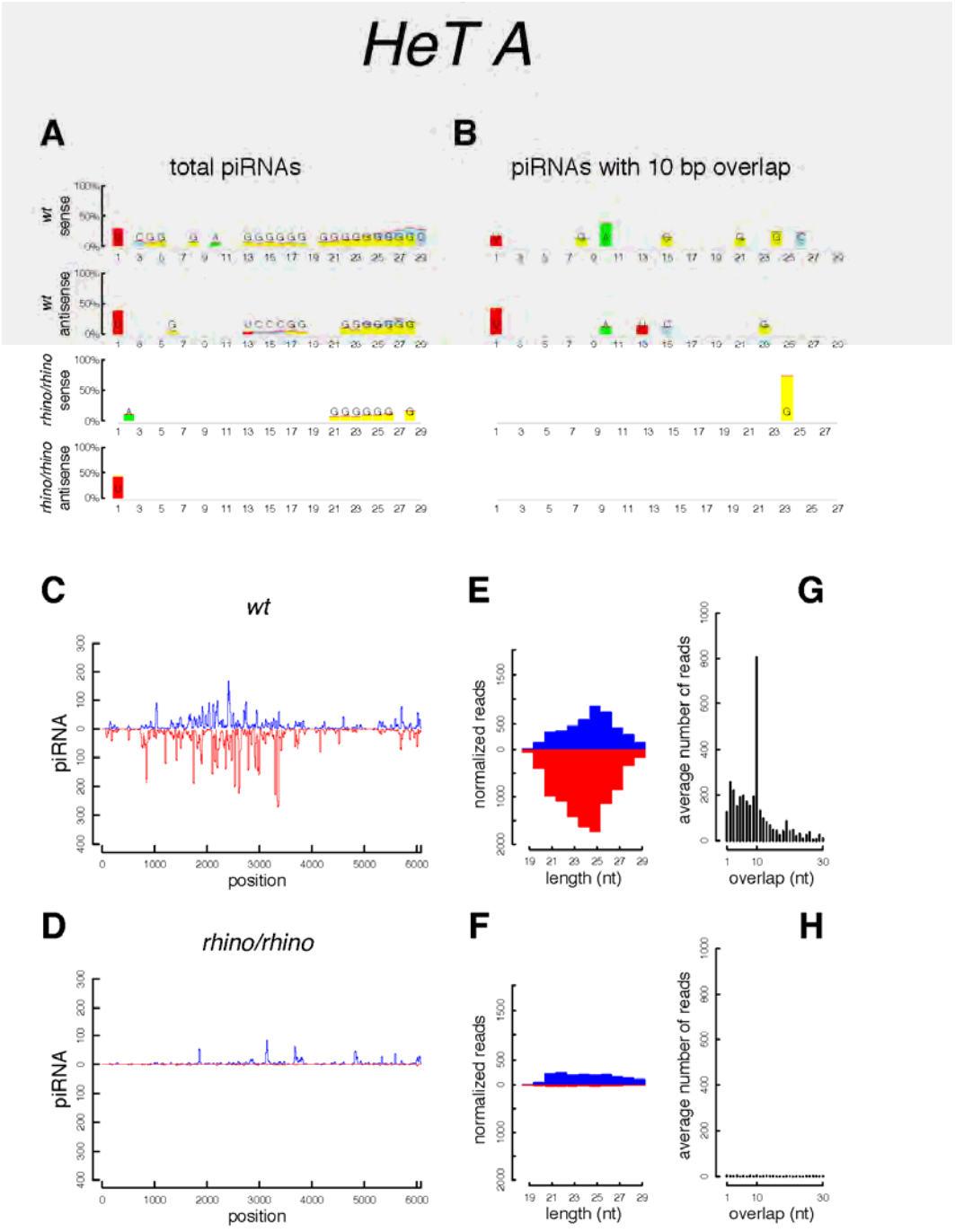
HeT A
A
total piRNAs
B
piRNAs with 10 bp overlap
wt sense
wt antisense
rhino/rhino sense
rhino/rhino antisense
C
wt
piRNA
position
D
rhino/rhino
piRNA
position
E
normalized reads
length (nt)
F
normalized reads
length (nt)
G
average number of reads
overlap (nt)
H
average number of reads
overlap (nt)

B’.

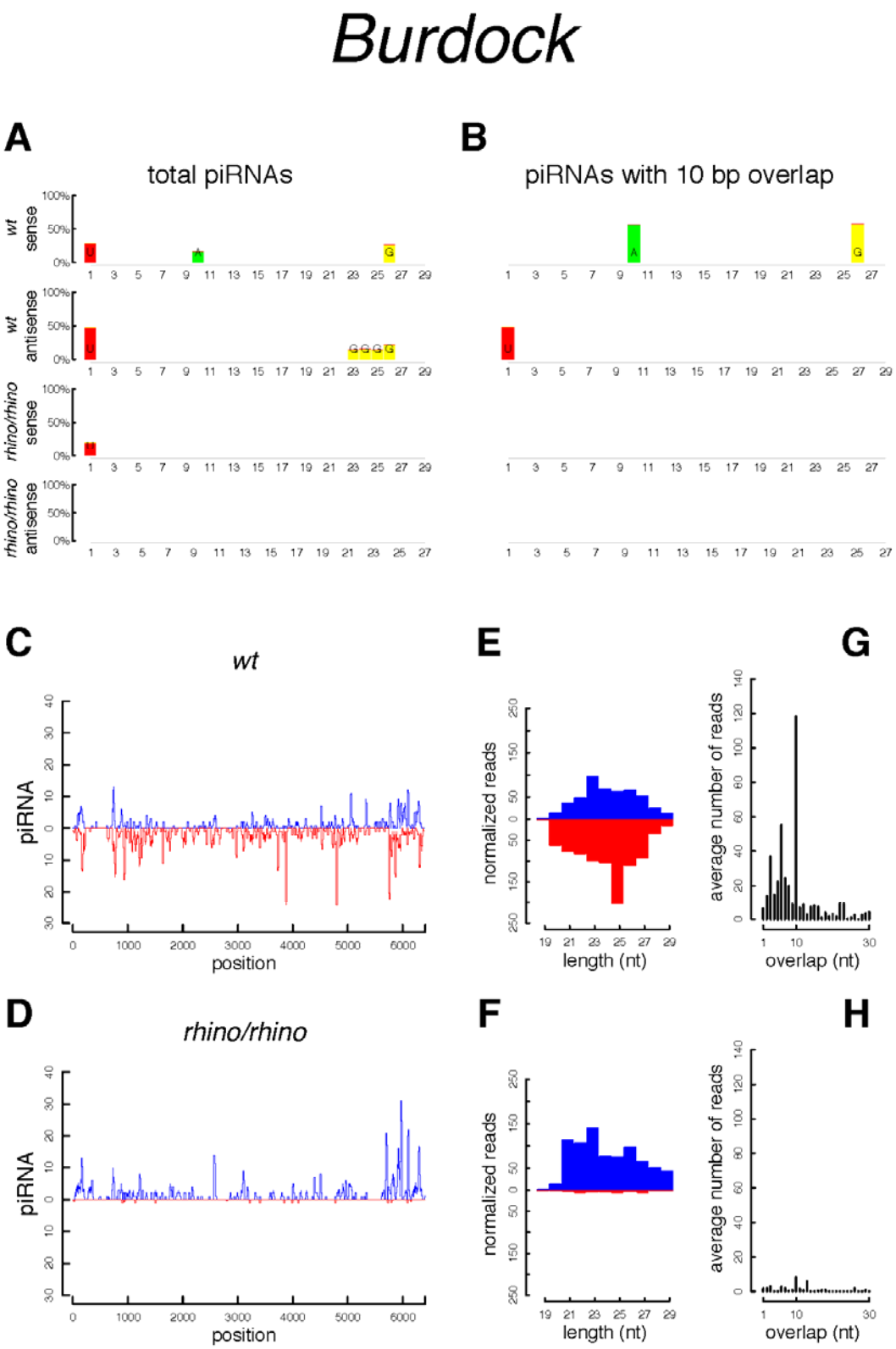
Burdock
A
total piRNAs
wt sense
wt antisense
rhino/rhino sense
rhino/rhino antisense
B
piRNAs with 10 bp overlap
C
wt
piRNA
position
D
rhino/rhino
piRNA
position
E
normalized reads
length (nt)
F
normalized reads
length (nt)
G
average number of reads
overlap (nt)
H
average number of reads
overlap (nt)

C’.

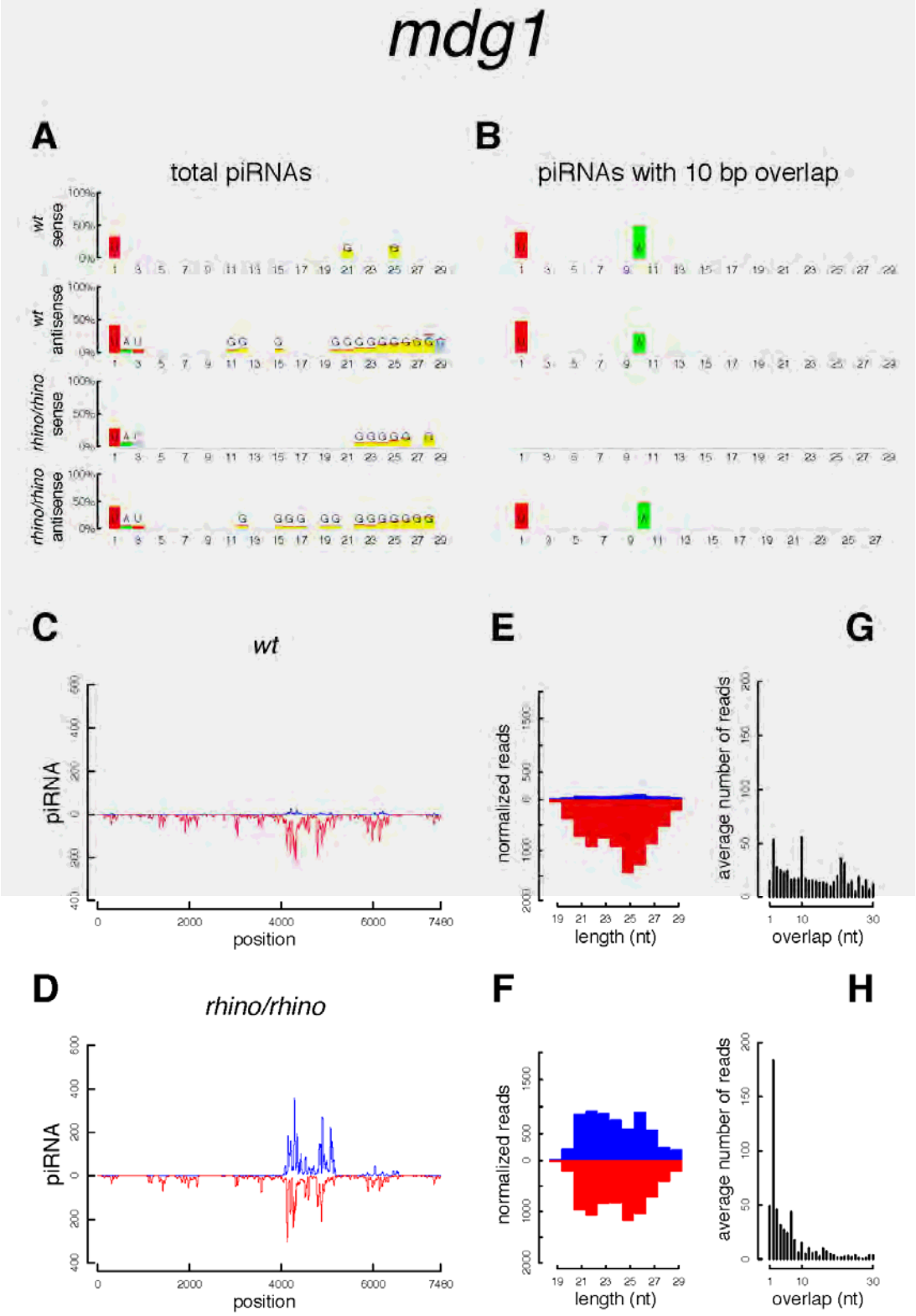
mdg1
A
total piRNAs
B
piRNAs with 10 bp overlap
wt sense
wt antisense
rhino/rhino sense
rhino/rhino antisense
C
wt
piRNA
position
D
rhino/rhino
E
normalized reads
length (nt)
F
G
average number of reads
overlap (nt)
H

Figure 6. piRNA production for *Het-A, Burdock* and *mdg-1* transposons.

piRNAs mapping to (A') *Het-A*, (B') *Burdock* and (C') *mdg-1* in ovaries.

(A) Nucleotide bias for every position across total piRNAs. (B) Nucleotide bias for every position across piRNAs with a 10 nt overlap. (C-D) Total piRNAs mapping across the transcript sequence in (C) control and (D) *rhi*. Blue bars represent sense and red bars represent antisense piRNAs. (E-F) Size distribution of piRNAs in (E) control and (F) *rhi* . Blue bars represent sense and red bars represent antisense piRNAs. (G-H) nt overlap between total piRNAs in (G) control and (H) *rhi*.

Figure 7.

A.

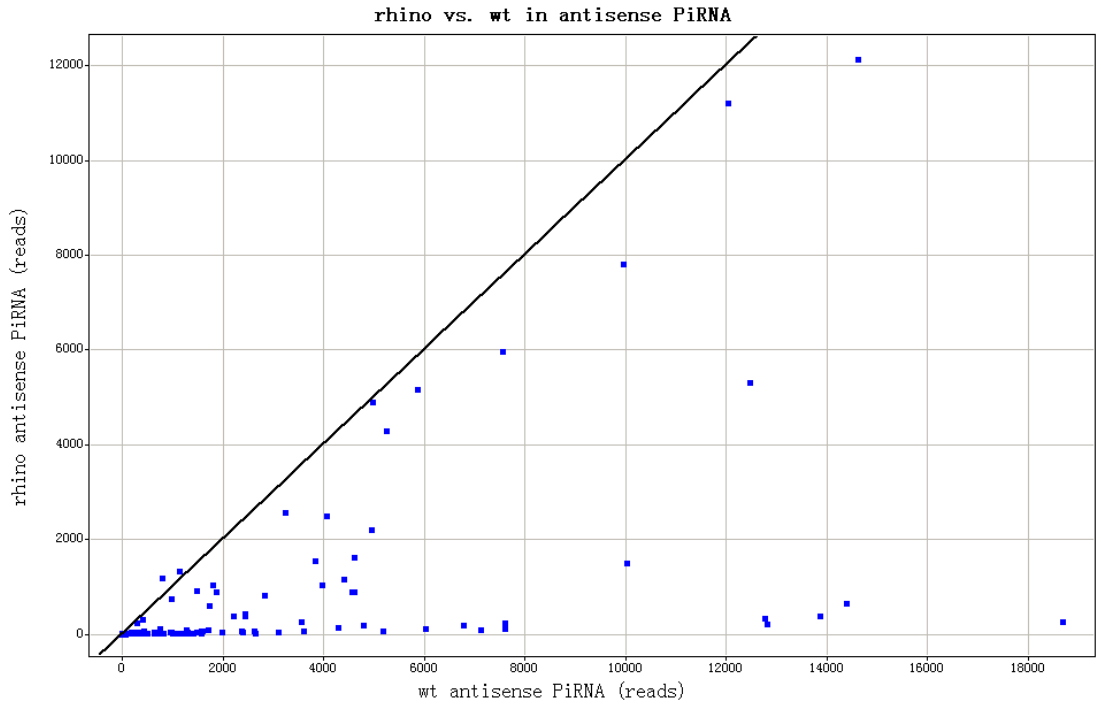
rhino vs. wt in antisense PiRNA
rhino antisense PiRNA (reads)
wt antisense PiRNA (reads)
0
2000
4000
6000
8000
10000
12000
14000
16000
18000

B.

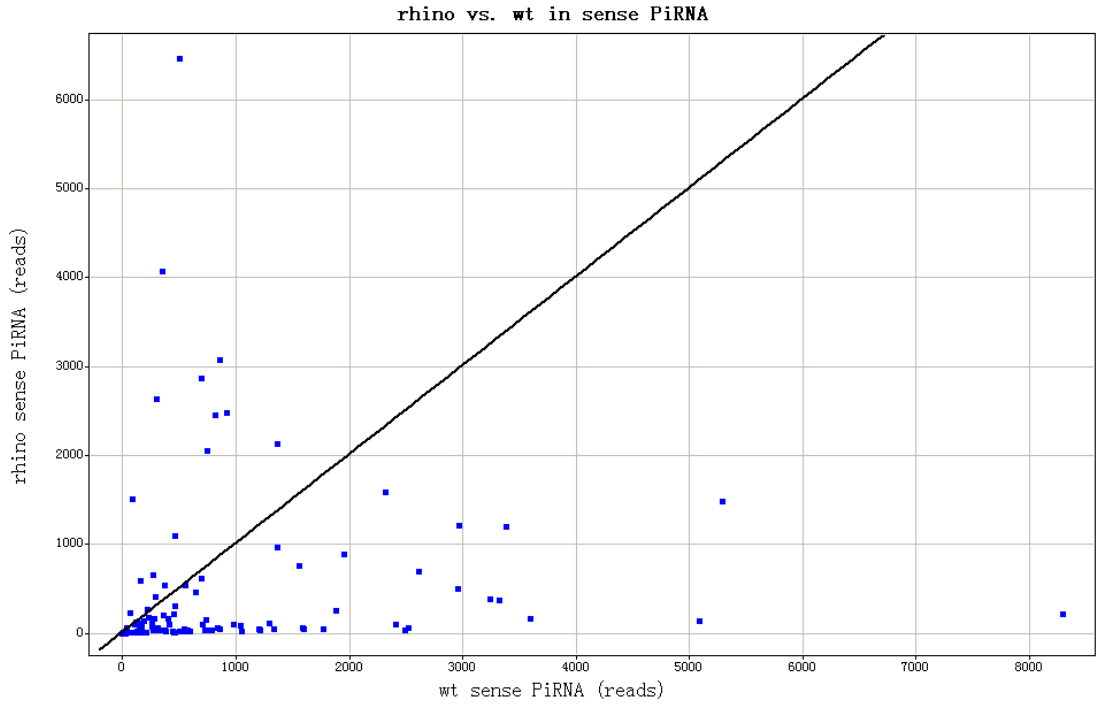
rhino vs. wt in sense PiRNA
rhino sense PiRNA (reads)
wt sense PiRNA (reads)
0
1000
2000
3000
4000
5000
6000
7000
8000

Figure 7. Antisense piRNAs for the majority of transposable elements is decreased in *rhi* mutant ovaries. Plots showing abundance of (A) antisense and (B) sense piRNAs in control vs *rhi* mutants, for all of the transposon families in *Drosophila.*

Figure 8.

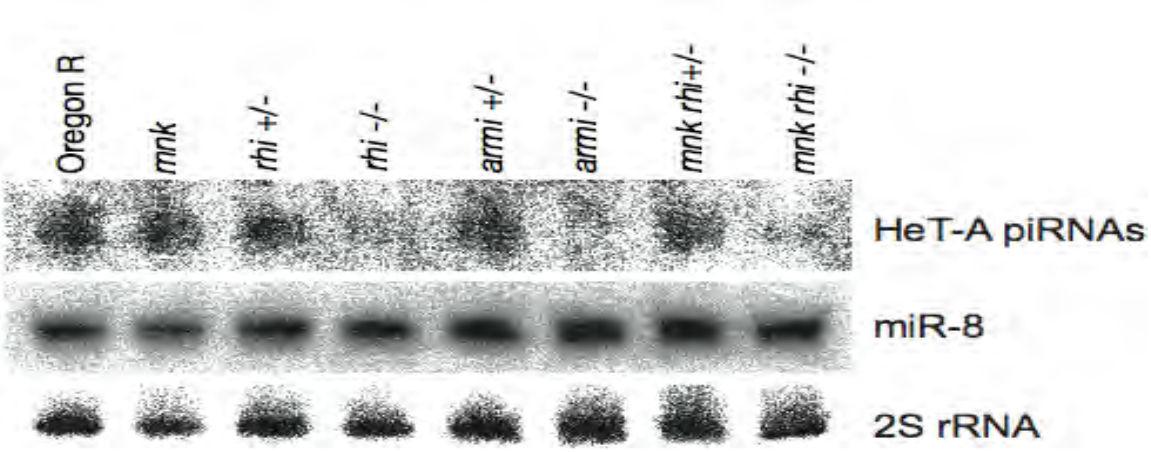
Oregon R
mnk
rhi +/-
rhi -/-
armi +/-
armi -/-
mnk rhi+/-
mnk rhi -/-
HeT-A piRNAs
miR-8
2S rRNA

Figure 8. *rhi* is required to produce and *HeT-A* piRNAs.

HeT-A piRNAs can be detected by Northern blot in RNA from Oregon R, *mnk* ,*rhi/+* , *armi/+*, and *mnk rhi/+* ovaries, but not from *rhi*, *armi* or *mnk rhi* ovaries. By contrast, the miRNA miR-8 is not affected by any of these mutations. 2SrRNA was used as a loading control.

Piwi class protein localization is disrupted in *rhino* mutants

The defects in piRNA production in *rhi* mutants raised the possibility that expression of genes involved in biogenesis of these RNAs is reduced. However, we did not observe a significant reduction in the expression of any protein coding genes (Figure 3C-D), including genes in the piRNA pathway, by whole genome tiling array (data not shown). We have not been able to quantify the amount of Piwi, Aub and Ago3 protein mutant ovaries, because the antibodies we generated do not work efficiently in western blotting. However, these antibodies efficiently label the expected germline structures in wild type ovaries, and signal is eliminated by mutations in the corresponding gene, indicating that these reagents are useful for immunofluorescence analysis of *in situ* protein localization (Figure 9). Nuclear localization of Piwi and peri-nuclear localization of Aub and Ago3 are disrupted in *rhi* mutants (Figure 9). Previous studies indicate that mutations in *spnE* and *aub* also disrupt piwi family protein localization (Lim and Kai, 2007). These findings provide further evidence that Rhino is a critical component of the piRNA biogenesis pathway, and suggest that wild type piRNA production is required for localization of piwi proteins to the correct subcellular compartment. Localization of Vasa, a core component of Nuage, is also disrupted by *rhi*, *spnE* and *aub* mutations (Figure 10 and (Lim and Kai, 2007). It is interesting to note that mutations in *rhi* do not eliminate piRNAs, and the levels of total piRNA from some transposons do not change or increases in these mutants (Figure 6). Assembly of nuage, which appears to represent an RNA processing compartment, thus appears to dependent on a subset of piRNAs that also appear to be critical to transposon silencing.

Figure 9.

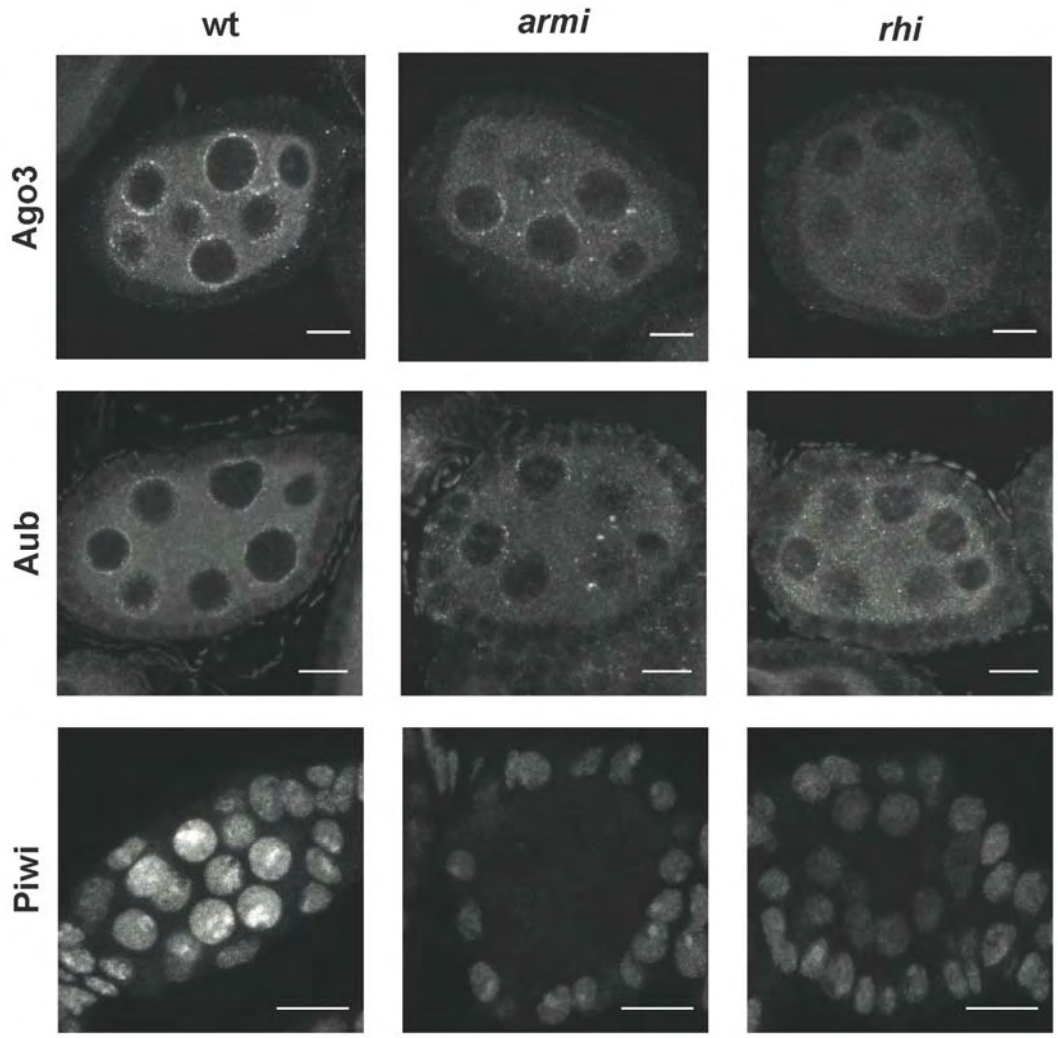

Figure 9. *rhi* mutation disrupts localization of Piwi class Argonautes in the female germline.

Stage 4-5 (Ago3 and Aub) and stage 2-3 (Piwi) egg chambers of wild type, *rhi* and *armi* mutants ovaries were immunostained with corresponding antibodies. Projection of 3 serial 1μm optical sections, scale bar 10 μm. Ago3 and Aub proteins localize to peri-nuclear nuage compartment in wild type germline. This localization is disrupted in *rhi* and *armi* mutants. Piwi protein localizes to the nuclei of both germline and somatic cells in wild type egg chambers. Only germline nuclear localization of Piwi is disrupted by mutations in *armi* and *rhi*.

Figure 10.

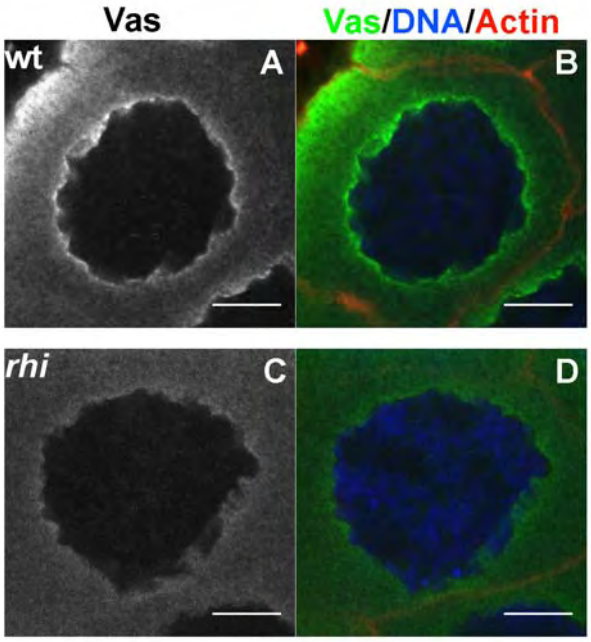

Figure 10. Nuage protein Vas is not localized properly in *rhi* mutants.

Vas localizes to nuage compartment around the nucleus of a stage-6 nurse cell in wild type (A-B), but fails to localize in *rhi* (C-D) mutants. Single optical section, scale bar is 10 μm.

Rhino protein localization

To define the subcellular distribution of Rhino during oogenesis, when this protein is required for transposon silencing and piRNA production, we raised anti-Rhino antibodies and generated transgenic animals expressing a functional GFP-Rhino protein. Immunolocalization with anti-Rhi antiserum and *in vivo* analysis of GFP-Rhino reveals foci within the nuclei of germline cells throughout oogenesis (figure 11A and 13). To determine if the Rhi foci are associated with centromeres or telomeres, we assayed colocalization with the centromere and telomere markers. CID is the *Drosophila* homologue of CENP-A, a centromere-specific histone H3-like protein that is found in the inner kinetochore (Blower and Karpen, 2001). Rhi labeling is associated with a subset of CID foci (Figure 11B). The heterochromatin protein 1/origin recognition complex-associated protein (HOAP) localizes to *Drosophila* telomeres (Cenci et al., 2003). We find that the Rhino is associated with a subset of the telomeric HOAP foci (Figure 11C). These finding suggest that Rhino associated with a subset of pericentromeric and telomeric regions. Significantly, the *rhino* mutations disrupt piRNA production from a subset of peri-centromeric and telomeric piRNA clusters (Figure 5).

Interestingly, Rhi localization to foci within germline nuclei is not disrupted by mutations in the piRNA pathway genes *armi* or *aub* (Figure 12). By contrast, *rhi* mutations disrupt piRNA production and the localization of Piwi, Aub and Ago3 (Figure 9). Taken together, these findings suggest that Rhi functions upstream of the Piwi proteins during piRNA biogenesis. We therefore speculated that Rhino binding may, in part, specify the piRNA cluster. To begin to address this possibility, we performed chromatin immunoprecipition studies using anti-GFP antibodies and females expressing

the functional GFP-Rhi fusion protein. GFP-Rhi localizes to distinct foci in germline nuclei (Figure 13), and rescues the patterning defects and sterility of *rhi* mutants (Table 1), indicating that this is a functional fusion protein. The *rhino* mutations affect production of piRNAs from major clusters located in chromosomes 2 and 4, but do significantly alter piRNA production for a major cluster on chromosome X. We therefore assayed for Rhino binding to regions within these three clusters, relative to the euchromatic *rp49* gene. Consistent with the piRNA profiles, Rhi is enriched at the 2R and 4th chromosome clusters, but shows only background binding to the X chromosome cluster (Figure 11D). These findings support the hypothesis that Rhi acts at the chromatin level to stimulate piRNA production from a set of piRNA clusters.

Figure 11.

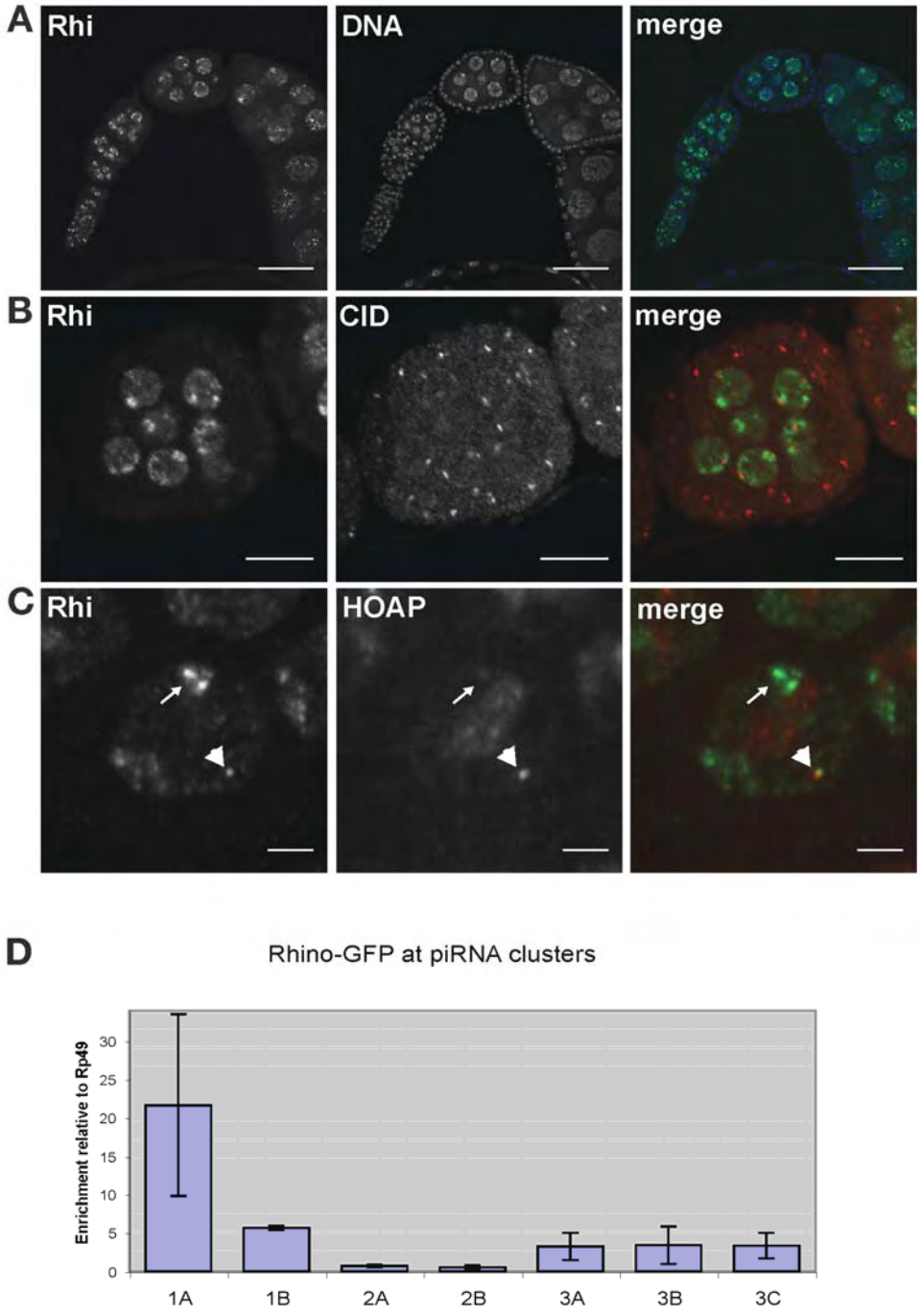
A
Rhi
DNA
merge
B
Rhi
CID
merge
C
Rhi
HOAP
merge
D
Rhino-GFP at piRNA clusters
Enrichment relative to Rp49
0
5
10
15
20
25
30
1A
1B
2A
2B
3A
3B
3C

Figure 11. Rhi localization

(A) Wild type ovaries immunostained with anti-Rhi antiserum show Rhi localizes predominantly to germline nuclei. Scale bar is 25 μm (B) Wild type ovaries immunostained with anti-Rhi antiserum and anti-CID antibody show that Rhi localizes to peri-centromeric regions in stage 3 nurse cell nuclei. Scale bar is 10μm (C) Wild type ovaries immunostained with anti-Rhi antiserum and anti-HOAP antibody show that Rhi partially co-localizes with HOAP in a stage 5 nurse cell nuclei. Arrow points to Rhi foci that do not co-localize with HOAP signal and arrowhead points to co-localized focus. Scale bar is 5 μm. Single optical sections for all panels.

(D) Chromatin Immunoprecipitation from GFP-Rhi expressing flies with anti-GFP antibody. Bars represent enrichment relative to *rp49*. 1A and 1B are different primer pairs for Cluster 1 located in chromosome 2R. 2A and 2B are different primer pairs for Cluster 2 located in chromosome X. 3A, 3B and 3C are different primer pairs for Cluster 3 located in chromosome 4. Rhi protein binds strongly to Cluster located in 2R and less dramatically to Cluster located in 4, but not to the Cluster in X.

Figure 12.

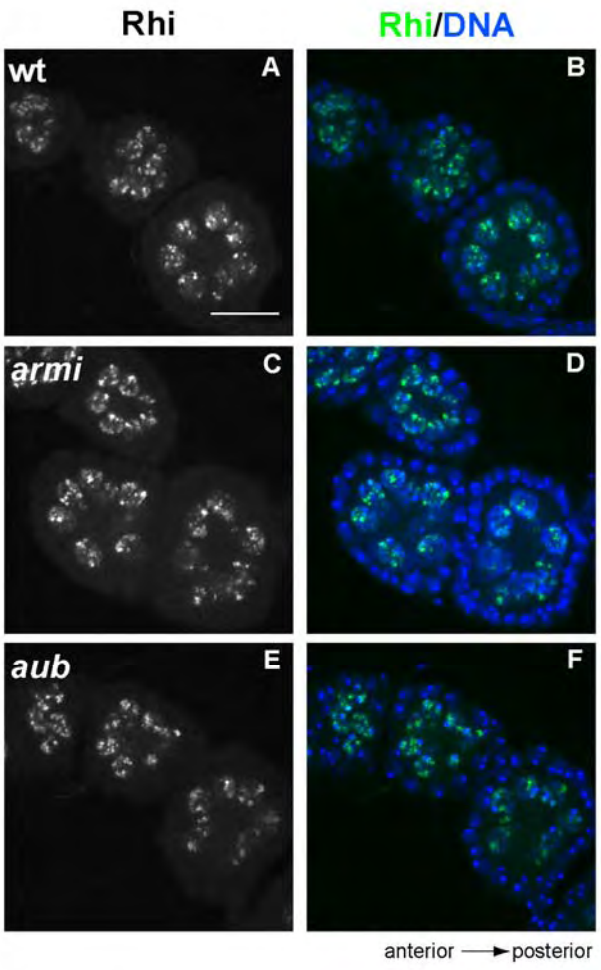

Figure 12. Rhi localization to the chromatin is independent of piRNAs.

Rhino localization appears similar in wild type (A-B), *armi* (C-D) and *aub* (E-F) stage 2 to stage 4 egg chambers. Projections of 5 serial 1μm optical sections are shown. Images were acquired under identical conditions. Scale bar is 20 μm.

Figure 13.

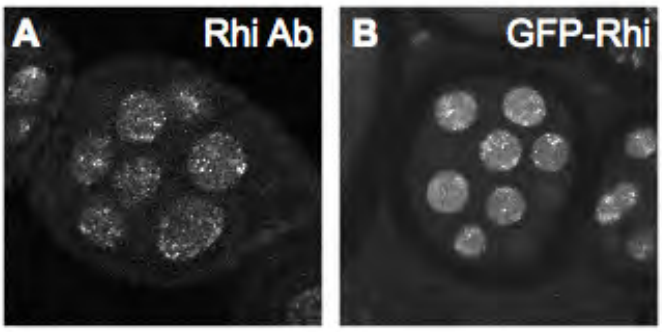

Figure 13. GFP-Rhi localization.

Endogenous Rhi detected with anti-Rhi antiserum and GFP-Rhi transgene show similar localization pattern in the germline nuclei of stage 4-5 egg chambers.

Discussion

The piRNA pathway is required for germline development in invertebrate and vertebrate systems. In *Drosophila*, the defects in germline development are linked to a loss of transposon silencing and accumulation of DNA break in germline nuclei. Deep sequencing studies suggest that Piwi proteins bound to piRNA catalyze cleavage of precursor RNAs, producing the 5' end of piRNA from the opposite strand (Brennecke et al., 2007; Gunawardane et al., 2007). However, the precursor RNAs have not been directly identified, the mechanism of 3'end generation is not understood, and the vast majority of piRNA cannot be assigned to "ping-pong" pairs. Transposons are over-represented in heterochromatic regions and piRNA pathway mutations modify position effect variagation in some somatic cells, suggesting that piRNAs may lead to transcriptional silencing of target transposons in the germline by promoting assembly of silent heterochromatin. By contrast, the Piwi proteins Aub and Ago3 localize to the cytoplasm and Piwi protein-piRNA complexes can catalyze homology dependent target RNA cleavage in vitro. These finding are consistent with post-transcriptional or co-transcriptional silencing mechanisms. The mechanisms that drive piRNA biogenesis and piRNA-dependent transposon silencing thus remain to be resolved.

Here we show that the HP1 homologue Rhino is a component of the piRNA biogenesis pathway. We also use whole genome tiling arrays to show that *rhi* and *armi* mutants lose transposon silencing but do not change the expression of protein coding genes in heterochromatin. These findings suggest that Rhino may specify chromatin domains that are required for piRNA biogenesis.

Mutations in the *rhino* locus lead to female sterility and disrupt posterior and dorsal-ventral patterning of the oocyte (Volpe et al., 2001). Mutations in the piRNA pathway lead to similar defects, and the axis specification defects associated with these mutations result from accumulation of DNA breaks in germline nuclei and the activation of a DNA-damage signaling pathway. We show that *rhino* mutations also lead to accumulation of DNA lesions. We also demonstrate that the patterning defects associated with *rhi* are dramatically suppressed by a null mutation in *mnk,* which encodes that *Drosophila* homologue of Chk2, a conserved kinase that functions in DNA damage signaling. The patterning defects associated with *rhi* are also suppressed by mutations in *mei-41,* which encodes the *Drosophila* ATR kinase homologue, and by caffeine, which inhibits ATM kinase and, to a lesser extent, ATR. ATR and ATM function upstream of Chk2 in the DNA damage signaling pathway and are activated preferentially by single stranded DNA and double strand break, respectively. Suppression by *mei-41* and caffeine thus suggests that the *rhi* mutation lead to both types of DNA lesions. We speculate that this results from mobilization of both retrotransposons, which form segments of single stranded DNA during integration, and transposable DNA elements, which generate double strand breaks during excision.

Based on these phenotypic observations, we speculated that Rhi may function in piRNA function or biogenesis. Analysis of gene expression using whole genome tiling arrays demonstrate that *rhi* disrupts silencing of transposons, and deep sequencing studies show that this is linked to a substantial reduction in piRNAs from these elements, with a particularly effect on anti-sense piRNAs. Intriguingly, *rhi* mutations do not lead to a uniform reduction in piRNA accumulation, but specifically affect piRNA production from

a number of clusters that are scattered throughout the genome. For example, piRNA production from clusters on chromosomes 2R and 4 is significantly reduced. However, piRNA production from the X chromosome is not significantly reduced. Consistent with these findings, ChIP studies suggest that Rhino binds to the clusters on 2R and 4, but not in the X chromosome. The ChIP studies are very limited, however, and a full understanding of the relationship between Rhino binding and piRNA production will require genome-wide studies.

Both sense and anti-sense RNAs are impacted by *rhi*, but reductions in anti-sense piRNA are more frequently observed, and the loss of these RNAs is linked to up-regulation of sense strand transcripts. Rhino appears to bind the piRNA clusters, and could therefore directly or indirectly activate transcription of precursors for the anti-sense piRNAs. Since piRNA biogenesis appears to be driven by a cycle of cleavage by sense and anti-sense piRNAs, loss of the anti-sense precursor would therefore lead to a breakdown in production of piRNAs from both strands. Current piRNA production models propose that piRNAs are derived from long precursor RNAs made at the clusters, and this model predicts that *rhi* will block production of these precursors. However, the hypothesized long piRNA precursors have not been identified, and it is therefore not feasible at this point to directly assay for loss of these precursors in *rhino* mutants. Alternatively, Rhino could recruit piRNA-processing machinery to chromatin, and thus promote co-transcriptional cleavage of precursor transcripts. The reduction in nuclear localization of Piwi protein in *rhi* mutants is consistent with this possibility. However, mutations in several piRNA pathway genes reduce Piwi localization to the nucleus,

making interpretation of the localization defect in *rhi* difficult. The precise role of Rhino in piRNA biogenesis thus remains to be determined.

All three domains of Rhino protein (chromo, chromo shadow and hinge) show evidence of rapid positive selection, and Rhino is the only HP1 paralog in *Drosophila* that displays this evolutionary behavior (Vermaak et al., 2005). Based on these observations, Vermaak et al. (2005) proposed that "…rhino is involved in a genetic conflict that affects the germline, belying the notion that heterochromatin is simply a passive recipient of "junk DNA" in eukaryotic genomes." Our findings indicate that Rhino is involved in the conflict between the drive for transposon propagation and the need to maintain germline DNA integrity, and suggest that heterochromatic loci that produce piRNAs may have a key role in this battle. The rapid pace of *rhino* evolution makes identification of homologues in other species difficult, but the conserved role for piRNAs in germline development suggests that HP1 variants may have critical roles in the conflict between selfish elements and genome integrity in humans.

Experimental Procedures

Drosophila stocks

All animals were raised at 25^{O}C on standard food. *Oregon R* was used for wild type, w^{1118} and $cn^{1}; ry^{506}$ were used as control when noted. The following alleles were used: mnk^{P6} (Brodsky et al., 2004; Takada et al., 2003); $rhi^{KG00910}$ (rhi^{KG}) and rhi^{02086} (rhi^{2}) (volpe 2001); $armi^{72.1}$ and $armi^{1}$ (Cook et al., 2004); $mei41^{D3}$, (Hari et al., 1995; Hawley and Tartof, 1983); P[*lacW*]*mei-W68*^{K05603}, *mei-W68*^{1} (McKim and Hayashi-Hagihara, 1998). The mnk^{P6} allele was kindly provided by M. Brodsky (Brodsky et al., 2004). All other stocks were obtained from the Bloomington *Drosophila* Stock Center (Consortium, 2003; http://flybase.org/). Standard genetic procedures were used to generate double mutant combinations.

Antibody Production

Rhino antibody

Primers annealing to each of the translation start and stop sites of a *rhino* cDNA (DGRC clone RE36324) were designed (Integrated DNA Technologies, Inc.) with attached Gateway (Invitrogen) sequences. The resulting PCR product was used to make a Rhi-DONR construct which in turn was used to subclone into the 6X-His-tagged Gateway vector pDest17 (Invitrogen), yielding a 6X-His tagged Rhino fusion protein. The fusion protein was purified over a Probond Ni matrix (Invitrogen) under denaturing conditions, isolated by SDS-PAGE and used to immunize 2 Guinea pigs (Pocono Rabbit Farm and Laboratory, Inc.) using standard protocols for antibody production. Anti-Rhi antibody was

affinity purified on fusion protein coupled to CNBr activated Sepharose 4B (Pharmacia) as described elsewhere (Harlow and Lane, 1999).

Piwi, Aub and Ago3 antibodies

Rabbit polyclonal antisera directed against the N-terminal 14-16 AA of Piwi, Aub and Ago3 (Brennecke et al., 2007) were raised by the Pocono Rabbit Farm and Laboratory, Inc. using their proprietary Quick Draw 49 Day protocol. Antisera were affinity purified over epoxy-activated Sepharose 6B (Pharmacia) columns coupled to their respective free peptides as described (Harlow and Lane, 1999).

HOAP antibody

A full length HOAP cDNA was cloned into the pQE31 6X his-tagged expression vector (Qiagen) and over-expressed in E. coli BL21(DE3) cells. The resulting fusion protein was purified on a Probond Ni matrix under denaturing conditions (Invitrogen). The purified protein was injected into rabbits and serum was produced by standard protocol at Pocono Rabbit Farm and Laboratory, Inc.

Immunohistochemistry

Egg chamber fixation and whole-mount antibody labeling were performed as previously described (Theurkauf, 1994). Vas protein was labeled with rabbit polyclonal anti-Vas antibody (Liang et al., 1994) at 1:1000. Gurken protein was labeled with mouse monoclonal anti-Gurken antibody (obtained from the Developmental Studies Hybridoma Bank, University of Iowa) at 1:10. Rhi protein was labeled with a guinea pig polyclonal anti-Rhi antiserum developed by our group (see above) at 1:2000. Piwi, Aub and Ago3 were labeled with rabbit polyclonal anti-Piwi, anti-Aub and anti-Ago3 antibodies

developed for this study (see above) at 1:1000. Antibody against γ-H2Av was kindly provided by Kim McKim (Gong et al., 2005) and egg chambers were labeled as described previously (Belmont et al., 1989). CID was labeled with an affinity purified chicken anti-CID antibody provided by Gary Karpen at 1:100 (Blower and Karpen, 2001). HOAP was labeled with a polylonal rabbit anti-Hoap antibody generated by our group (see above) at 1:1000.

Rhodamine-conjugated phalloidin (Molecular Probes) was used at 1:100 to stain F-actin, and TOTO3 (Molecular Probes) was used at 1:500 (0.2 μM final concentration) to visualize DNA.

GFP-Rhino transgenic animals

GFP-Rhi transgene was generated by recombining the Rhi-DONR (see above) construct with a modified pCasper vector containing the GFP sequence and Gateway cloning cassette B (invitrogene). The resulting vector contained GFP fused in frame to the N-terminus of Rhino under the control of the Gal4 promoter. Transgenic animals were generated using standard embryo microinjection techniques at Genetic Services, Inc.

Microscopy

All tissues were mounted in 90% glycerol / PBS, with 1 mg/ml p-Phenylenediamine (Sigma). Samples were analyzed using a Leica TCS-SP inverted laser scanning microscope with 63X NA 1.32 PlanApo oil and 40X NA 1.25 Planapo oil objectives. Identical imaging conditions were used for each set of wild type and mutant samples. Images were processed using Image J software.

Northern Blot

Fly ovaries were dissected in 1× Robb's medium (55mM Potassium Acetate, 40mM Sodium Acetate, 100mM Sucrose, 10mM Glucose, 1.2mM MgCl2, 1mM CaCl2, and 100mM HEPES, pH7.4). Total RNA was isolated from approximately 30 mg of ovaries using RNeasy® Mini Kit following manufacturer's instructions (Qiagen). Total RNA was quantified and 20μg total RNA of each sample were resolved electrophoretically on a 1%Agarose/Formaldehyde gel. RNA was transferred to a positively charge nylon membrane (Roche) by the use of standard capillary transfer. Following transfer, RNA was fixed to the membrane via UV crosslinking (Stratalinker UV Crosslinker 2400). Loading and transfer steps were controlled by staining the membrane with methylene Blue (data not shown). Following pre-hybridization, Northern analysis was performed using the DIG RNA labeling kit following manufacturer's recommendations (Roche). Blots were developed using CDP-Star (Tropix) according to manufacturer's directions. Images were acquired using the Kodak 4000MM Image Station.

Small RNA Northern blot

Total RNA was isolated from manually dissected ovaries from 2-4 day flies using mirVana (Ambion, Austin, TX, USA) according to the manufacturer's instructions. The RNA was quantified by absorbance at 260 nm. 10 μg of total RNA was resolved by 15% denaturing urea-polyacrylamide gel (National Diagnostics, Atlanta, GA, USA). 5´-32P-radiolabeled synthetic RNA oligonucleotides were used as size markers. After electrophoresis, the gel was transferred to Hybond N+ (Amersham-Pharmacia, Little Chalfont, UK) in 0.5x TBE by semi-dry transfer (Transblot SD, Bio-Rad) at 20 V for 1 h.

The RNA was crosslinked to the membrane by UV irradiation (1200 μjoules/cm; Stratalinker, Stratagene, La Jolla, CA, USA) and pre-hybridized in Church buffer for 2 h at 37°C. 25 pmol of DNA (IDT, Coralville, IA, USA) probe was 5´-32P-radiolabeled with polynucleotide kinase (New England Biolabs, Beverly, MA, USA) and 330 μCi γ-32P-ATP (7,000 μCi/mmol; New England Nuclear, Boston, MA, USA) and purified with a Sephadex G-25 spin column (Roche, Basel, Switzerland). To detect 2S rRNA, 1/50 of the 32P-radiolabeled probe was diluted with unlabeled 2S rRNA probe. The 32P-radiolabeled probes were hybridized in Church buffer for 2–12 h. After hybridization, membranes were washed three times with 1x SSC/0.1% (w/v) sodium dodecyl sulfate (SDS) for 30 min. Membranes were analyzed by phosophorimagery (Fuji, Tokyo, Japan). To strip probes, membranes were boiled in 0.1% (w/v) SDS for 10 min, then re-exposed to confirm probe removal.

Probes for Northern hybridization

Small RNA detected	Sequence (5′ to 3′)
HeT-A piRNA	GGCGTTACGCATCTTGTTATT
miR-8	GACATCTTTACCTGACAGTATTA
2S rRNA	TACAACCCTCAACCATATGTAGTCCAAGCA

Total RNA isolation and tiling array hybridization

Total RNA was isolated from manually dissected ovaries from 2-4 day old w^{1118}, rhi^{KG}/rhi^{2} and *armi72.1/armi1* flies using RNeasy (Qiagen) according to the manufacturer's instructions. The RNA was quantified by absorbance at 260 nm. Double-stranded cDNA was prepared using GeneChip® WT Amplified Double-Stranded cDNA

Synthesis Kit (Affymetrix). DNA was labeled using GeneChip® WT Double-Stranded DNA Terminal Labeling Kit (Affymetrix). Labeled DNA was hybridized to GeneChip® Drosophila Tiling 2.0R Arrays (Affymetrix) in triplicate using GeneChip® Hybridization, Wash, and Stain Kit (Affymetrix) at the University of Massachusetts Medical School genomic core facility.

Deep sequencing of small RNAs

Total RNA was isolated from manually dissected ovaries from $cn^{1};ry^{506}$ and rhi^{KG}/rhi^{2} 2-4 day flies using mirVana (Ambion, Austin, TX, USA) according to the manufacturer's instructions. The RNA was quantified by absorbance at 260 nm. To deplete 2S rRNA, 100µg total RNA was incubated with 200 pmole of DNA oligonucleotides (5′AGTCTTACAACCCTCAACCATATGTAGTCC AAGCAGCACT-3′) complementary to 2S rRNA sequences in 20µl reaction at 95°C for 2min, then gradually decrease temperature over one hour to room temperature. 2S rRNA was digested with 2 units of RNase H (Invitrogen, Carlsbad, CA, USA) in 30 µl reaction containing 50 mM Tris-HCl (pH 8.3), 75 mM KCl, 3 mM MgCl2, and 10mM DTT. After 2S rRNA depletion, 18-29nt small RNA was purified with 15% denaturing urea-polyacrylamide gel (National Diagnostics, Atlanta, GA, USA). Half of purified RNA was oxidized with 25 mM NaIO4 in borax/boric acid buffer (60 mM borax, 60 mM boric acid, pH 8.6) for 30 min at room temperature followed by ethanol precipitation. The other half was subject to the same treatment except that NaIO4 was omitted. 100pmole of 3´ preadenylated adapter (5´-rAppTCGTATGCCGTCTTCTGCTTGT/ddC/-3´) was ligated to oxidized or un-oxidized small RNAs with Mutant Rnl2_1-249_K227Q (17-23B) (Addgene,

Cambridge, MA, USA) at 4°C for 12 hrs in 20 µl reaction containing 50mM Tris-HCl (pH 7.5), 10mM MgCl2, 10mM DTT, 60µg/mL BSA, 10% (v/v) DMSO, and 40 units of RNasin (Promega, Madison, WI, USA). 3´ ligated product was purified with 15% denaturing urea-polyacrylamide gel (National Diagnostics, Atlanta, GA, USA), and then ligated to 100 pmole of 5´ adapter (5´-rGrUrUrCrArGrArGrUrUrCrUrArCrArGrUrCrCrGrArCrGrArUrC-3´) with T4 RNA ligase (Ambion, Austin, TX, USA) at room temperature for 6 hrs in 20 µl reaction containing 50 mM Tris-HCl (pH 7.8), 10 mM MgCl2, 10 mM DTT, 1 mM ATP, and 10% DMSO. The ligated product was purified with 10% denaturing urea-polyacrylamide gel (National Diagnostics, Atlanta, GA, USA). Half of ligated product was used to synthesize cDNA with Superscript III (Invitrogen, Carlsbad, CA, USA) and reverse transcription primer (5´CAAGCAGAAGACGGCATACGA-3´), and half was used as –RT control. Small RNA library was amplified with forward primer (5´AATGATACGGCG ACCACCGACAGGTTCAGAGTTCTACAGTCCGA-3´) and reverse primer (5´CAAGCAGAAGACGGCATACGA-3´), and then purified with % NuSieve GTG agarose gel (Lonza). Purified libraries were submitted for illumina-solexa high-throughput sequencing at the University of Massachusetts Medical School deep sequencing core facility.

Statistical Analysis of tiling array and deep sequencing data

Tiling array analysis

Since transposons account for more than 10% of the probes on the tiling array, a special normalization workflow has been taken to avoid over-normalization of signals. Coordinates and raw signal values for Drosophila tiling 2.0R array probes were extracted

from Affymetrix Tiling Array Software. Then probes mapped to transposon regions were identifed. The remaining non-transposon probes were quantile-normalized across wild type and mutant replicates based on the assumption that the overall signal distribution of these probes should remain the same across the different strains. Then the signals for transposon probes were calculated by looking up the normalized values of non-transposon probes at same raw signal level. To summarize the signal for each transposon element, probes mapped to any copy of the element were grouped together and Hodges-Lehmann estimator (Hollander, M. and Wolfe, D.A. Nonparametric Statistical Methods, 2nd edition. John Wiley and Sons, Inc. 1999) was used to calculate the pseudomedian of their normalized signals. We used pseudomedian as it is less sensitive to the large number of outlier probes (probes with value of 1) in the tiling array experiments. Differentially expressed transposon elements were identified by contrasting their pseudomedian values in mutant replicates against wild type replicates. To correct for multiple testing, False Discovery Rates (FDRs) were calculated from t-test P-values. FDR<0.02 were used to call significantly changed transposons. Similarly, expression values of mRNAs were summarized by calculating the pseudomedian of probes mapped to each of the RefSeq mRNA transcripts. Differentially expressed transcripts were identified using FDR<0.02 cutoff.

Deep sequencing analysis

The extracted inserts were mapped to the female *Drosophila melanogaster* genome (Flybase Release R5.5, excluding chromosome YHet). Only the inserts that are perfectly matched to a genomic sequence were collected, using an internally developed suffix tree-based software. The annotated genes and transposons were downloaded from Flybase

(R5.5). The transposon consensus sequence downloaded from Flybase was blasted against the female genome, with e-value cutoff 10^{-10}. For a set of sequences (possibly of various lengths), the frequency of each nucleotide at each position was computed as a foreground count matrix. The background frequencies at each position were computed by averaging over all possible k-mers (k=23~29) in transposon sequences, strand-specifically (either sense or antisense), weighted by the length distribution of each foreground set. A binomial testing was performed for each nucleotide at each position in the foreground matrix, using the corresponding element in the background matrix as the probability parameter. The significance level of testing used was $\alpha=5\times10^{-7}$. This stringency corrects for multiple testing. Only the nucleotides significantly above background were displayed, with the Y values being the relative frequency of foreground minus background. This background correction is important in determining whether a certain A or U-bias is biologically meaningful. Transposon sequences are generally AU-rich. Within each set of sequences mapped to transposons, the nearest sequence on the opposite strand was chosen and the length of 5' overlaps were computed. The histogram of the overlaps was generated using the average normalized reads of the two partners of the pairing as the abundance. For each blast-hit transposon copy, all the ungapped segments of the consensus-hit sequence alignment were collected and were used for coordinate conversion. The genomic coordinate of any insert that overlaps with an ungapped segment of a blast hit was converted relative to the consensus sequence. Overlaps of an insert to multiple segments were corrected to avoid double-counting, as well as multiple hits on the same genomic position caused by repetitive sequences. An advantage of coordinate conversion over direct sequence matching to the consensus sequence is that it allows consistency in the

small RNAs included in different analyses, i.e. the same set of the small RNAs mapped to transposon regions in the genome are included in the set mapped on the consensus sequence. The total reads of PiRNA (23-29nt) normalized by number of times mapped to the genome were calculated using 5kb non-overlap window.

Chromatin Immunoprecipitation and qPCR

30 wild type ovaries were dissected and treated for subsequent ChIP analysis as previously described (Austin et al., 1999) with modifications. ChIP and input DNA fragments were PCR amplified in triplicate and quantitated using the ABI prism 7500 sequence detection system and SYBR Green PCR master mix (Applied Biosystems). Using primers C1A-F (CGTCCCAGCCTACCTAGTCA),C1AR(ACTTCCCGGTG AAGACTCCT), C1B-F (GCAGATGAGCTGAAACGAAA),C1BR(TCGCAGTCGT GTAATCCAAA), C2A-F(GCCTACGCAGAGGCCTAAGT),C2AR(CAGATGT GGTCCAGTTGTGC), C2BF(CTGCTTTGTGCTTGGAGATG),C2BR(TCTG CACAGATTCTGAAATTGA A), C3A-F(CGGATGTGTTGAGGTGAGTG), C3A-R(CGGCTGCTCTCAAATTTCTT), C3B-F(TGGAGACTGCAGCAAGAAAA), C3B-R(GCCTAGCGACACATACACCA), C3C-F(TCTTTGGCCATGGCTATCTC), C3C-R(GATTCCAAGCACGTTTCGTT). A ratio of ChIP DNA to input DNA was calculated for all samples, and fold enrichment was determined relative to *rp49*.

References:

Abdu, U., Brodsky, M., and Schupbach, T. (2002). Activation of a meiotic checkpoint during Drosophila oogenesis regulates the translation of Gurken through Chk2/Mnk. Curr Biol *12*, 1645-1651.
Aravin, A. A., Hannon, G. J., and Brennecke, J. (2007). The Piwi-piRNA pathway provides an adaptive defense in the transposon arms race. Science *318*, 761-764.
Austin, R., Orr-Weaver, T., and Bell, S. (1999). Drosophila ORC specifically binds to ACE3, an origin of DNA replication control element. Genes and Development *13*, 2639-2649.
Bartek, J., Falck, J., and Lukas, J. (2001). CHK2 kinase--a busy messenger. Nat Rev Mol Cell Biol *2*, 877-886.
Belmont, A. S., Braunfeld, M. B., Sedat, J. W., and Agard, D. A. (1989). Large-scale chromatin structural domains within mitotic and interphase chromosomes in vivo and in vitro. Chromosoma *98*, 129-143.
Blower, M. D., and Karpen, G. H. (2001). The role of Drosophila CID in kinetochore formation, cell-cycle progression and heterochromatin interactions. Nat Cell Biol *3*, 730-739.
Bozzetti, M. P., Massari, S., Finelli, P., Meggio, F., Pinna, L. A., Boldyreff, B., Issinger, O. G., Palumbo, G., Ciriaco, C., Bonaccorsi, S., and et al. (1995). The Ste locus, a component of the parasitic cry-Ste system of Drosophila melanogaster, encodes a protein that forms crystals in primary spermatocytes and mimics properties of the beta subunit of casein kinase 2. Proc Natl Acad Sci U S A *92*, 6067-6071.
Brennecke, J., Aravin, A. A., Stark, A., Dus, M., Kellis, M., Sachidanandam, R., and Hannon, G. J. (2007). Discrete small RNA-generating loci as master regulators of transposon activity in Drosophila. Cell *128*, 1089-1103.
Brodsky, M. H., Weinert, B. T., Tsang, G., Rong, Y. S., McGinnis, N. M., Golic, K. G., Rio, D. C., and Rubin, G. M. (2004). Drosophila melanogaster MNK/Chk2 and p53 regulate multiple DNA repair and apoptotic pathways following DNA damage. Mol Cell Biol *24*, 1219-1231.
Brower-Toland, B., Findley, S. D., Jiang, L., Liu, L., Yin, H., Dus, M., Zhou, P., Elgin, S. C., and Lin, H. (2007). Drosophila PIWI associates with chromatin and interacts directly with HP1a. Genes Dev *21*, 2300-2311.
Cenci, G., Siriaco, G., Raffa, G. D., Kellum, R., and Gatti, M. (2003). The Drosophila HOAP protein is required for telomere capping. Nat Cell Biol *5*, 82-84.
Chen, Y., Pane, A., and Schupbach, T. (2007). Cutoff and aubergine mutations result in retrotransposon upregulation and checkpoint activation in Drosophila. Curr Biol *17*, 637-642.
Cook, H., Koppetsch, B., Wu, J., and Theurkauf, W. (2004). The Drosophila SDE3 Homolog armitage Is Required for oskar mRNA Silencing and Embryonic Axis Specification. Cell *116*, 817-829.
Du, T., and Zamore, P. D. (2005). microPrimer: the biogenesis and function of microRNA. Development *132*, 4645-4652.
Ghabrial, A., and Schupbach, T. (1999). Activation of a meiotic checkpoint regulates translation of Gurken during Drosophila oogenesis. Nat Cell Biol *1*, 354-357.
java/Propub/cellbio/ncb1099_1354.fulltext java/Propub/cellbio/ncb1099_1354.abstract.

Gong, W. J., McKim, K. S., and Hawley, R. S. (2005). All paired up with no place to go: pairing, synapsis, and DSB formation in a balancer heterozygote. PLoS Genet *1*, e67.
Gonzalez-Reyes, A., Elliott, H., and St Johnston, D. (1995). Polarization of both major body axes in Drosophila by gurken-torpedo signalling. Nature *375*, 654-658.
Gunawardane, L. S., Saito, K., Nishida, K. M., Miyoshi, K., Kawamura, Y., Nagami, T., Siomi, H., and Siomi, M. C. (2007). A slicer-mediated mechanism for repeat-associated siRNA 5' end formation in Drosophila. Science *315*, 1587-1590.
Hannon, G. J. (2002). RNA interference. Nature *418*, 244-251.
Hari, K. L., Santerre, A., Sekelsky, J. J., McKim, K. S., Boyd, J. B., and Hawley, R. S. (1995). The mei-41 gene of D. melanogaster is a structural and functional homolog of the human ataxia telangiectasia gene. Cell *82*, 815-821.
Harlow, E., and Lane, D. (1999). Purifying Antibodies, In Using Antibodies: A Laboratory Manual (Cold Spring Harbor Laboratory Press), pp. 70-80.
Hawley, R. S., and Tartof, K. D. (1983). The effect of mei-41 on rDNA redundancy in Drosophila melanogaster. Genetics *104*, 63-80.
Houwing, S., Kamminga, L. M., Berezikov, E., Cronembold, D., Girard, A., van den Elst, H., Filippov, D. V., Blaser, H., Raz, E., Moens, C. B., *et al.* (2007). A role for Piwi and piRNAs in germ cell maintenance and transposon silencing in Zebrafish. Cell *129*, 69-82.
Jang, J. K., Sherizen, D. E., Bhagat, R., Manheim, E. A., and McKim, K. S. (2003). Relationship of DNA double-strand breaks to synapsis in Drosophila. J Cell Sci *116*, 3069-3077.
Klattenhoff, C., Bratu, D. P., McGinnis-Schultz, N., Koppetsch, B. S., Cook, H. A., and Theurkauf, W. E. (2007). Drosophila rasiRNA pathway mutations disrupt embryonic axis specification through activation of an ATR/Chk2 DNA damage response. Dev Cell *12*, 45-55.
Liang, L., Diehl-Jones, W., and Lasko, P. (1994). Localization of vasa protein to the Drosophila pole plasm is independent of its RNA-binding and helicase activities. Development *120*, 1201-1211.
Lim, A. K., and Kai, T. (2007). Unique germ-line organelle, nuage, functions to repress selfish genetic elements in Drosophila melanogaster. Proc Natl Acad Sci U S A *104*, 6714-6719.
McKim, K. S., and Hayashi-Hagihara, A. (1998). mei-W68 in Drosophila melanogaster encodes a Spo11 homolog: evidence that the mechanism for initiating meiotic recombination is conserved. Genes Dev *12*, 2932-2942.
Modesti, M., and Kanaar, R. (2001). DNA repair: spot(light)s on chromatin. Curr Biol *11*, R229-232.
Pal-Bhadra, M., Bhadra, U., and Birchler, J. A. (2002). RNAi related mechanisms affect both transcriptional and posttranscriptional transgene silencing in Drosophila. Mol Cell *9*, 315-327.
Pal-Bhadra, M., Leibovitch, B. A., Gandhi, S. G., Rao, M., Bhadra, U., Birchler, J. A., and Elgin, S. C. (2004). Heterochromatic silencing and HP1 localization in Drosophila are dependent on the RNAi machinery. Science *303*, 669-672.
Pane, A., Wehr, K., and Schupbach, T. (2007). zucchini and squash encode two putative nucleases required for rasiRNA production in the Drosophila germline. Dev Cell *12*, 851-862.

Prud'homme, N., Gans, M., Masson, M., Terzian, C., and Bucheton, A. (1995). Flamenco, a gene controlling the gypsy retrovirus of Drosophila melanogaster. Genetics *139*, 697-711.
Redon, C., Pilch, D., Rogakou, E., Sedelnikova, O., Newrock, K., and Bonner, W. (2002). Histone H2A variants H2AX and H2AZ. Curr Opin Genet Dev *12*, 162-169.
Roth, S., Neuman-Silberberg, F. S., Barcelo, G., and Schupbach, T. (1995). cornichon and the EGF receptor signaling process are necessary for both anterior-posterior and dorsal-ventral pattern formation in Drosophila. Cell *81*, 967-978.
Saito, K., Nishida, K. M., Mori, T., Kawamura, Y., Miyoshi, K., Nagami, T., Siomi, H., and Siomi, M. C. (2006). Specific association of Piwi with rasiRNAs derived from retrotransposon and heterochromatic regions in the Drosophila genome. Genes Dev *20*, 2214-2222.
Sarkaria JN, Busby EC, Tibbetts RS, Roos P, Taya Y, Karnitz LM, and RT., A. (1999). Inhibition of ATM and ATR kinase activities by the radiosensitizing agent, caffeine. Cancer Res *59*, 4375-4382.
Schupbach, T. (1987). Germ line and soma cooperate during oogenesis to establish the dorsoventral pattern of egg shell and embryo in Drosophila melanogaster. Cell *49*, 699-707.
Takada, S., Kelkar, A., and Theurkauf, W. E. (2003). Drosophila checkpoint kinase 2 couples centrosome function and spindle assembly to genomic integrity. Cell *113*, 87-99.
Theurkauf, W. E. (1994). Immunofluorescence analysis of the cytoskeleton during oogenesis and early embryogenesis. Methods Cell Biol *44*, 489-505.
Vagin, V. V., Sigova, A., Li, C., Seitz, H., Gvozdev, V., and Zamore, P. D. (2006). A distinct small RNA pathway silences selfish genetic elements in the germline. Science *313*, 320-324.
Verdel, A., and Moazed, D. (2005). RNAi-directed assembly of heterochromatin in fission yeast. FEBS Lett *579*, 5872-5878.
Vermaak, D., Henikoff, S., and Malik, H. S. (2005). Positive selection drives the evolution of rhino, a member of the heterochromatin protein 1 family in Drosophila. PLoS Genet *1*, 96-108.
Volpe, A. M., Horowitz, H., Grafer, C. M., Jackson, S. M., and Berg, C. A. (2001). Drosophila rhino encodes a female-specific chromo-domain protein that affects chromosome structure and egg polarity. Genetics *159*, 1117-1134.
Wang, X. Q., Redpath, J. L., Fan, S. T., and Stanbridge, E. J. (2006). ATR dependent activation of Chk2. J Cell Physiol *208*, 613-619.

CHAPTER IV

Perspectives and Open Questions

Protecting the genome of their germline is one of the most crucial tasks that organisms confront. Transposable elements are genetic parasites that can mobilize, causing DNA damage. To protect themselves from transposable elements, organisms need a system that can silence various elements and respond to their rapid evolution. The piRNA pathway is responsible for silencing transposable elements in the *Drosophila* germline. piRNAs bind to the piwi class of Argonaute proteins, which are conserved proteins required for germline development in flies, fish and mice.

Source of DNA damage in the germline of piRNA mutants

This thesis is focused on piRNA function and production in the *Drosophila* female germline. In the studies presented in Chapter II, I determined that the piRNA pathway is not directly responsible for patterning *Drosophila* embryos. The patterning defects in these mutants are caused by activation of a DNA damage response. Although we demonstrated that there was increased phosphorilation of histone H2Av in mutant germline nuclei, which is generally accepted as a consequence of DNA damage, we did not directly show the presence of DNA double stranded breaks or other DNA lesions. Work is currently underway in the laboratory to address this point. Using pulse field gel elctrophoresis and comet assays (Fairbairn et al., 1995) our group has now determined that the DNA is indeed fragmented in ovaries from *armi* and *aub* mutants, probably as a result of DNA double strand breaks. The cause of DNA damage in piRNA mutants, however, is not known. The simplest explanation is that DNA damage is caused by insertion of de-repressed transposable elements. This hypothesis has been very quickly accepted as a cause-effect relationship by the field, without any direct conclusive data. To date there is

no direct evidence of transposon mobilization in the ovary and only one retrotransposon has been shown to mobilize in mutant testes. If the DNA double stranded breaks are caused by transposable elements integrating into the genome, one would expect to find sequences corresponding to such elements in the DNA closest to the break. Cloning strategies to try to isolate the DNA adjacent to the breaks using DNA end-labeling have been attempted by our group with no success. PCR strategies to determine if there are new transposon insertion sites in the mutants are currently being performed and it appears that there is indeed increased transposition in the mutant ovaries.

Hybrid dysgenesis is an event that occurs in *Drosophila* when a transposon, carried by a male that has established control over that element, is introduced into a female that does not carry the element (Bucheton, 1990). Transposon mobilizes in the progeny cause sterility and a variety of abnormalities in the germline, including axial patterning defects (Engels and Preston, 1979). It has been established that the molecular basis of this phenomenon is the inability to silence the transposable element in the germline of the progeny (Pelisson, 1981; Rubin et al., 1982). Over several generations the progeny that survive become resistant and acquire the ability to silence the transposable element (Pelisson and Bregliano, 1987). The piRNA pathway has been involved in this process of acquired resistant (Brennecke, unpublished observations). It would be interesting to determine if the pattering defects associated with hybrid dysgenesis are due to activation of the DNA-damage signaling pathway. This would be hard to address genetically, but treatment with caffeine could be used to inactivate ATM and ATR. Furthermore, if γ-H2Av staining in the germline is increased, as observed in piRNA mutants, it would indicate that transposon overexpression can lead to break formation in the germline.

Downstream target of mnk that mediate patterning defects

in piRNA mutant oocytes

The downstream targets of *mnk* that cause the disruption of the microtubule network and result in oocyte patterning defects also remain to be defined. We determined that *mnk* is genetically required for the axis specification defects, but have not directly demonstrated that the Chk2 kinase is activated in the mutants. Chk2 protein is expressed at low levels during oogenesis and the antibodies that are available do not show any strong signal at this stage. Our group has generated a human Chk2 transgene (huChk2) that can rescue the *mnk* phenotype in response to DNA damage, suggesting that these proteins are functionally conserved. As shown in figure 1 of Appendix 1, we expressed the huChk2 transgene in mutant and wild type ovaries and stained with an antibody raised against the active (phosphorylated) form of huChk2. We observed that activated huChk2 was present in mutant oocytes but not in wild type. Chk2 kinase is therefore active and in the right location to directly modify components of the microtubule network.

However, we do not know the downstream targets of Chk2. During oogenesis, the nurse cells centrioles migrate into the oocyte and become clustered at the posterior pole (Mahowald and Strassheim, 1970). It is possible that this material organizes the microtubule network between stages 3 and 6. I have found that, in *armi* mutants, the centrioles partially migrate into the oocyte but fail to cluster at the posterior pole (Appendix 1, figure 2). In *Drosophila* embryos, DNA damage results in Chk2-dependent centrosome inactivation, and centrioles lie at the center of centrosomes. I speculatue that Chk2 has the same centrosome targets in oocytes and embryos. The embryos provide a

much better system to address Chk2 targets at the centrosome, suing both genetic and biochemical approaches. Analysis of Chk2-depenendent centrosome inactivation in the embryo may provides significant insight into Chk2-dependent defects in axis specification during oogenesis.

Function of Rhino in the piRNA pathway

In the studies presented in Chapter III, I demonstrate that the HP1 homologue Rhino is required for piRNA production and transposon silencing in the *Drosophila* female germline. Our ChIP results suggest that Rhi binds to only a subset of piRNA production clusters. We show that Rhi specifically binds to piRNA production clusters in chromosomes 2R and 4 and that production of piRNAs from these loci is severely affected in *rhi* mutants. By contrast, we did not detect binding of Rhi to the cluster located in chromosome X, and piRNAs mapping to that clusters are not noticeably affected in *rhi* mutants. Rhi is predominantly expressed in the germline and thus it could be binding to only the clusters that have a specific function in this tissue. Further experiments, including ChIP on ChIP or ChIP-deep sequencing, would give us a more comprehensive view of all the sites where Rhi binds in the genome and perhaps suggest whether or not its function is limited to piRNA production.

Defining the sites where Rhi binds in the genome will also open the question of what recruits Rhi to those regions. It will be interesting to determine if Rhi is recruited to the chromatin by mechanisms similar to HP1. However, the rapid pace of evolution of the chromo and chromo shadow domains in Rhino suggests that Rhino does not bind to a very conserved protein, such as a histone (Vermaak et al., 2005). Furthermore, studies in

Drosophila cell lines suggest that Rhi might define a distinct heterochromatic domain, as it only partially co-localizes with HP1 and methylated H3K9 (Vermaak et al., 2005). Initial studies from our group suggest that this might also be the case in the germline.

The mechanism by which Rhi functions to promote piRNA biogenesis remains to be elucidated. We hypothesize that it could direct transcription of piRNA precursors from the clusters. However, precursor transcripts from these loci have not been detected, suggesting that they are perhaps very transient. For example, piRNAs could be processed directly from nascent transcripts. Alternatively, Rhi could have no effect on transcription and rather be involved in recruiting factors that would process transcripts originating from these loci. This hypothesis can be tested by directing Rhi to specific loci. For example, a GAL4 DNA binding domain-Rhi chimera could be expressed in flies with target transgenes carrying GAL4 binding sites, as has been done for HP1 (Seum et al., 2001). If Rhi is responsible for defining piRNA production clusters and directing piRNA processing machinery to these loci, piRNAs should be produced from the target transgenes. Furthermore these piRNAs should be capable of silencing GFP genes inserted in other places in the genome in trans.

References

Bucheton, A. (1990). I transposable elements and I-R hybrid dysgenesis in Drosophila. Trends Genet *6*, 16-21.
Engels, W. R., and Preston, C. R. (1979). Hybrid dysgenesis in Drosophila melanogaster: the biology of female and male sterility. Genetics *92*, 161-174.
Fairbairn, D., Olive, P., and O'Neill, K. (1995). The comet assay: a comprehensive review. Mutat Res *339*, 37-59.
Mahowald, A. P., and Strassheim, J. M. (1970). Intercellular migration of centrioles in the germarium of Drosophila melanogaster. An electron microscopic study. J Cell Biol *45*, 306-320.
Pelisson, A. (1981). The I--R system of hybrid dysgenesis in Drosophila melanogaster: are I factor insertions responsible for the mutator effect of the I--R interaction? Mol Gen Genet *183*, 123-129.
Pelisson, A., and Bregliano, J. (1987). Evidence for rapid limitation of he I element copy number in a genome submitted to several generations of I-R hybrid dysgenesis in Drosophila melanogaster. Mol GenGenet, 306–313.
Rubin, G. M., Kidwell, M. G., and Bingham, P. M. (1982). The molecular basis of P-M hybrid dysgenesis: the nature of induced mutations. Cell *29*, 987-994.
Seum, C., Delattre, M., Spierer, A., and Spierer, P. (2001). Ectopic HP1 promotes chromosome loops and variegated silencing in Drosophila. Embo J *20*, 812-818.
Vermaak, D., Henikoff, S., and Malik, H. S. (2005). Positive selection drives the evolution of rhino, a member of the heterochromatin protein 1 family in Drosophila. PLoS Genet *1*, 96-108.

APPENDIX 1

Studies to determine Chk2 activation and downstream targets of the DNA-damage signaling pathway in *armi* mutants

huChk2 transgene is activated in *armi* mutant oocytes

Mnk protein is expressed at low levels during oogenesis and the antibodies that are available do not show any strong signal at this stage. Our group has generated a human Chk2 transgene (huChk2) that can rescue the *mnk* embryonic phenotype in response to DNA damage, suggesting that these proteins are functionally conserved. We expressed the huChk2 transgene in *armi* mutant and armi heterozygous ovaries and stained with an antibody raised against the active (phosphorylated) form of huChk2 (P-T68, Tsvetkov L. et al. J Biol Chem 2003). We observed that activated huChk2 was present only in mutant oocytes but not in wild type.

Figure 1.

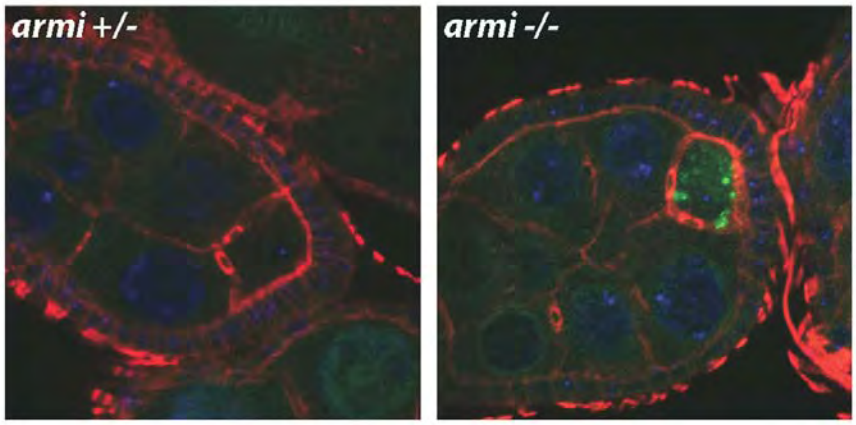

Figure 1. huChk2 transgene is activated in *armi* mutant oocytes

A full length human Chk2 transgene was expressed in *armi* heterozygous and homozygous flies. An antibody against the active for of Chk2 only labels the oocyte in homozygous but not heterozygous egg chambers.

GFP-PACT fails to localize in *armi* oocytes

During oogenesis the nurse cells centrioles migrate into the oocyte and become clustered at the posterior pole (Mahowald and Strassheim, 1970). It is possible that this material organizes the redistribution of the microtubule network between stages 3 and 6. We used a transgene expressing the Pericentrin/AKAP450 centrosomal targeting (PACT) domain of the *Drosophila* pericentrin-like protein fused to GFP (GFP-PACT) (Martinez-Campos, et al., 2004) to detect centrioles in egg chambers from heterozygous and homozygous *armi* mutant ovaries. We observe that in *armi* mutants the centrioles partially migrate into the oocyte and fail to cluster at the posterior pole (figure 2).

Figure2.

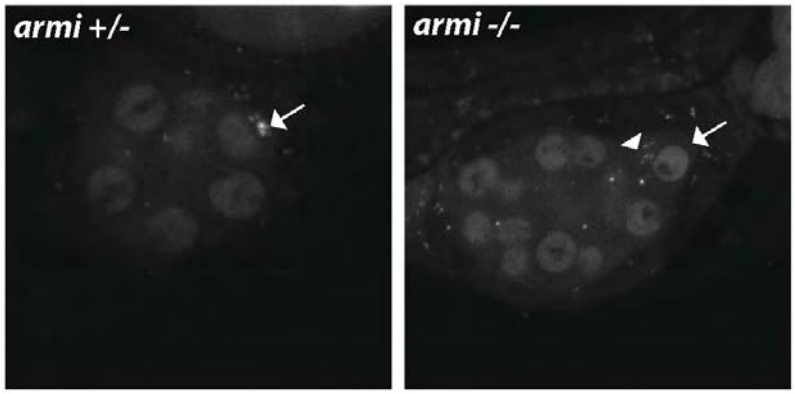

Figure 2. GFP-PACT fails to localize to the posterior pole of the oocyte at stage 5 in *armi* mutant egg chambers.

GFP-PACT localizes forming a tight aggregate at the posterior pole in *armi* heterozygous oocytes (arrow), but fails to localize in *armi* homozygous and is detected in dispersed foci at the anterior of the oocyte (arrowhead). Images were acquired using identical conditions.

huChk2 transgene

Full length of human Chk2 was amplified from plasmid pGEX2TKcs-huChk2 by PCR. The DNA fragment was sequenced and cloned via KpnI and XbaI sites into pUASP (2). The resultant plasmid, pUASp-Chk2 was introduced into the Drosophila germline by P-element-mediated transformation (3). Fly stocks were constructed carrying pUASP-Chk2 insertions and the maternal nos-GAL4-VP16 driver for expression in the ovary or early embryos (4).

1. Matsuoka S (2000) PNAS. 97, 10389-94.

2. Roth, P. (1998) Mech. Dev. 78, 113-8.

3. O'Connor,M.J. (2002) Methods Mol Biol 180, 27-36

4. Van Doren, M., Williamson, A. L. & Lehmann, R. Regulation of zygotic gene expression in Drosophila primordial germ cells. Curr Biol 8, 243-6 (1998)